



Turun yliopisto  
University of Turku

**EFFECTS OF OBESITY AND RESISTANCE EXERCISE  
ON BONE HEALTH  
STUDIED WITH MODERN IMAGING METHODS**

---

Ville Huovinen

Turun yliopiston julkaisu – Annales universitatis turkuensis  
Sarja - ser. D osa - tom. 1279 | Medica – Odontologica | Turku 2017

## **University of Turku**

---

Faculty of Medicine  
Department of Radiology  
University of Turku Doctoral Programme of  
Clinical Investigation

## **Supervised by**

---

Professor Riitta Parkkola  
Turku PET Centre  
Department of Radiology  
Turku University Hospital and  
University of Turku, Turku, Finland

Professor Pirjo Nuutila  
Turku PET Centre  
Department of Endocrinology  
Turku University Hospital and  
University of Turku, Turku, Finland

## **Reviewed by**

---

Professor Ritva Vanninen  
Department of Clinical Radiology  
Kuopio University Hospital and  
University of Eastern Finland, Kuopio, Finland

Professor Seppo Koskinen  
Department of Clinical Science, Intervention  
and Technology  
Karolinska Institutet, Stockholm, Sweden

## **Opponent**

---

Adjunct professor Kirsi Timonen  
Department of Clinical Physiology and  
Nuclear Medicine  
Central Finland Health Care District  
Jyväskylä, Finland

The originality of this thesis has been checked in accordance with the University of Turku quality assurance system using the Turnitin OriginalityCheck service.

ISBN 978-951-29-6791-9 (PRINT)

ISBN 978-951-29-6792-6 (PDF)

ISSN 0355-9483 (Print)

ISSN 2343-3213 (Online)

Painosalama Oy - Turku, Finland 2017

*To Minna, Milla and Ellen*

## **ABSTRACT**

Ville Huovinen

Effects of obesity and resistance exercise on bone health studied with modern imaging methods

University of Turku, Faculty of Medicine, Department of Radiology, University of Turku Doctoral Programme of Clinical Investigation

*Annales Universitatis Turkuensis. Painosalama Oy, 2017.*

Altered metabolic states, such as obesity and resistance exercise, may affect bone health either in a negative or positive manner. In clinical practice, bone health may be easily understood as a synonym for bone mineral density or osteoporosis, which is defined as a skeletal disorder resulting from decreased bone strength. In addition, bone glucose metabolism and bone marrow adiposity may contribute to bone overall health status.

The aims of this thesis were to investigate the effects of obesity and resistance exercise on bone glucose metabolism, bone marrow adiposity and bone mineral density using modern imaging methods, such as positron emission tomography, magnetic resonance imaging and quantitative computed tomography, in various study settings. It was found that obesity did not alter bone glucose metabolism or bone marrow adiposity. However, resistance exercise resulted in improved bone glucose metabolism and bone mineral density.

In conclusion, resistance exercise, but not obesity, had an impact on bone health studied with modern imaging methods. The obtained results may offer new insights into quantification and into the follow-up of bone health during altered metabolic conditions. In addition, more individualized and accurately allocated lifestyle interventions may be administered in the treatment or prevention of diseases associated with obesity or insulin resistance.

Keywords: obesity, exercise, bone, positron emission tomography, magnetic resonance imaging, quantitative computed tomography

# TIIVISTELMÄ

Ville Huovinen

Ylipainon ja lihasvoimaharjoittelun vaikutus luun terveyteen tutkittuna modernien kuvantamismenetelmien avulla

Turun yliopisto, Lääketieteellinen tiedekunta, Radiologia, Turun yliopiston kliininen tohtorihjelma

Turun yliopiston julkaisuja. Painosalama Oy, 2017.

Aineenvaihduntaa muuntelevat fysiologiset tilat kuten lihavuus ja lihasvoimaharjoittelu voivat mahdollisesti vaikuttaa luun terveyteen joko negatiivisesti tai positiivisesti. Luun terveys kuitenkin ymmärretään usein vain synonyymina luuntiheydelle tai osteoporoosille, joka on luun alentuneesta lujudesta johtuva sairaus. Luun terveyteen voi kuitenkin olla osallisena muitakin vähemmän tunnettuja potentiaalisia tekijöitä kuten luun sokeriaineenvaihdunta ja luuytimen rasvoittuminen.

Väitöskirjan tarkoituksena oli tutkia lihavuuden ja lihasvoimaharjoittelun vaikutuksia luun sokeriaineenvaihduntaan, luuytimen rasvoittumiseen sekä luuntiheyteen modernien kuvantamismenetelmien kuten positroniemissiotomografian, magneettikuvauksen ja kvantitatiivisen tietokonetomografian avulla erilaisissa tutkimusasetelmissä. Tulosten mukaan lihavuudella ei ollut vaikutusta luun sokeriaineenvaihduntaan tai luuytimen rasvoittumiseen. Sen sijaan lihasvoimaharjoittelu näytti parantavan luun sokeriaineenvaihduntaa ja luuntiheyttä.

Yhteenvedon voidaan siis todeta, että lihasvoimaharjoittelulla on positiivinen vaikutus luun terveyteen modernien kuvantamismenetelmien avulla tutkittuna. Sen sijaan lihavuudella ei ole siihen vaikutusta. Väitöskirjatutkimuksen tulokset voivat tuottaa uusia oivalluksia aineenvaihdunnallisiin häiriötiloihin liittyvässä luun terveyden määrittämisessä ja seurannassa. Lisäksi tuloksia soveltaen voidaan suunnitella aiempaa yksilöllisempiä ja kohdistetumpia elämäntapainterventioita lihavuuteen ja insuliiniresistenssiin liittyvien luun häiriötilojen ehkäisyssä ja hoidossa.

Avainsanat: lihavuus, liikunta, luu, positroniemissiotomografia, magneettikuvaus, kvantitatiivinen tietokonetomografia

## TABLE OF CONTENTS

ABSTRACT.....	4
TIIVISTELMÄ.....	5
ABBREVIATIONS.....	8
LIST OF ORIGINAL PUBLICATIONS.....	10
1 INTRODUCTION.....	11
2 REVIEW OF LITERATURE.....	13
2.1 Bone.....	13
2.1.1 Bone anatomy.....	13
2.1.2 Bone modeling and remodeling.....	16
2.1.3 Bone marrow fat (BMF).....	17
2.1.3.1 Obesity, exercise and BMF.....	20
2.1.4 Bone marrow glucose uptake (GU).....	21
2.1.4.1 Obesity, exercise and bone marrow GU.....	22
2.1.5 Bone mineral density (BMD) and osteoporosis.....	23
2.1.5.1 Exercise and BMD.....	24
2.2 In vivo imaging of bone.....	25
2.2.1 Magnetic resonance imaging (MRI).....	25
2.2.1.1 <sup>1</sup> H MR Spectroscopy.....	26
2.2.1.2 In-phase and out-of-phase MRI.....	31
2.2.2 FDG-PET imaging.....	32
2.2.3 Quantitative computed tomography (QCT).....	35
3 AIMS OF THE STUDY.....	38
4 MATERIALS AND METHODS.....	39
4.1 Study designs.....	39
4.2 Study subjects.....	42
4.3 MRI methods.....	44
4.4 PET methods.....	45
4.5 QCT and CT methods.....	48
4.6 Biochemical and clinical methods.....	49
4.7 Statistical methods.....	50
5 RESULTS.....	52
5.1 Association between VBM GU and VBM fat content (Study I).....	52
5.2 Effect of obesity BMF UI (Study II).....	53
5.3 Effects of obesity and exercise on bone marrow insulin-stimulated GU (Study III).....	55
5.4 Effects of exercise on BMD and serum sclerostin (Study IV).....	58

6	DISCUSSION .....	62
6.1	BMF (Bone marrow fat).....	62
6.2	Bone marrow GU (Glucose uptake).....	64
6.3	BMD (Bone mineral density) .....	67
6.4	Strengths and limitations .....	69
6.5	Clinical implications and future directions .....	72
7	CONCLUSIONS.....	74
	ACKNOWLEDGEMENTS.....	75
	REFERENCES .....	77
	ORIGINAL PUBLICATIONS .....	93

## **ABBREVIATIONS**

<sup>1</sup> H	Hydrogen, proton
BMD	Bone mineral density
BMF	Bone marrow fat
BMI	Body mass index
CT	Computed tomography
CTXA	Computed tomography x-ray absorptiometry
DXA	Dual x-ray absorptiometry
FBM	Femoral bone marrow
FDG	Fluorine-18 fluorodeoxyglucose
GE	Gradient echo
GU	Glucose uptake
HBCS	Helsinki Birth Cohort Study
HRT	Hormonal replacement treatment
HSC	Hematopoietic stem cell
HU	Hounsfield unit
LC	Lumped constant
MSC	Mesenchymal stem cell
MRI	Magnetic resonance imaging
OLM	Offspring of lean/normal-weight mother
OOM	Offspring of obese/overweight mother
PET	Positron emission tomography
PPAR $\gamma$	Peroxisome proliferator-activating receptor gamma
ppm	Parts per million
PRESS	Point resolved spectroscopy
RANKL	Receptor activator of nuclear factor kappa-B ligand
RF	Radio frequency
RM	Repetition maximum
ROI	Region of interest
SAT	Subcutaneous adipose tissue
SNR	Signal-to-noise ratio
STEAM	Stimulated echo acquisition mode
SUV	Standardized uptake volume



## *Abbreviations*

---

T1DM	Type 1 diabetes mellitus
T2DM	Type 2 diabetes mellitus
TAC	Time-activity curve
TAG	Triacylglycerols
tBMF	Tibial bone marrow fat
TE	Time of echo
TR	Time of repetition
UI	Unsaturation index
VBM	Vertebral bone marrow
vBMF	Vertebral bone marrow fat
VOI	Volume of interest
QCT	Quantitative computed tomography

## LIST OF ORIGINAL PUBLICATIONS

This thesis is based on the following original publications, which are referred in the text by the Roman numerals I-IV:

- I           **Huovinen V**, Saunavaara V, Kiviranta R, Tarkia M, Honka H, Stark C, Laine J, Linderborg K, Tuomikoski P, Badeau RM, Knuuti J, Nuutila P, Parkkola R. Vertebral bone marrow glucose uptake is inversely associated with bone marrow fat in diabetic and healthy pigs: [<sup>18</sup>F]FDG-PET and MRI study. *Bone* 2014 Apr;61:33-8.
- II           **Huovinen V**, Viljakainen H, Hakkarainen A, Saukkonen T, Toiviainen-Salo S, Lundbom N, Lundbom J, Mäkitie O. Bone marrow fat unsaturation in young adults is not affected by present or childhood obesity, but increases with age: a pilot study. *Metabolism* 2015 Nov;64(11):1574-81.
- III          **Huovinen V**, Bucci M, Lipponen H, Kiviranta R, Sandboge S, Raiko J, Koskinen S, Koskensalo K, Eriksson JG, Parkkola R, Iozzo P, Nuutila P. Femoral bone marrow insulin sensitivity is increased by resistance training in elderly female offspring of overweight and obese mothers. *PLoS One* 2016 Sep 26;11(9):e0163723
- IV          **Huovinen V**, Ivaska KK, Kiviranta R, Bucci M, Lipponen H, Sandboge S, Raiko J, Eriksson JG, Parkkola R, Iozzo P, Nuutila P. Bone mineral density is increased after a 16-week resistance training intervention in elderly women with decreased muscle strength. *Eur J Endocrinol* 2016 Sep 15. pii: EJE-16-0521.

The original publications have been reproduced with the permission of the copyright holders.

# 1 INTRODUCTION

Bone health is a sweeping and informal term describing the wellbeing or fitness of bones as they contribute to the musculoskeletal system. Different characteristics such as age, gender, obesity and physical activity levels may affect bone health either in negative or positive manner (Office of the Surgeon General (US) 2004). In clinical practice, bone health is often understood as a synonym for bone mineral density (BMD) or osteoporosis, which is defined as a skeletal disorder resulting from decreased bone strength. Osteoporotic hip fracture has a significant negative effect on an individual's quality of life. However, there may be other potential parameters contributing in the bone overall health. The parameters that are particularly focused on in this thesis include bone marrow glucose metabolism, bone marrow adiposity and BMD.

The early imaging methods for assessing bone health were replaced with dual-energy X-ray absorptiometry (DXA) in the late 1980s (Cullum, Ell & Ryder 1989). Computed tomography (CT) was introduced in 1973 for head scanning, but a couple of years later when whole-body scanners were emerging, its capability to study the skeleton was recognized (Kreel 1976). However, the use of quantitative CT (QCT) was eventually diminished because DXA was already widely used in majority of studies. In addition, DXA possessed lower radiation dose than QCT (Adams 2009). Nowadays, the use of QCT in musculoskeletal studies and the amount of CT scanners is increasing.

Modern bone marrow imaging methods consist of magnetic resonance imaging (MRI) and positron emission tomography (PET). MRI offers supreme soft-tissue contrast, is non-ionizing and offers valuable applications such as spectroscopy, which can be used as an analytical tool identifying various chemical compounds, e.g., bone marrow fat (BMF), without destructing the sample. PET, on the other hand, is a novel non-invasive imaging method that produces information pertaining to physiological tissue function. Especially with fluorine-18 fluorodeoxyglucose (FDG), the most widely used tracer, tissue-specific glucose metabolism can be measured.

The main aim of this thesis was to investigate the possible effects of obesity and physical exercise on bone health with modern imaging modalities. It was hypothesized that obesity negatively affects and physical exercise positively affects bone health. To ad-

dress this question, PET, MRI and QCT were used to assess bone marrow glucose metabolism, bone marrow adiposity and BMD within prospective cohort studies and non-randomized clinical trials (Studies I-IV).

## 2 REVIEW OF LITERATURE

### 2.1 Bone

#### 2.1.1 Bone anatomy

Human skeleton contains approximately 200 bones, which can roughly be categorized into long bones, short bones, flat bones and irregular bones. In this thesis's review of the literature, I concentrate on the femur (long bone) and vertebral body (irregular bone). Simplified, long bones consist of a hollow shaft, diaphysis, cone-shaped metaphysis below the growth plates and rounded epiphyses above the growth plates. Diaphysis of the long bone is mainly trabecular bone surrounded by thick cortical bone. Meta- and epiphyses of the long bones consists mainly of trabecular bone within bone marrow, which is surrounded by a thin layer of cortical bone (Figure 1). Irregular bones, for example, vertebral bodies are composed of a thin layer of cortical bone surrounding the trabecular bone within bone marrow (Figure 2) (Moore KL 2006).

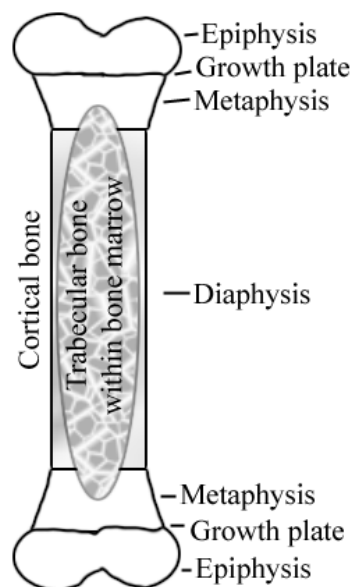


Figure 1 Schematic anatomy of a long bone, e.g., tibia or femur. Illustration by V Huovinen 2016.

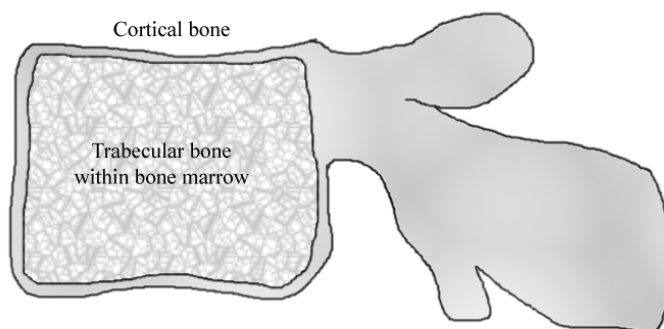


Figure 2 Schematic anatomy of a vertebral bone. Illustration by V Huovinen 2016.

Cortical bone is solid tissue that consists of multiple microscopic columns, which are called osteons. Osteons are composed of concentric layers of bone resorptive osteoclasts and osteocytes as well as bone forming osteoblasts (Clarke 2008). In the center of the osteon, the Haversian canal, running vertically, provides blood supply and nutrition for the bone cells. Osteons are connected via horizontally running Volkmann's canals (Seeman 2013). The walls and interspaces of the osteons are formed by concentric lamellar bone in which collagen fibrils produced by osteoblasts are laid in alternating orientations compared to weaker woven bone in which collagen fibrils are laid in a disorganized manner. Woven bone is normally produced rapidly by osteoblasts during conditions with high bone turnover such as fracture healing (Fazzalari 2011). Lamellar and woven bones are composed of actual bone cells and bone extracellular matrix, which is mineralized by osteoblasts. A thin membrane called the periosteum surrounds the outer surface of cortical bone and its activity is important for bone growth and fracture repair. Endosteum, also a thin membrane, is located between the bone marrow and inner surface of cortical bone (Clarke 2008).

Connective tissue of bone marrow consists of the trabecular bone, which is an interlinked structure of bony plates and rods composed of osteons and lamellar bone. Soft marrow tissue, located in between trabecular bone, consists of yellow fatty marrow, red hematopoietic marrow, blood vessels and sinusoids (Hardouin, Pansini & Cortet 2014). The function and regulation of yellow fatty marrow is mainly unknown (Gimble, Nuttall 2004), but, in short, these cells may act as an energy supply (Rosen, Bouxsein 2006) or have a function as a passive endocrine organ (Gimble et al. 1996).

---

Red hematopoietic marrow consists of differentiated hematopoietic stem cells (HSCs), hematopoietic progenitor and precursor cells and non-differentiated HSCs, and these cells constitute only a minority of the bone marrow microenvironment, also called as “the niche” (Challen et al. 2009) (Figure 3). One of the main functions of these pluripotent cells is to maintain a physiologically normal immune system by differentiating into a great variety of cells, e.g., red blood cells, a dozen types of lymphoid and myeloid white blood cells and osteoclasts. To maintain homeostasis of the hematopoietic system, these pluripotent cells respond to pathologic environmental signals, e.g., infection (Singh et al. 2008). In addition to HSCs, red marrow consists of differentiated and non-differentiated mesenchymal stem cells (MSCs), which also constitute a minority of the bone marrow cells (Pittenger et al. 1999) that support HSCs (Pontikoglou et al. 2011). MSCs have a capability to differentiate into specialized cells, e.g., osteoblasts and adipose tissue cells, through very convoluted and several stochastic autonomous cell processes. Alternatively, differentiation can occur through signals from the bone microenvironment, and this is called “the niche theory” (Calvi, Link 2014).

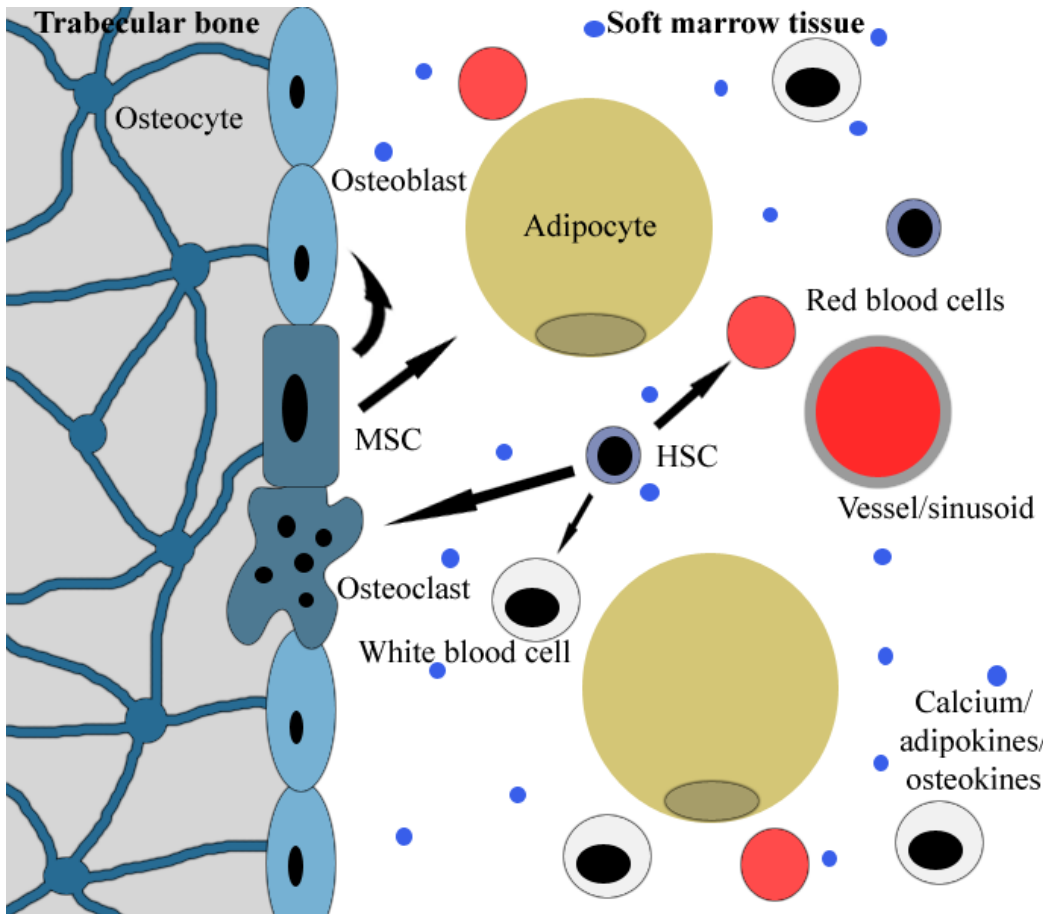


Figure 3 Simplified bone marrow in “the niche”. MSCs differentiate into osteoblasts or adipocytes and their progenitors. Eventually osteoblasts end up trapped surrounded by connective tissue with trabecular bone and transform into osteocytes that form a tentacle-like network connecting to other osteocytes and bone-lining osteoblasts. HSCs differentiate into red blood cells and their progenitors, a variety of white blood cells and their progenitors and osteoclasts. Differentiation of MSCs and HSCs is regulated by a variety of biochemical factors such as adipokines and osteokines. Calcium, which aids orienteering of HSCs to the cells at the bone-lining, is produced by bone resorptive osteoclasts. Illustration by V Huovinen 2016. MSC: mesenchymal stem cell. HSC: hematopoietic stem cell.

### 2.1.2 Bone modeling and remodeling

Bone modeling is a process where bone shape and size is changed in response to a mechanical or physiological stimulus such as growth (Clarke 2008), whereas bone remodeling is a process in which bone is renewed (Parfitt 2002). The main purpose of bone remodeling is to maintain bone mechanical strength by repairing bone microdamage and



sustaining mineral, e.g., calcium, homeostasis (Raggatt, Partridge 2010). During bone remodeling, new bone formation by osteoblasts and old bone resorption by osteoclasts are tightly coupled (Kylmaja, Nakamura & Tuukkanen 2015). Remodeling is considered to be a cycle of four different consecutive stages consisting of: activation, resorption, reversal and formation (Parfitt 2002). During the activation process, osteoclast precursors are recruited from circulation. This is followed by the formation of the multinucleated preosteoclasts. These cells bind to the bone matrix via different receptors to form bone-resorbing zones beneath multinucleated osteoclasts. Bone is then resorbed by osteoclasts via secretion of hydrogen ions and a great variety of enzymes forming empty resorption cavities (Eriksen 1986). Phagocytic cells complete the resorption phase, which can last a couple of weeks (Delaisse 2014). In the reversal phase, bone resorption switches to bone formation. Resorption cavities are filled with a wide variety of cells including osteocytes and osteoblast precursors. Activation signals that end the bone resorption and start the bone formation may include bone matrix-derived factors or a stretching gradient in the cavities (Smit, Burger & Huyghe 2002). The bone formation phase lasts approximately 4-6 months (Clarke 2008). During this phase, osteoblasts synthesize connective tissue components such as collagen and regulate matrix mineralisation. Eventually osteoblasts become trapped within the synthesized matrix and transform into osteocytes, which have an extensive tentacle-like network connecting themselves to other osteoblasts and osteocytes (Burger, Klein-Nulend & Smit 2003). The majority of the osteoblasts undergo apoptosis but some become bone-lining cells that maintain their ability to transform into osteoblasts upon exposure of stimuli, e.g., mechanical stress (Dobnig, Turner 1995). Osteon is the result of a remodeling cycle process that resembles a similar composition to trabecular and cortical bone (Clarke 2008).

### **2.1.3 Bone marrow fat (BMF)**

Bone marrow is the only place in human body where adipose tissue cells and other bone cells lie adjacently to each other (Devlin, Rosen 2015). This suggests a communication between these cells. The mean diameter of a bone marrow adipocyte is around 50  $\mu\text{m}$ , and it contains big lipid vacuole of triglycerides consisting of saturated or unsaturated fatty acids (Hardouin, Pansini & Cortet 2014). These cells are interspersed within the hematopoietic tissue and, importantly, have the same MSC progenitor that can differentiate into osteoblasts that eventually transform into an osteocyte (Van Damme et al.

2002, Calvi, Link 2014). In short, the complex differentiation of MSCs is regulated by chemical, physical and biochemical factors. These factors lead to the triggering of microenvironmental cell signals including a variety of transcription factors. For example, the upregulation of *Runx2* (runt-related transcription factor-2) may induce osteogenic differentiation, while upregulation of *PPAR $\gamma$*  (peroxisome proliferator-activating receptor gamma) induces adipogenic differentiation (Chen et al. 2016).

Mitochondria-moderate yellow BMF differs from mitochondria-sparse white subcutaneous and mitochondria-enriched brown adipose tissue (Krings et al. 2012). Brown adipose tissue is known to be metabolically very active according to earlier PET-studies (Virtanen et al. 2009, Matsushita et al. 2014, Orava et al. 2013), while white subcutaneous adipose tissue (SAT) seems to be less metabolically active compared to visceral fat in healthy obese subjects (Viljanen et al. 2009). Unfortunately, no previous PET-studies that specifically target BMF have been conducted. Nonetheless, BMF, which is accumulated in between the trabecular area of the bone diaphysis and epiphysis, has been considered as an intermediately metabolic active tissue in animal studies (Pagnotti, Styner 2016). This hypothesis is supported by the fact that BMF responds to systemic changes in energy metabolism, for example, in postmenopausal osteoporosis (Li et al. 2011) and in patients with anorexia nervosa (Bredella et al. 2014), which is a condition of undernutrition associated with various physiological changes in the body including a decrease in subcutaneous and visceral fat depots (Misra, Klibanski 2013). In addition, BMF is increased in response to a high-fat diet, while running exercise suppresses this accumulation of BMF in mice (Styner et al. 2014). Moreover, BMF is related with subcutaneous and body total fat amounts in postmenopausal women with and without T2DM (Baum et al. 2012) indicating a similar systemic regulation of these fat depots.

Yellow BMF bears its name due to its yellowish appearance, which is caused by a moderate number of cytoplasmic mitochondria. However, the precise function of yellow BMF is unknown. Yellow bone marrow is involved in thermogenesis because of its similar characteristics to brown adipose tissue (Krings et al. 2012). It may also act as a local energy supply for bone formation by storing and releasing triglycerides (Gimble, Nuttall 2004). From a secretory perspective, yellow bone marrow may act as a target endocrine organ secreting a variety of cytokines and hormones resulting in systemic consequences and local regulation in the bone marrow microenvironment (Greco, Lenzi

& Migliaccio 2015). Several data suggest an active role of BMF cells in their microenvironment by having a negative effect on osteoblasts by secreting saturated fatty acids (Rosen et al. 2009), favouring osteoclast differentiation of HSCs by expressing factors such as *RANKL* (receptor activator of nuclear factor kappa-B ligand) (Teitelbaum 2000). In addition, BMF cells may inhibit the HSC differentiation (Lecka-Czernik 2012) or act as a passive placeholder by occupying space not needed for hematopoiesis or bone formation (Devlin, Rosen 2015).

There is variation in BMF amount in a site-specific manner. At birth, bone marrow tissue is mainly composed of red hematopoietic marrow (Proytcheva 2013). Conversion of red hematopoietic marrow to yellow fatty marrow takes place gradually during childhood and continues centripetally from the peripheral skeleton to the axial skeleton (Moore, Dawson 1990). For example, femoral bone marrow (FBM) contains only fat by the time of adulthood. However, vertebral bone marrow (VBM) contains approximately 50 % yellow fatty marrow and 50 % red hematopoietic marrow by the time of adulthood (Machann, Stefan & Schick 2008). The ratio of fatty and hematopoietic marrow gradually increases with age (Liney et al. 2007). At old age, VBM fat content is at its highest (Rosen et al. 2009). Thus, BMF content correlates positively with age (Rosen et al. 2009). However, some gender variation occurs. Younger men appear to have more VBM fat than women (Kugel et al. 2001), but elderly women tend to have slightly more VBM fat than men (Griffith et al. 2012). Interestingly, VBM fat content associates inversely with BMD (Schwartz et al. 2013), but a causal relationship of the association has been found to be controversial. Lecka-Czernik et al. found that bone loss is preceded by increased BMF in mice (Lecka-Czernik et al. 2015). On the contrary, Li et al. found that the increase in BMF content was preceded by the decrease in BMD in rabbits with a setting of glucocorticoid-induced osteoporosis (Li et al. 2016). However, human studies have shown that aging (Okano et al. 1998) and marrow adiposity (Schwartz et al. 2013) have been linked with decreased BMD suggesting that an increase in BMF and a decrease in BMD is a mutual process. In addition, the finding that decrease in a BMD during menopause is corrected by estrogen administration supporting the theory of mutual process (Gallagher 2001).

Marrow adiposity arises via several mechanisms that activate intracellular pathways, which may eventually lead to having an impact on *PPAR* $\gamma$  receptor that promotes adi-

pogenesis. In short, BMF is increased by physiological factors, e.g., age, gender, anatomic location and mechanical unloading (Sadie-Van Gijsen, Hough & Ferris 2013). Pathophysiological factors promoting BMF includes anorexia nervosa (Bredella et al. 2014), T1DM (Kawai, de Paula & Rosen 2012) and pharmacological agents such as the long-term use of *PPAR* $\gamma$  agonists (thiazolidinediones) (Kawai, de Paula & Rosen 2012) or glucocorticoids (Hamrick, McGee-Lawrence & Frechette 2016). Persistence of existing BMF caused by different conditions varies, but, for example, anorexia nervosa-induced increase in marrow adiposity is reversed with weight gain possibly due to dietary changes (Fazeli et al. 2012), but mechanical unloading-induced (Trudel et al. 2009) and diabetes-induced marrow adiposity are not easily reversed. This has led to suspicions that there might be two types of BMF deposits, which are constitutive and regulated (Devlin, Rosen 2015).

Therapeutic implications targeted at BMF in order to promote differentiation of MSCs towards osteoblastogenesis are clinically relevant. Treatment of malignant diseases with chemotherapy or radiation during childhood results in increased skeletal fragility in later life (Wilson, Ness 2013). These patients usually have decreased BMD and increased BMF compared to age-matched controls (Georgiou, Hui & Xian 2012). In addition, T1DM is associated with decreased BMD with concomitantly increased BMF probably due to oxidative stress (Coe et al. 2011) or via increased *PPAR* $\gamma$  expression and activation (Botolin et al. 2005). Increased BMF saturation measured with  $^1\text{H}$  MRI spectroscopy is also related with osteoporosis and T2DM (Baum et al. 2012). Screening of the individuals at risk would prove to be a cost-effective means to identify the patients in need for anti-osteoporosis medication (Devlin, Rosen 2015).

### **2.1.3.1 Obesity, exercise and BMF**

Obesity increases BMF by adipose tissue hyperplasia and hypertrophy (Rosen, MacDougald 2006), but no previous studies addressing the effect of obesity on BMF UI has been conducted. As earlier stated, there are three types of fat depots in the human body: white, brown and yellow adipocyte containing depots. Under healthy conditions, bone marrow adipocytes are classified as yellow that store lipids, produce adipokines and are responsive to the systemic energy balance via changes in fat volume (Krings et al. 2012). However, obesity among other metabolic challenges such as aging and T2DM

drives the expression of the yellow adipocyte phenotype towards the white adipocyte phenotype. This movement may be caused by inflammation and has many negative consequences on normal function of bone marrow such as blunted white blood cell production that eventually leads to a compromised immune system (Adler, Kaushansky & Rubin 2014). In addition, a link between body adiposity and chronic diseases indicates that bone marrow haematopoiesis does not working properly in obesity (van den Berg et al. 2016).

Exercise is known to have beneficial effects on systemic health before having an effect on body composition (Adler, Kaushansky & Rubin 2014). However, BMF is known to reduce after high-impact loading exercise in female athletes (Rantalainen et al. 2013) and in young children (Casazza et al. 2012). In animal studies, exercise reduces BMF with a simultaneous increase in bone quantity in both subjects with high-fat diet-induced obesity as well as in lean controls (Styner et al. 2014). In addition, there is evidence that bone marrow phenotype is preserved in obese animals without reducing systemic adiposity (Styner et al. 2014) indicating that the protective effect of exercise on bone phenotype is caused by mechanical stimulation rather than changes in energy balance (Adler, Kaushansky & Rubin 2014). The effect of exercise or physical activity on BMF UI has not been earlier investigated.

#### **2.1.4 Bone marrow glucose uptake (GU)**

Bone marrow GU can be determined with positron emission tomography (PET), which is a non-invasive, functional imaging method to study physiologic, metabolic and malignant diseases and conditions. FDG is the most commonly radiotracer in oncologic PET-imaging and is transported in the cell via the same mechanism as glucose (Aras et al. 2014). Semi-quantitative GU in the bone marrow is usually modest (SUV < 3). However, semi-quantitative uptake values of the axial bone marrow in healthy conditions are somewhat higher than uptake of peripheral bone marrow. This may be explained by the different distribution of red hematopoietic marrow and yellow fatty marrow (Fan et al. 2007). Red hematopoietic marrow is known to have a much higher uptake value compared to yellow fatty marrow (Basu et al. 2007). In addition, uptake values of red hematopoietic marrow have been found to have a negative correlation with increasing age (Fan et al. 2007), but no differences between the male and female gender

in human studies have been found in the uptake of bone marrow (Fan et al. 2007). Axial bone marrow GU is normally lower than liver GU (Shreve, Anzai & Wahl 1999) but increases in pathological conditions such as bone marrow lymphoma (Adams et al. 2014), leukemia (Arimoto et al. 2015) and multiple myeloma (Sachpekidis et al. 2015).

#### **2.1.4.1 Obesity, exercise and bone marrow GU**

Prenatal maternal obesity increases fetal insulin resistance (Catalano et al. 2009), which increases the risk of T2DM in female offspring (Eriksson et al. 2014, Mingrone et al. 2008). The genetic background of the mother interacts with intrauterine programming, but this may be a less important factor determining health in later life than maternal obesity (Vaag et al. 2014). There were no previous studies investigating the effect of maternal obesity on bone marrow insulin-stimulated GU until the EU funded DORIAN project (Developmental ORIGins of healthy and unhealthy AgeiNg) was carried out in Turku and Helsinki during the years 2012 to 2014. The original purpose of this project was to study the long-term effect of prenatal maternal obesity on the health of the offspring (Iozzo et al. 2014). In first part of the study, Bucci et al. showed that whole-body and skeletal muscle insulin-stimulated GU is increased after resistance training regime in the offspring of obese mothers (OOM).

There are no previous studies investigating the long-term effect of exercise on bone marrow GU. Isometric muscle exercise is known to acutely increase femoral bone GU (Heinonen et al. 2013). Moreover, the effect of exercise on skeletal muscle GU has been widely investigated and outcomes in these studies have been beneficial. Reichkender et al. found that femoral skeletal muscle GU increased after 11-week aerobic exercise training in moderately obese and sedentary male subjects (Reichkender et al. 2013). They also observed a decrease in SAT GU but not in intra-abdominal visceral adipose tissue. Hällsten et al. investigated skeletal muscle GU during isometric strength training in obese and non-obese males. Their main finding was that skeletal muscle GU is blunted due to insulin resistance but muscle mass compensates for this effect (Hallsten et al. 2003). The same compensating effect of muscle has been also found in subjects with T1DM (Peltoniemi et al. 2001). Insulin-stimulated GU in skeletal muscle is known to correlate with exercise intensity (Heinonen et al. 2012).

### **2.1.5 Bone mineral density (BMD) and osteoporosis**

BMD is defined as bone mass per volume of bone (NIH Consensus Development Panel on Osteoporosis Prevention, Diagnosis, and Therapy 2001). Osteoporosis is defined as a skeletal disorder resulting from decreased bone strength, which is reported with T-score (number of standard deviations above or below the average BMD value for young healthy white women), Z-score (number of standard deviations above or below the average BMD for age and gender matched controls) or absolute BMD value ( $\text{g}/\text{cm}^2$  or  $\text{mg}/\text{cm}^3$ ). A T-score lower than -2.5 is considered a diagnostic score for osteoporosis measured with DXA from lumbar spine or hip (NIH Consensus Development Panel on Osteoporosis Prevention, Diagnosis, and Therapy 2001). The gold standard for measuring BMD is dual X-ray absorptiometry (DXA) (NIH Consensus Development Panel on Osteoporosis Prevention, Diagnosis, and Therapy 2001). Other possible applications for measuring BMD are quantitative computed tomography (QCT) (Adams 2009) and qualitative ultrasound (Casciaro et al. 2015).

A condition with decreased BMD is known as osteoporosis or osteopenia depending on the magnitude of bone loss. As BMD decreases, the risk for osteoporotic fractures increases (Kanis 1994). Osteoporotic hip fracture has a tremendous negative effect on the quality of life. Approximately 1/3 of the hip fractures in over 75-year old women lead to death, approximately 1/3 lead to permanent nursing home replacement and approximately 1/3 regain their pre-fracture function level (NIH Consensus Development Panel on Osteoporosis Prevention, Diagnosis, and Therapy 2001).

BMD declines with age and the most rapid decrease takes place right after menopause in women (Okano et al. 1998). In addition to age, female gender, estrogen deficiency, smoking, low BMI, a family history for osteoporosis, history of prior fracture, alcohol consumption, late menarche, early menopause and low endogenous estrogen levels are known risk factors for decreased BMD (Kanis et al. 2009, Sambrook, Cooper 2006). Normal handgrip strength and active exercise habits are predictors for high BMD (NIH Consensus Development Panel on Osteoporosis Prevention, Diagnosis, and Therapy 2001). As decreased BMD is the most common risk factor for osteoporotic fracture, other risk factors are also recognized. These are related to factors that increase the risk for falls (Kanis et al. 2013). The risk for osteoporotic fracture has been associated with history of falls, low physical function, low gait speed, decreased muscle strength, im-

paired cognition, impaired vision and the presence of environmental hazards such as low illumination, doorsteps and throw rugs. In addition, residents of nursing homes and other long-term facilities are at risk for fracture probably because of high rates of dementia and multiple medications (Kanis et al. 2000).

### **2.1.5.1 Exercise and BMD**

The human skeleton is a metabolically active organ, which responds to mechanical stimulus by increasing or decreasing bone modelling and remodelling (Frost, Schonau 2000). Exercise has been found to have a different effect on BMD regarding age, gender, underlying pathologic conditions, type of the exercise (e.g. low and high-impact resistance training, endurance training or whole body vibration training), site of the BMD measurement (Karlsson, Rosengren 2012) and method of the BMD measurement. In this chapter, only the effect of moderate to high-impact resistance training on BMD of hip and vertebral body in elderly women is reviewed.

The effect of resistance training on BMD in elderly women seems to vary among studies since some have found that BMD remains unchanged but other studies have found significant increases in BMD. For example, Bemben et al. found that resistance training, regardless of intensity and frequency, increases BMD of the proximal femur and spine (Bemben, Bemben 2011). On the contrary, Maddalozzo et al. did not find a significant increase in BMD in women after a 24-week high-intensity resistance training intervention (Maddalozzo, Snow 2000). However, various meta-analyses addressing this matter have concluded that physical exercise seems to have a significant positive effect on BMD at different skeleton sites (Howe et al. 2011, Martyn-St James, Carroll 2006, Zhao, Zhao & Xu 2015, Hamilton, Swan & Jamal 2010).

The precise mechanism behind the increasing effect of resistance training on BMD remains unclear. High mechanical strains may stimulate site-specific osteogenesis (Heinonen et al. 2002). This theory is supported by Marques et al. who suggested that the positive effect of exercise observed at total hip BMD may be related with the inclusion of movements, for example, hip abduction stimulating the gluteus muscles, which insert on the greater trochanter of the proximal femur (Marques et al. 2011). In addition, a positive correlation between muscle strength and bone mass has been found (Armamen-



to-Villareal et al. 2014, Huh et al. 2014). Muscle-bone interaction may result in the positive BMD outcome, which may partly be explained by the spatially heterogeneous response of bone to resistance training that targeted to different muscle groups (Lang et al. 2014). Exercise can cause microdamage in bone (Luo et al. 2014), which may serve as a strengthening mechanism for bone.

Exercise may also induce an osteogenic effect via bone mechanosensor activation. Mechanical stimuli induce bone cellular activity in osteocytes and osteoblasts, which communicate with each other through gap junctions (Donahue et al. 1995). Osteocytes are the mechanosensors in bone tissue (Clarke 2008) that coordinate the osteogenic response to mechanical loading at least in part through the expression of sclerostin (Tu et al. 2012). Sclerostin is a soluble antagonist of the Wnt/ $\beta$ -catenin signaling pathway. It is secreted by osteocytes, and it regulates osteoblast activity and differentiation. It is also a negative regulator of bone mass (Clarke, Drake 2013). However, in some studies, sclerostin has been found to positively associate with BMD especially in postmenopausal women (Polyzos et al. 2012, Modder et al. 2011, He et al. 2014).

## 2.2 In vivo imaging of bone

### 2.2.1 Magnetic resonance imaging (MRI)

MRI is the best non-invasive imaging method to study bone marrow due to its supreme soft-tissue contrast, spatial resolution and non-ionizing nature. The magnetic resonance principle is based on Larmor's equation, which states that the nucleus resonance frequency  $\nu_0$  (Hz) is proportional to the static magnetic field  $B_0$  (T).  $\gamma$  is the gyromagnetic ratio, which is specific for each nucleus. For example, at a magnetic field of 1.5T, the Larmor frequency of a proton is 63.8 MHz. according to the Larmor equation:

$$\nu_0 = \gamma / 2\pi B_0$$

To disturb the alignment of a proton located in the external magnetic field formed by MRI scanner, a burst of RF pulses is sent with the same frequency that the proton possesses. This leads to a decrease of longitudinal magnetization and an increase of the

transversal magnetization of the proton. When the RF pulse is switched off, the transversal magnetization decreases, while longitudinal magnetization increases. The spiraling motion of relaxing protons' magnetic sum vector leads to MR signal that is used in the reconstruction of the MRI image. The longitudinal relaxation is described by a time constant of  $T_1$  and the transversal relaxation time is described by a time constant of  $T_2$  that is specific to different tissues (Schild 2012).

### **2.2.1.1 $^1\text{H}$ MR Spectroscopy**

$^1\text{H}$  MR spectroscopy is a non-invasive MRI imaging application that can be used *in vivo* to identify various chemical states of certain elements. It can be used to quantify fat amount and composition of different organs, e.g., bone marrow (Yeung et al. 2005). The basic principle of MR spectroscopy is that different nuclei have a different distribution of electrons leading to slightly different magnetic fields among the measured compounds. Technically, the bone marrow frequency spectrum of fat and water peaks provide visualisation of the presence of fat and water content within the placed voxel allowing expression of marrow adiposity in relation to water content (Figure 4). Triglyceride properties, including the level of carbon chain saturation, can be investigated by assessing the ratios of fat resonances. Spectral analyses are performed on an MR system or with commercial packages (Hu, Kan 2013).

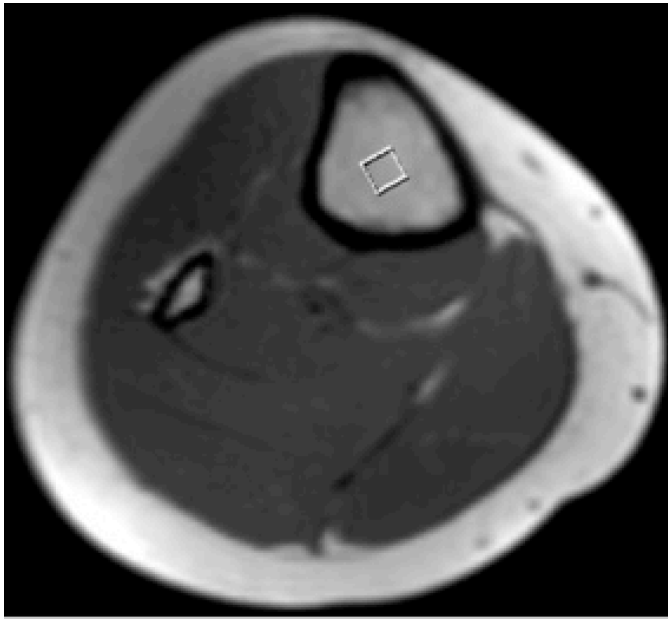


Figure 4 Axial magnetic resonance image of calf from study II. Voxel is placed on tibial bone marrow. Reprinted with permission from Study II.

MR spectroscopy is performed with different pulse sequences. The two commonly used single-voxel approaches for assessing BMF are the Stimulated Echo Acquisition Mode (STEAM) (LeBlanc et al. 1999) and Point RESolved Spectroscopy (PRESS) pulse sequences (Kugel et al. 2001, Schick et al. 1994) with or without water suppression. STEAM uses a  $90^\circ$  refocusing pulse to collect the signal in a similar way than GE sequence. Shorter TEs are achieved with STEAM at the expense of less signal-to-noise. PRESS sequence refocuses the spins with a  $180^\circ$  radiofrequency pulse in a similar way to spin echo (Hesselink 2005). In a single-voxel method, a series of slice-selective radio frequency (RF) pulses excite a volume of interest (VOI). This is subsequently followed by data acquisition of a TE domain in the absence of spatial-encoding gradients. Spectroscopy voxels are bigger in size compared to voxels in regular MRI. Voxel volumes range from 5-20 ml. This is beneficial from a signal-to-noise ratio (SNR) perspective and increases detection sensitivity of small fat concentrations. However, voxel placement requires accuracy to avoid adjacent tissues, for example, arteries and cortical bone (Hu, Kan 2013).

To report the resonance frequency of measured nucleus, the use of a ppm chemical shift scale ( $S_i$ , dimensionless parameter) is more practical than absolute frequency scale (Hz) because the value of external magnetic field  $B_0$  is not a constant. The chemical shift scale is calculated by the difference between  $\nu_i$  (frequency of nuclei) and  $\nu_{ref}$  (reference

frequency), which is divided by  $\nu_{\text{ref}}$ .  $\nu_{\text{ref}}$  is practically replaced by the spectrometer frequency.

$$S_i = 10^6 (\nu_i - \nu_{\text{ref}}) / \nu_{\text{ref}}$$

MR spectroscopy imaging results in a spectrum of signals that are placed on X- and Y-axis (Figure 5). The X-axis describes the signal position in a frequency scale (Chemical shift scale, relative in ppm) and the Y-axis represents the signal intensity, which is directly proportional to proton amount that produces the signal. The common quantitative endpoint from spectral analysis is a T2-corrected fat-signal fraction computed as the sum of the areas under all quantifiable fat peaks divided by the sum of the water and fat peak areas (Hu, Kan 2013). MR spectroscopy can measure the spectrum from all known nuclei, which are able to absorb radiofrequency energy. In biomedical imaging, it is mainly focused on protons, carbon and phosphorus (Hajek, Dezortova 2008).

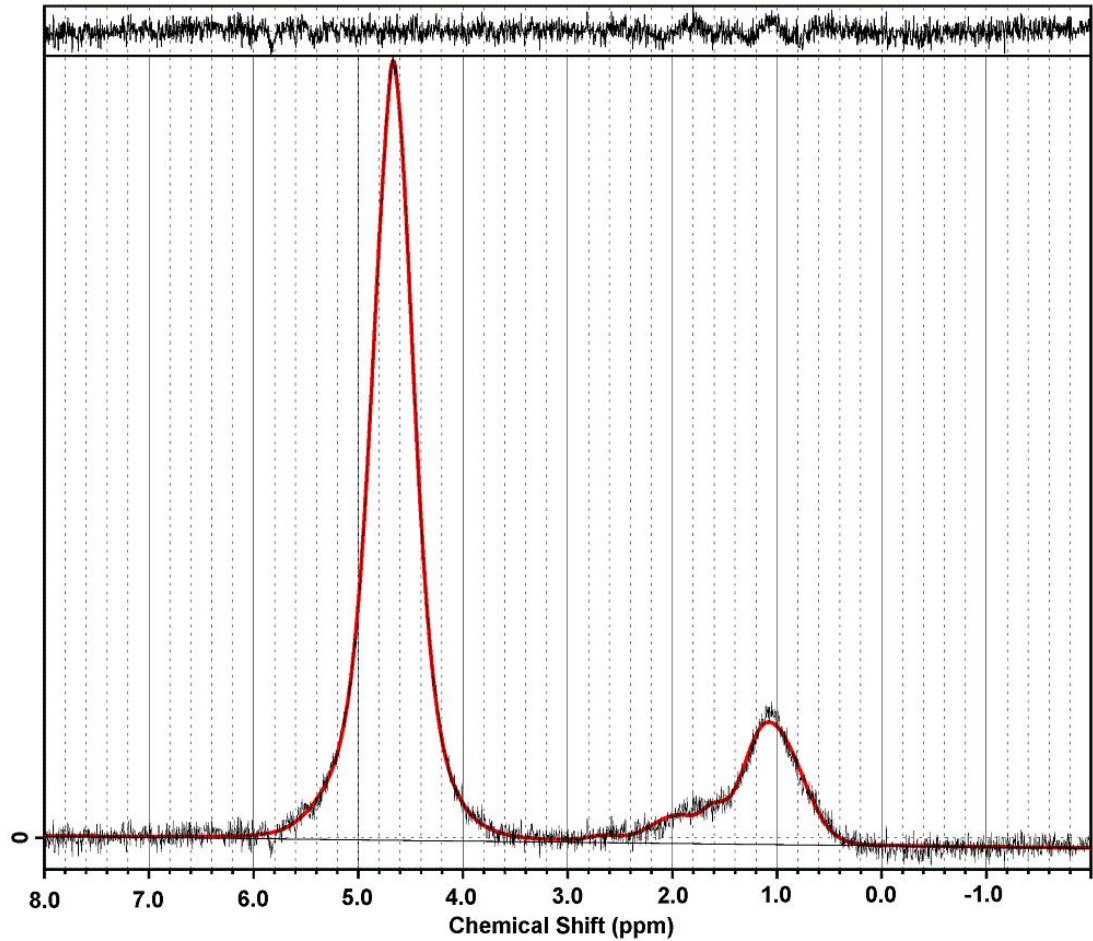


Figure 5  $^1\text{H}$  MR spectra of vertebral bone marrow from Study I. Water peak at 4.9 ppm, main lipid peak at 1.1 ppm and smaller lipid peak at 2.0 ppm. Residual is depicted on top of the image. Reprinted with permission from Study I.

*In vivo* MR spectroscopy usually uses N-acetylaspartate methyl signal (resonates at 2.02 ppm) as the reference. The best separation of the spectrum signals is achieved by highest possible magnetic field. However, homogeneity is more important than the intensity of the magnetic field. Homogeneity of the magnetic field is characterized by the half-width (full width of the half height) of the signal. In addition, SNR is another basic parameter, which characterizes the quality of the spectrum and tells how strong is signal compared to the noise.

$$\text{SNR} = 2.5 \cdot h / \text{noise}$$

SNR = signal-to-noise ratio

noise = peak to peak distance in a range around 100 points without signals

h = height of the signal

2.5 = constant

SNR is increased proportionally with the square number of the repetition of pulses sequences, which are also called acquisitions. The acquisition is the time needed for the measurement of one spectrum. SNR also increases with an increase in the size of VOI. Magnetic field homogeneity is a limiting factor, because it is more homogenous in small VOI compared to large VOI (Hajek, Dezortova 2008).

Normal bone marrow spectrum of femoral diaphysis consists mainly of lipid peaks that are composed of triglycerides stored in adipocytes. In the fat spectrum, the olefinic, i.e., double bond, proton resonance (at 5.3 ppm) is well-resolved from other fat resonances (at 2.8–0.9 ppm). An intense water resonance (at 4.7 ppm) may, however, obscure the olefinic resonance from fat hampering analysis of fat composition (Yeung et al. 2005). Lundbom et al. have recently introduced a method using long TE  $^1\text{H}$  MR spectroscopy to assess fat unsaturation in tissues with an intense water resonance (Lundbom et al. 2011). Usage of long TE suppresses the intense water resonance at 4.7 ppm resulting in a well-resolved olefinic resonance and a more accurate measurement of fat unsaturation. Recently, Troitskaia et al. also applied the long TE  $^1\text{H}$  MR spectroscopy method to determine the unsaturation of BMF (Troitskaia, Fallone & Yahya 2013). Water content is usually less than 5 % compared to lipid peaks (Machann, Stefan & Schick 2008).

The normal spectrum of VBM consists around half-half of fat and water-signals. The water signal is visible on 4.5-4.7 ppm and lipid signal is visible at 0.0-2.0 ppm (Machann, Stefan & Schick 2008). The relative water intensity is known to correlate with cellularity of the bone marrow (Ballon et al. 1991).

The fat-to-water-ratio of VBM increases with age and is lower in women subjects compared to male throughout the lifespan (Kugel et al. 2001). As stated earlier, hematopoietic bone marrow consists of hematopoietic cells that produce majority of water signal and lipid cells that partly produce the fat signal. Hematological malignancies and lymphoma cause the fat-to-water-ratio decrease, which results from the pathological fat depletion of bone marrow by malignant cells and reactive stimulation (Kugel et al.

2001). Moreover, successful treatment with chemotherapy or bone marrow transplantation leads to increasing fat-to-water -ratio, which is caused by the destruction of malignant tumour cells. In addition to bone marrow biopsy,  $^1\text{H}$  MR spectroscopy is an important tool in follow-up of the hematological malignancies (Machann, Stefan & Schick 2008). However, the invasive nature limits the possible amounts of biopsies conducted. Moreover, a diminutive target area limits its use in controlling the therapeutic effects. The fat-to-water ratio of  $^1\text{H}$  MR spectroscopy and cellular findings of the bone marrow biopsy are known to have a high correlation (Ballon et al. 1991).

### ***2.2.1.2 In-phase and out-of-phase MRI***

In-phase and out-of-phase MRI (also known as chemical shift MR or opposed-phase imaging) can show small amounts of fat in tissues and may help to separate osteoporotic fractures from a neoplastic process (Ragab et al. 2009). However, in-phase and out-phase MRI is more inaccurate in quantitation of fat compared to  $^1\text{H}$  MR spectroscopy. Potential advantages of in-phase and out-of-phase MRI compared to  $^1\text{H}$  MR spectroscopy are simpler post-processing and have shorter acquisition times (Ojanen et al. 2014). In-phase and out-of-phase imaging techniques rely on the fact that water and fat have different resonance frequencies (3.5 ppm or 222 Hz at 1.5T) (Ma 2008). When resonating is aligned, their signal is summed (in-phase). While they are out-of-phase, the magnetic moments of fat and water protons are subtracted with subsequent signal drop (Disler et al. 1997). Simple summation and subtraction of these images can yield water-only and fat-only images. Limitations of this technique include false negative results from fat containing metastases and false positive results from marrow fibrosis (Nouh, Eid 2015), sensitivity to external magnetic field inhomogeneity without proper phase correction (Ma 2008), increased scanning time leading to increased motion artefact and image blurring. A high correlation among results obtained with in-phase and out-of-phase MRI and  $^1\text{H}$  MR spectroscopy of VBM fat content has been observed in human subjects (Ojanen et al. 2014).

Water and fat-signal can be derived after leaving out phase correction for the sake of simplicity (Schild 2012):

$$SI_{\text{in-phase}} = SI_{\text{water}} + SI_{\text{fat}}$$

$$SI_{\text{out-phase}} = SI_{\text{water}} - SI_{\text{fat}}$$

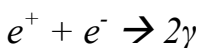
$$SI_{\text{sum}} = (SI_{\text{water}} + SI_{\text{fat}}) + (SI_{\text{water}} - SI_{\text{fat}}) = 2SI_{\text{water}}$$

$$SI_{\text{diff}} = (SI_{\text{water}} + SI_{\text{fat}}) - (SI_{\text{water}} - SI_{\text{fat}}) = 2SI_{\text{fat}}$$

SI = Signal intensity

### 2.2.2 FDG-PET imaging

A PET system detects paired gamma-radiation (high energy photons) that is emitted by  $^{18}\text{F}$  radioligand bound to tracer.  $^{18}\text{F}$  is an unstable isotope with excess amount of protons in its nucleus.  $^{18}\text{F}$  isotope is not found in nature and thus have to be produced with cyclotron. The widespread use of  $^{18}\text{F}$  isotope is based on its relatively long half-life (109 min) allowing long imaging protocols e.g., whole-body and production of the isotope in different facility than the actual PET-imaging takes place. The isotope undergoing positron decay emits a positron that travels in the tissue only few millimeters until it is annihilated with a nearby electron after losing all its kinetic energy. In annihilation, positrons and electrons are converted into two 511 keV photons travelling in opposite directions (equations). The PET system detects these photons in a certain period of time (frames) and are reconstructed into an image as spatial distribution of coincide annihilation events. Thus, the observed PET-image reconstruction reflects the spatial distribution of tracer radioactivity concentration over time. The spatial resolution of PET technique is limited and due to this limitation PET cameras are usually paired with CT or MRI to achieve excellent spatial resolution in combination with functional data of the tissue (Rudroff, Kindred & Kalliokoski 2015). The formula for positron decay:



A = mass number

Z = proton number

N = neutron number

$e^+$  = positron

$e^-$  = electron



$\gamma$  = high energy photon

$\nu$  = neutrino

FDG is the most used radiotracer to measure tissue-specific GU in physiological conditions (Rudroff, Kindred & Kalliokoski 2015). In dynamic FDG-PET imaging, tracer kinetics in the tissue over time is imaged. After administration of FDG tracer, it eventually accumulates in the tissue cells. The tracer is transported through the cell membrane in a similar way than glucose. After transportation, FDG is phosphorylated preventing its re-transportation back into bloodstream. However, modeling is needed to convert the acquired PET data into a meaningful graphical interpretation. Gjedde–Patlak graphical analysis (Patlak, Blasberg 1985) can be used to quantitate the tracer influx rate  $K_i$ , which reflects the fractional rate of tracer phosphorylation in the target tissue.

$$K_i = (k_1 \cdot k_3/k_2 + k_3)$$

$k_1$  = transfer coefficient from vascular space into tissue

$k_2$  = initial clearance and efflux coefficient

$k_3$  = phosphorylation rate constant

The Gjedde-Patlak graphical analysis assumes that the dephosphorylation rate  $K_4$  is zero, and the tracer is irreversibly trapped in the cell (Dhawan et al. 1989). The steady state of the tracer (FDG concentrations between compartments are in equilibrium) is achieved at certain time point after the tracer administration. Tracer plasma activity is high a certain time after the intravenous tracer administration and gradually decreases while tracer is transported into the target tissue. Data of arterialised plasma and regional time-activity curves (TAC) are plotted as a function of the normalized integral of plasma FDG levels, and this function becomes linear after the steady state has been achieved.

$$C_t(t)/P(t) = K_i \left[ \int_0^t P(t) dt \right] / P(t) + V_B$$

$C_t(t)$  = tissue radioactivity level at timepoint  $t$

$P(t)$  = plasma radioactivity level at timepoint  $t$

$K_i$  = influx rate of tracer

$V_B$  = initial distribution of tracer volume in the tissue

In steady state equation above can be expressed as a straight line

$$y = K_i x + V_B$$

Thus, the slope of the fit data  $K_i$  represents the transfer rate of FDG from plasma into tissue (Figure 6), and  $V_B$  is the intercept of the fit line. To obtain rates of bone marrow GU ( $\mu\text{mol/L} \cdot \text{min}$ ), the transfer rate  $K_i$  of FDG is multiplied with plasma glucose levels and divided by the lumped constant (LC), which accounts for differences in the transport and phosphorylation of FDG and glucose (Phelps et al. 1979). LC is assumed to be 1.0 for bone marrow and is known to be 1.2 for skeletal muscle and 1.14 for adipose tissue (Peltoniemi et al. 2000). The formula to calculate GU:

$$\text{GU} = (K_i \cdot [\text{Glc}]_p) / \text{LC}$$

$K_i$  = influx rate of tracer

$[\text{Glc}]_p$  = plasma glucose concentration

LC = lumped constant

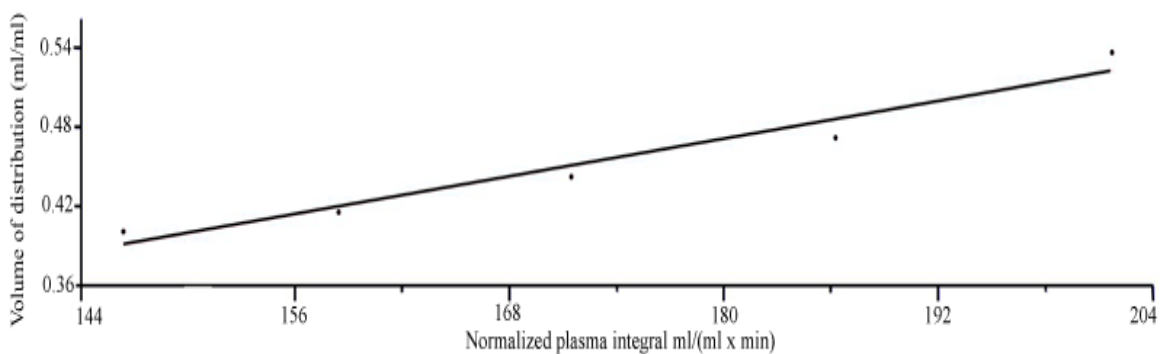


Figure 6 Slope of the linear phase of femoral bone marrow from Study III. The influx rate  $K_i$ , depicts the amount of accumulated tracer in bone marrow in relation to tracer amount in plasma. In this case, the goodness of fit was  $r = 0.99$ . It expresses a line fit to measured points.

This thesis focuses mainly on femoral (peripheral) and vertebral (axial) bone marrow dynamic FDG-PET-imaging under hyperinsulinemic euglycemic clamp technique to standardize the insulin action and to quantify tissue-specific GU in relation to whole-body GU. The basic physiological assumption is that diaphysis of FBM is composed mainly of fat as previously stated. It is also assumed that VBM is composed of varying ratios of hematopoietic and fat content that varies by gender and age as previously stated. There are few previous studies, excluding malignant or pathological conditions, focusing on dynamic FDG-PET imaging of bone marrow or BMF under insulin-stimulated conditions. Dynamic FDG-PET is by far the only imaging method combined with hyperinsulinemic euglycemic clamp that can quantify site-specific GU of insulin sensitivity (DeFronzo, Tobin & Andres 1979).

In clinical cases, the relative tracer uptake is usually of interest, e.g., in cancer diagnosis, static FDG-PET imaging can be used. It offers information on spatial distribution of administered tracer. FDG-tracer activity in the tissue is measured semi-quantitatively by drawing a region of interest (ROI) or volume of interest (VOI). The results are represented as standardized maximal uptake values ( $SUV_{max}$ ) that is standardized PET quantifier. The SUV is calculated by the tissue's maximal radioactivity concentration (kBq/mL) at time T ( $C_T$ ) divided by injected tracer radioactivity dose in MBq that is divided by the subject weight in kilograms.

### **2.2.3 Quantitative computed tomography (QCT)**

The gold standard technique in clinical use for assessing BMD is DXA (NIH Consensus Development Panel on Osteoporosis Prevention, Diagnosis, and Therapy 2001). QCT is a CT imaging application technique to assess volumetric trabecular BMD of the spine with a calibration phantom to convert Hounsfield units (HU) into BMD values (Adams 2009). As simplified principle, CT image is based on the linear X-ray absorption in target tissues. Bone tissue possesses a high atomic number, and thus, absorbs X-rays very efficiently. This results in bone appearing densely white on the image leading to having a higher HU number. To transform HU into BMD unit ( $g/cm^2$  or  $mg/cm^3$ ), a bone mineral calibration phantom is required in the field of view (Adams 2009). Calibration phantoms contain different concentrations of material that is composed of solid material such as hydroxyapatite. Conversion of HU into BMD is calculated from the regression

of attenuation and concentration of the calibration phantom (Adams 2009). The same calibration phantom must be used in longitudinal study scanings to achieve reliable results and good reproducibility (Engelke et al. 2008)

Limitations of QCT include the fact that the WHO has defined osteoporosis as a T-score lower than -2.5 measured with DXA (Lewiecki et al. 2008), which means that formal diagnosis of osteoporosis cannot be made with QCT. However, the American College of Radiology has published guidelines for the performance of QCT in 2008. Due to these guidelines, trabecular BMD values from 80 - 120 mg/cm<sup>3</sup> are defined as osteopenic, and BMD values lower than 80 mg/cm<sup>3</sup> are defined as osteoporotic (Felsenberg, Gowin 1999, American College of Radiology 2008). In addition, radiation doses are higher when scanning central sites compared with DXA (3D QCT of spine L1-L2 ~1.5 mSv with voltage of 120 kV, current 100 mAs *versus* DXA of spine ~ 0.013 mSv *versus* annual background radiation ~2.7 mSv) (Damilakis et al. 2010).

CTXA (Computed Tomography X-Ray Absorptiometry) of the hip is a commercial extension of the classical DXA measurement using QCT. CTXA of the hip utilizes 3D volumetric projections to generate hip images that look similar generated by DXA. While DXA rely on dual-energy X-ray method, CTXA of the hip rely on the 3D anatomical image (Figure 7) combined with the separation of soft tissue from surrounding bone. Both the CTXA and DXA of the hip provide the same information, which is reported as total bone mass per projected area. In addition, excellent correlations between the results of CTXA of the hip and DXA of the hip have been observed (Cann et al. 2014, Khoo et al. 2009). Precision error of total hip CTXA measurement have been reported to be approximately 2 % and interobserved error approximately 1 % (Cann et al. 2014).

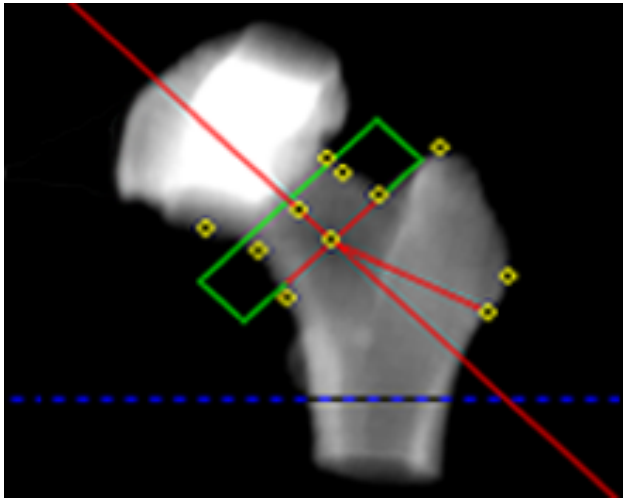


Figure 7 Image of 3D rendered proximal femur with QCT Pro software with femoral neck region of interest. Reprinted with permission from Study IV.

### **3 AIMS OF THE STUDY**

- I To study the differences in vertebral bone marrow glucose uptake and bone marrow fat amount between diabetic and healthy control experimental animals and, in addition, whether vertebral bone marrow glucose uptake is associated with vertebral bone marrow adiposity (I)
  
- II To study whether current or early-onset obesity decreases bone marrow fat unsaturation in adolescent male and female subjects (II)
  
- III To investigate the role of prenatal maternal obesity in bone marrow insulin-stimulated glucose uptake and to investigate whether 16-week resistance training increases bone marrow insulin-stimulated glucose uptake in elderly female offspring of lean/normal-weight mothers and offspring of obese/overweight mothers (III)
  
- IV To test the effect of 16-week resistance training and accompanying one-year follow-up on total hip bone mineral density and serum sclerostin in elderly female subjects with decreased muscle strength (IV)

## 4 MATERIALS AND METHODS

Summary of the materials and methods is depicted in Table 1.

Table 1 Summary of study designs, subjects, imaging methods and outcome variables of the original studies. OLM: offspring of lean/normal-weight mothers. OOM: offspring of obese/overweight mothers. VBM: vertebral bone marrow. FBM: femoral bone marrow. GU: glucose uptake. vBMF: vertebral bone marrow fat. tBMF: tibial bone marrow fat.

Study	Study design	Subjects	Age	Imaging	Outcome variable
I	Prospective cohort	n=10 male pigs (5 overweight diabetic, 5 normal-weight control)	7-9 months	PET, MRI	VBM GU, vBMF
II	Prospective cohort	n=35 subjects (18 normal-weight of which 2 male, 16 female and 17 overweight of which 9 male, 8 female)	15-27 years	MRI	tBMF UI
III	Non-randomized clinical trial	n=46 women (20 frail OLM, 17 frail OOM, 9 non-frail OLM)	68-78 years	PET, MRI	VBM and FBM GU, vBMF
IV	Non-randomized clinical trial	n=48 women (37 frail, 11 non-frail controls)	68-78 years	QCT	Total hip BMD

### 4.1 Study designs

In Study I (prospective cohort study), the difference in VBM GU and BMF content was assessed between diabetic and control groups. In addition, the association between VBM GU and BMF was tested in pooled population. VBM GU was measured with FDG-PET imaging, and BMF was assessed with  $^1\text{H}$  MR spectroscopy with in-phase and out-of-phase MRI and with biochemical TAG-analysis in 10 pigs.

In Study II (prospective cohort study), the effect of current and early-onset obesity (before age of 7 years) on BMF UI of tibial diaphysis was studied with  $^1\text{H}$  MR spectroscopy in 35 adolescent subjects with varying BMI.

The design of Study III is depicted in Figure 8. In Study III (interventional non-randomized single blind study design), we investigated the role of maternal obesity in bone marrow GU. In addition, we studied the effect of 16-week resistance training intervention on bone marrow GU with FDG-PET in 37 frail elderly female offspring with a known history of prenatal maternal obesity status. 9 non-frail age-and sex-matched controls were studied at baseline.

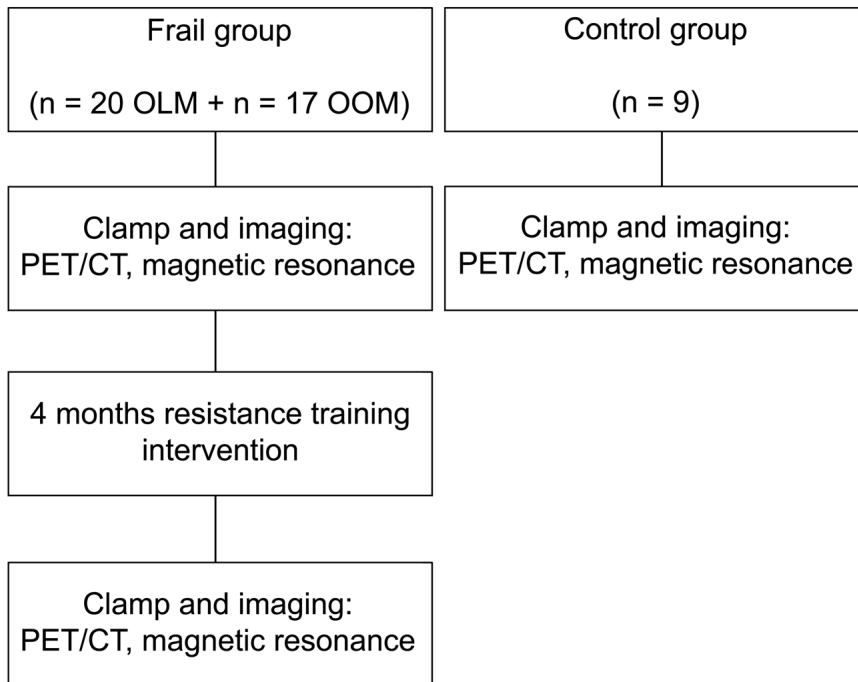


Figure 8 Study design of Study III. Reprinted with permission from Study III.

The study design of Study IV is depicted in Figure 9. In Study IV (interventional non-randomized single blind study design with a follow-up), the effect of 16-week resistance training intervention on BMD and on serum sclerostin in 37 frail elderly female was assessed. 11 non-frail age- and sex-matched controls were studied at baseline. A subset of 25 subjects (19 intervention, 6 controls) was studied one year after the end of the intervention. Reprinted with permission from Study III.



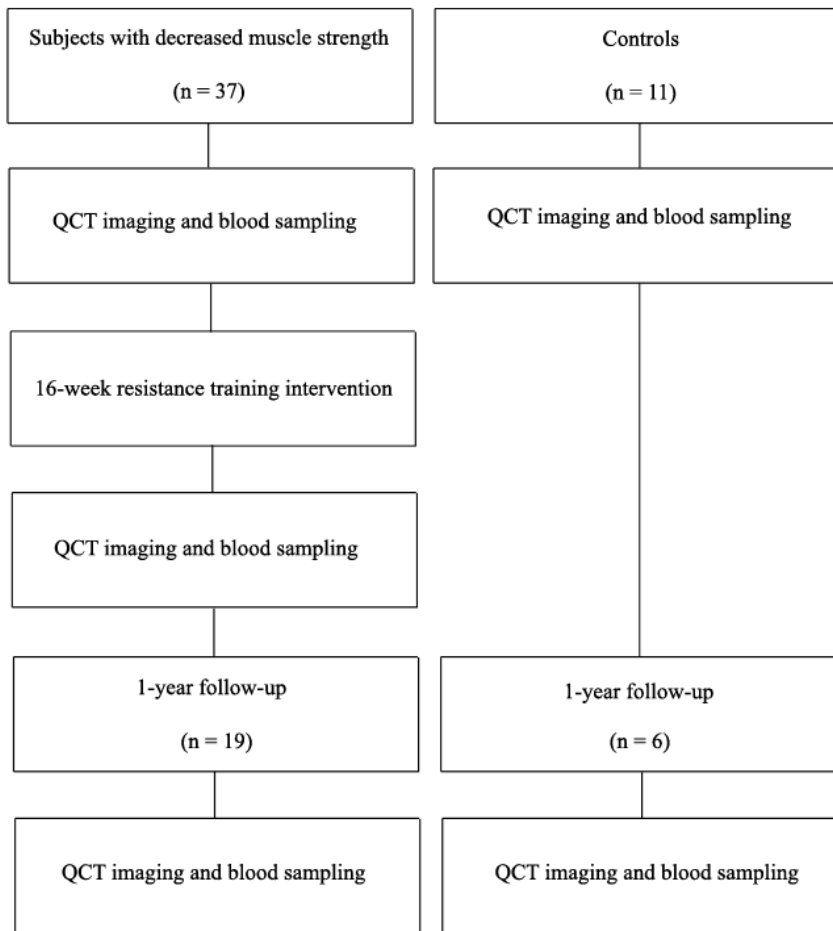


Figure 9 Study design of Study IV. All the subjects who were not prescribed an anti-osteoporotic treatment other than calcium or vitamin D after the intervention (32 from intervention group and 11 controls) were invited to a follow-up visit. Altogether 19 intervention and 6 control subjects participated this visit. Reprinted with permission from Study IV.

In Studies III and IV, after the first study visit, the frail/interventional subjects underwent an individualized four-month resistance training intervention three times a week, 60 minutes per session under supervision of a trained, licensed physiotherapist for four months. Resistance training sessions started with a 10-minute warm-up using a cycle or elliptical ergometer. It proceeded with eight different resistance exercises targeting large muscle groups of the lower and upper body (leg presses, chest presses, seated rows, abdominal crunches, back extensions, seated leg extensions, seated leg curls and hip abductions). Subjects completed three sets of 8–15 repetitions at each station with a load that corresponded to 50–80 % of estimated 1 repetition maximum (RM). Progress in muscle strength was measured monthly, and the loads for the following month were adjusted as appropriate. Adherence (actualized individual exercise frequency per week

divided by maximum exercise amount per week) of the pooled population to exercise was  $78.6 \pm 10.8$  %.

## **4.2 Study subjects**

In Study I, altogether ten 7-9 old month pigs were included either in obese diabetic or control group based on their demographic profile. Animals were raised in animal facility of Biocity, Turku. Originally, diabetes had been induced to the diabetic group with 3-day lasting administration of streptozotocin (dosage 50 mg/kg per day, Zanosar, Pharmacia & Upjohn, MI, USA) at the age of 12 weeks. The diabetic group had also been fed with high fat diet for 6 months (basic fodder supplemented with 1.5 % cholesterol, 15 % lard, 1.5 % sodium cholate, Pekoni 90, Suomen Rehu/Hankkija–Maatalous Oy, Hyvinkää, Finland). The control group had been fed with basic fodder without any supplementation (Pekoni 90, Suomen Rehu/Hankkija–Maatalous Oy, Hyvinkää, Finland).

In Study II, a random sub-group of altogether 35 subjects (18 normal-weight of which 2 male, 16 female with current BMI  $< 25$  kg/m<sup>2</sup> and 17 overweight of which 9 male, 8 female with current BMI  $> 25$  kg/m<sup>2</sup>) were included in the study from 68 (18.6 %) eligible study subjects consented from Children's hospital patient registry during 2011-2013 including altogether 366 patients fulfilling the inclusion criteria. Inclusion criteria for the overweight subjects were: 1) weight-for-height ratio exceeding 60 % before age 7 years, according to Finnish growth standards; 2) referral due to severe obesity to Children's Hospital, Helsinki University Central Hospital, during childhood; 3) at the age of 7 years living in the capital region of Helsinki and 4) aged between 15 and 27 years at the time of the study. For each overweight subject, an age- and sex matched normal-weight control was selected from the population register. Sampling of controls was limited to the capital region of Helsinki. Exclusion criteria for the controls were obesity (weight-for-height ratio above 40 %) before the age of 10 years. In Study II, we also performed a second analysis by grouping the subjects based on their BMI by the age of 7 years: 13 subjects developed severe obesity before age 7 years, while 22 were non-obese at age 7 and were regarded as controls.

In Studies III and IV, study subjects were recruited from Helsinki Birth Cohort Study II (HBCS II), which included 13345 subjects born during 1934 to 1944. The HBCS cohort

is a longitudinal study cohort with information of prenatal life through medical records of birth and child welfare clinics, and in addition, throughout the life span including for example, characteristic, metabolic and exercise data. The eligible study subjects were selected from a sub-cohort of 2003 subjects that had been thoroughly clinically characterized throughout the years. Exclusion criteria for studies III and IV included diabetes requiring insulin treatment or measured plasma fasting glucose over 7 mmol/l measured at the last visit before enrolment. Individuals currently smoking and those with comorbidities influencing insulin sensitivity and contraindications for participating in an exercise intervention (i.e., chronic atrial fibrillation and pacemaker) or an MRI study were also excluded.

In Study III, altogether 46 study subjects aged 68-78 years (20 frail offspring of lean/normal-weight mothers (OLM), 17 frail offspring of obese/overweight mother (OOM), 9 OLM non-frail controls) were included in the study. Frailty is a syndrome that can be characterized by e.g. muscle weakness, exhaustion, unintentional weight-loss and low physical activity (Abbatecola, Paolisso 2008) but our definition of frailty was not multi-factorial and was based only on handgrip strength (Syddall et al. 2003). Frail OLM and OOM subjects belonged to the lower half of handgrip strength values and control OLM subjects belonged to the upper half of handgrip strength values, as measured from all HBCS participants in 2001–04. OLM had prenatal maternal BMI  $\leq 26.3 \text{ kg/m}^2$  (lowest two quartiles of the entire population), and OOM had a prenatal maternal BMI  $\geq 28.1 \text{ kg/m}^2$  (highest quartile of the entire population). BMI of the participant's mothers was measured prior to delivery. The BMI was calculated as weight (kg) divided by height squared ( $\text{m}^2$ ).

In Study IV, altogether 48 study subjects (37 subjects with decreased handgrip strength, 11 controls with normal handgrip strength) were included in the study. Inclusion criteria for the subjects with decreased handgrip strength were a handgrip strength value below the median value of all HBCS participants assessed between 2001 and 2004, age between 68-78 years, female gender and none of the exclusion criteria present. Inclusion criteria for the control subjects were handgrip strength values above the median value of all HBCS participants assessed between 2001 and 2004, age between 68-78 years, female gender and none of the exclusion criteria present.

### 4.3 MRI methods

In Study I, a block of two to three adjacent thoracic vertebral bodies was extracted from the pigs. The MRI of the vertebral blocks was done using a 1.5-T MRI scanner (Gyrosan Intera CV Nova Dual, Philips Medical Systems, The Netherlands). Single voxel  $^1\text{H}$  MR spectroscopic studies of the vertebrae of the pigs were obtained using the time of repetition (TR) of 5000 ms, time of echo (TE) of 25 ms. Voxel size was 13 mm x 15 mm x 18 mm. The voxel was placed in the middle of the vertebral body avoiding hard cortical bone. The lipid ratio (peaks at 0.9 ppm, 1.3 ppm and 1.6 ppm) to water was measured. Spectra analysis was performed with LCModel (version 6.2–1 L) (Provencher 1993). The in-phase and out-of-phase MRI was performed in VBM at the spectroscopy using the same scanner in sagittal plane of the vertebrae of the pigs using the image parameters of TR of 120 ms, TE of 2.3 and 4.6 ms and slice thickness of 8 mm.

Signal intensity (SI) was measured at a standard workstation (AW 3.1; GEMedical Systems). ROI had a shape of a rectangle, and they were drawn manually in the middle of two to three adjacent VBM cavity excluding the cortex. Average SI was calculated from the two to three separate SI of ROIs. Signal intensity index was calculated with the formula:

$$(\text{SI}_{\text{in}} - \text{SI}_{\text{out}}) / \text{SI}_{\text{in}} \text{ (Borra et al. 2009)}$$

$\text{SI}_{\text{in}}$  = signal intensity measured with in-phase-image

$\text{SI}_{\text{out}}$  = signal intensity measured with out-phase-image

In Study II, the MRI experiment was performed on a 3.0T clinical imager (Siemens, Verio, Erlangen, Germany). In the supine position, the right calf was positioned and fixed in an 8-channel knee coil. Localizers were obtained in three planes and a stack of 32 transaxial T1-weighted images (FOV 280 x 280 mm<sup>2</sup>; matrix 256 x 256; TE = 2.31 ms; TR 240 ms; FA 70°; slice thickness 3 mm; slice gap 3.45 mm) were collected in the proximal tibial diaphysis covering the leg from the tibial tubercle 20 cm distally. A 7 mm x 7 mm x 20 mm voxel was placed in the bone marrow of the proximal tibia and PRESS localization was used to collect long TE spectra with TR and TE of 4000 and 200 ms, respectively.

The spectra were analyzed with jMRUI v3.0 software using AMARES algorithm (Vanhamme, van den Boogaart & Van Huffel 1997). Intensities of methylene (CH<sub>2</sub>), methyl (CH<sub>3</sub>) and olefinic (CH = CH) resonances were determined as previously described (Lundbom et al. 2010). The unsaturation index (UI) was calculated as the percentage of the olefinic resonance intensity to total fat resonance intensity.

$$UI = 100 \cdot I_{\text{olefinic}} / (I_{\text{olefinic}} + I_{\text{methylene}} + I_{\text{methyl}})$$

UI = unsaturation index

I = resonance intensity

In Study III, <sup>1</sup>H MR spectroscopy was performed on the bone marrow of the 10<sup>th</sup> thoracic vertebral body. Typical acquisition parameters for the PRESS sequence were: TR/TE 5000/25 ms, bandwidth 1 kHz, number of data points 2048, number of acquisitions 32, voxel size 15 mm x 18 mm x 15 mm. A single element of Sense Body coil was used for the signal reception. LCModel (version 6.3-0C, protocol “lipid-4” for lipid quantification) (Provencher 1993) was used for the analysis of the spectra. Triglyceride signals from around 0.9 to around 2.0 ppm were considered as the “fat” signal because the water signal overlapped the resonances around 5.3 ppm. Both fat and water resonance areas were corrected for the T<sub>2</sub> relaxation effect using the T<sub>2</sub> times (75.4 ms for fat and 26.9 ms for water) measured by Kugel et al. (Kugel et al. 2001). T<sub>1</sub> effects were considered to be negligible because of the long duration of the repetition. T<sub>2</sub> corrections were performed using the equation  $SI = SI_0^{-TE/T_2}$  where SI is the corrected and SI<sub>0</sub> the uncorrected resonance area. The fat-fraction (Reeder, Hu & Sirlin 2012) was calculated by dividing the T<sub>2</sub> corrected resonance area of fat by the sum of T<sub>2</sub> corrected areas of water and fat.

#### 4.4 PET methods

In Study I, animals were studied under the fasting state. Pigs were anesthetized with 1.0 g ketamine into the neck muscles before moving the pigs into the operating room. They were kept anesthetized with ketamine and pancuronium (total of 1.5 g and 40 mg) and mechanically ventilated via tracheal intubation with oxygen and normal room air during

the imaging. After the induction of anesthesia, peripheral catheters were placed in both ears and arterial catheter was placed in the right carotid artery. Saline was infused through the venous catheters and FDG-tracer ( $890 \pm 180$  MBq) was injected at the zero time point. 70 minutes after the injection of the tracer, the dynamic PET imaging of the upper abdomen (field of view included upper and lower thoracic vertebrae) was performed lasting for 20 minutes with PET-scanner (hybrid PET/CT scanner Discovery VCT; General Electric, Milwaukee, WI, USA). Blood samples were drawn on a regular basis during the imaging in order to measure FDG-tracer concentration in circulation.

The PET study design for Study III is depicted in Figure 10. Abdominal and thigh PET-imaging was conducted with FDG after an overnight fasting state during hyperinsulinemic euglycemic clamp with a GE Advance PET-CT scanner (Discovery 690, General Electric (GE) Medical systems, Milwaukee, WI, USA). For Studies I and III, FDG was synthesized with a computer-controlled apparatus in accordance with a modified method described by Hamacher et al (Hamacher, Coenen & Stocklin 1986). After 90 minutes of hyperinsulinemia, an FDG bolus ( $188 \pm 10$  MBq) was injected through the cannula on the left antecubital vein. Forty minutes after the injection, the upper abdomen and lumbar spine were imaged for 15 minutes and 55 minutes after the injection thigh area and diaphysis of the femoral bone were imaged for 15 minutes (frames, 5 x 180 seconds). Hyperinsulinemic euglycemic clamp (1 mU/kg x min, Actrapid; Novo Nordisk) was performed as previously described (Nuutila et al. 1992), and the whole-body GU (M-value) representing systemic insulin sensitivity was calculated from the glucose infusion rates during 60–120 minutes of the clamp.

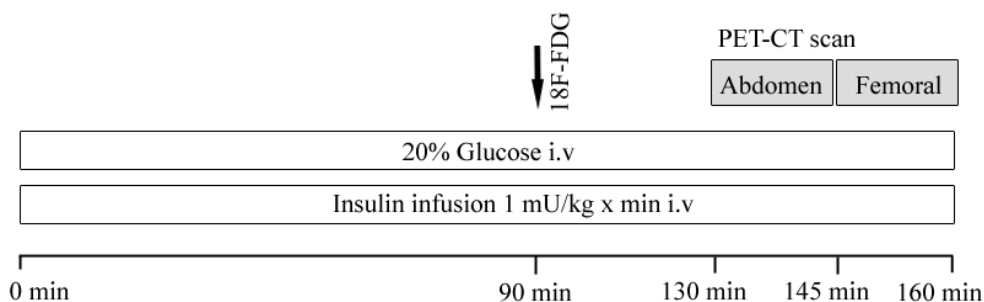


Figure 10 PET study design for Study III.

In Studies I and III, PET image data was corrected for tissue attenuation, dead time and time decay. Reconstruction was made using standard algorithms in a 256 x 256 matrix.

PET image analysis was carried out with Carimas 2.6 (study I) and Carimas 2.7 (study III) software (Turku PET Centre, University of Turku, Turku, Finland). First, in Study I, to obtain time activity curves (TACs), volumes of interests (VOIs) shaped as cylinders were manually drawn into the marrow cavity of the two to three adjacent vertebral bodies excluding the cortex. In Study III, VOIs were drawn on the diaphysis of the right FBM and on the VBM (L1-L2), excluding the cortex (Figure 11), on the psoas major muscle and on SAT of the hip. Second, the transfer rate of FDG from plasma into VOIs was calculated from TACs using Gjedde-Patlak graphical analysis (Patlak, Blasberg 1985). Third, data of TACs was plotted as a function of the normalized integral of plasma FDG levels, and the function became linear after the steady state (plasma FDG levels entering the tissue are constant). Last, to obtain rates of bone marrow GU ( $\mu\text{mol/L} \cdot \text{min}$ ), the transfer rate of FDG was multiplied with plasma glucose levels divided by the LC that was set to 1.0 for bone marrow, 1.2 for skeletal muscle and 1.14 for SAT.

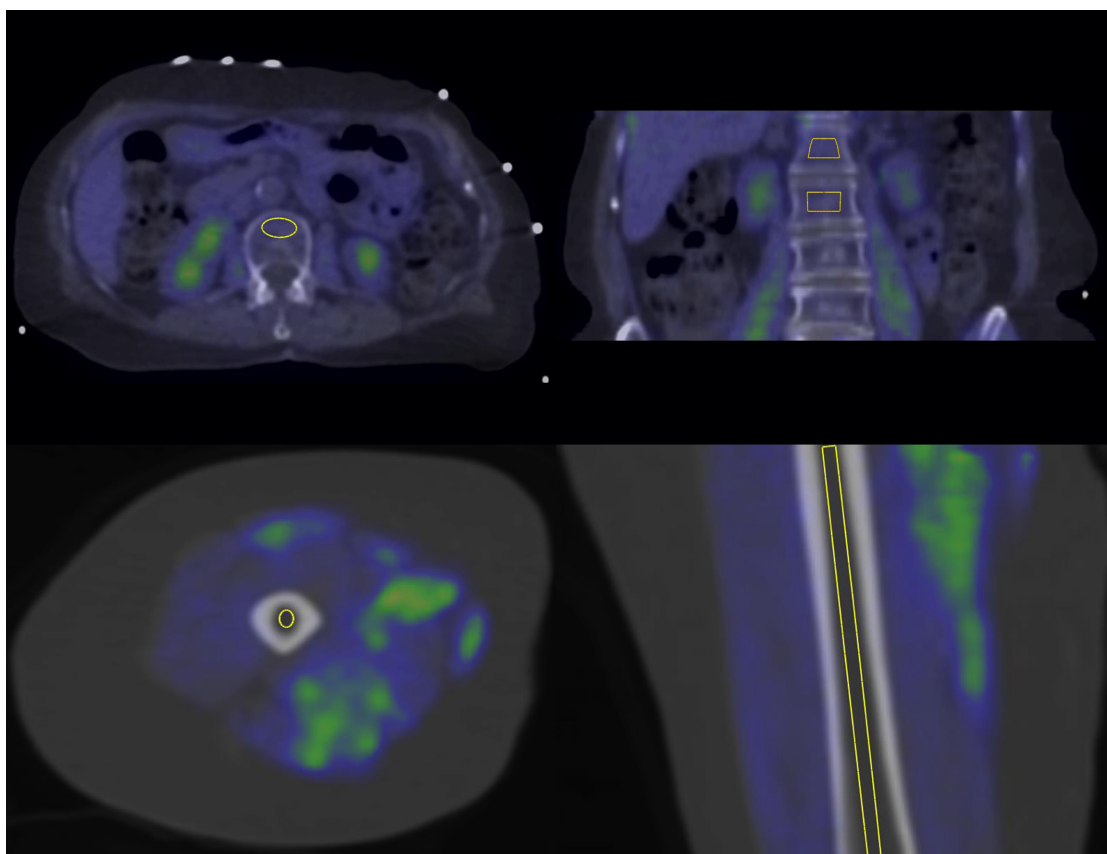


Figure 11 Volumes of interest drawn on vertebral bone marrow (upper row) and femoral bone marrow (lower row) in PET-CT images. Reprinted with permission from Study III.

## 4.5 QCT and CT methods

Hip CTXA from proximal femur in  $\text{g}/\text{cm}^2$  was assessed using QCT (Discovery 690, General Electric (GE) Medical systems, Milwaukee, WI, USA) with a resolution of 3.75 mm. A region located between the superior level of the femoral head and inferior level of the lesser trochanter was imaged while the patient was in a supine position on the CT table. The CT values were converted to a BMD-scale using a solid calibration phantom (Mindways) that was placed under the subject during the imaging. All imaging was done at SFOV 500 mm, pitch 1.375, 120 kV and 79 mAs. Images were transferred to a QCT workstation and analyzed using the CTXA hip function version 4.2.3 of Mindways QCT pro software (Mindways Software Inc., Austin, TX, USA). First, isolation and rotation of the hip were performed with a default threshold value of  $100 \text{ mg}/\text{cm}^3$  to isolate bone from soft tissue. The femoral neck axis was identified automatically with an algorithm in the QCT software. A rectangular-shaped femoral neck ROI with a thickness of 15 mm was used, and it was set in the femoral column resting on top of the trochanters excluding the femoral head (Figure 7). The distal extent line was set to the level of lesser trochanter. QCT Pro software assessed the trochanteric and intertrochanteric BMD automatically.

For obtaining muscle masses, thigh CT images were semi-automatically co-registered to the whole-body MRI images and then measures were taken to select a 1.5 cm thick section (1.6 cm mask in the imaging software) that was 5 cm distant (perpendicularly) from the pubic region (with right and left inguinal lines showed in coronal view). It followed the manual segmentation of the different muscle groups by drawing ROIs in the 5-6 selected slices in the Carimas 2.7 software. The selected compartments were quadriceps, adductor magnus, hamstring and adductor longus muscles. After drawing the ROIs surrounding the muscle groups, the muscle tissue volume on the CT image was segmented via Hounsfield Unit (HU) thresholding. A threshold of 0 to 100 HU was used. The different muscle group volumes were converted into masses using the skeletal muscle density ( $1.04 \text{ g}/\text{cm}^3$ ).



## 4.6 Biochemical and clinical methods

In Study I, the vertebral bone was crushed by pressure after dipping it into liquid nitrogen. The lipids were extracted from the crashed bone with chloroform:methanol (2:1 v/v) (Folch, Lees & Sloane Stanley 1957). Triplicate, consequent extractions were performed to ensure complete extraction from the porous material. Triacylglycerols (TAGs) were isolated from the extracted lipids with prepacked Silica-columns (Hamilton, Comai 1988). Fatty acid methyl esters were prepared from the isolated TAGs by the boron trifluoride method (Agren, Julkunen & Penttila 1992) and analyzed with gas chromatography (Shimadzu GC-2010 equipped with AOC-20i auto injector, flame ionization detector (Shimadzu corporation, Kyoto, Japan) and a wall-coated open-tubular column DB-23 (60 m x 0.2 mm i.d., liquid film 0.25  $\mu\text{m}$  (Agilent technologies, J.W. Scientific, Santa Clara, CA, USA)). Splitless/split injection was used and the split was opened after 1 min. Triheptadecanoin and trionadecanoin (Larodan AB, Malmö, Sweden) were used as internal standards. The TAG content in the samples was calculated by comparing the area of the internal standard to the total area of the sample peaks. The fatty acids were identified by comparing their retention times with those in external standards: Supelco 37 Component FAME Mix (Supelco, St. Louis, MO, USA) and 68D (Nu-Check-Prep, Elysian, MN, USA).

In Study II, anthropometry including height, weight, and waist and hip circumferences was collected during the study visit. Weight was measured with a Seca digital scale ([www.seca.com](http://www.seca.com)). Height was measured with a fast stadiometer connected to the scale. Waist circumference was measured with non-stretch narrow tape at between the ribs and the iliac crest. Hip circumference was measured at the level of the greater trochanters. Fasting blood samples were collected for glucose, insulin and HbA1c. Plasma fasting glucose was analyzed by a spectrophotometric hexokinase and a glucose-6-phosphate dehydrogenase assay (Gluko-quant glucose/hexokinase; Roche Diagnostics). Serum fasting insulin was measured with a time-resolved immunofluorometric assay (PerkinElmer Life Sciences). HOMA2-IR was calculated with the HOMA2 calculator (<https://www.dtu.ox.ac.uk/homacalculator>). Body composition was determined with dual-energy X-ray absorptiometry (DXA) (Lunar Prodigy, GE Medical Systems, Madison, WI). Basal metabolic rate was calculated by the Harris-Benedict equation (Japur et al. 2009).

History of the Study II subjects' physical activity was collected 12 months retrospectively. The questionnaire consisted of supervised and unsupervised physical activity in leisure time and physical activity during school attendance. Total physical activity expressed as minutes per day was used. The subjects filled in the questionnaire before the study visit and reviewed it with one of the researchers during the study visit. Subjects used a pedometer (Omron Walking Style III, OMN, The Netherlands) for seven days. Height, weight and step length were assessed and set to the pedometer prior to the study period. Number of steps, travelled distance and energy expenditure were recorded.

In Studies III and IV, clinical examination included sitting blood pressure from the left arm (Omron M3 HEM-7200-E2, OMN, The Netherlands) and measurements of waist and hip circumference between the ribs and the iliac crest and at the level of greater trochanters. In addition, weight, height and total body fat percentage were measured (Omron HBF-400-E, OMN, The Netherlands) and fasting serum insulin (automatized electro-chemiluminescence immunoassay, ECLIA; Cobas 8000, Roche Diagnostics GmbH, Mannheim, Germany) and fasting plasma glucose (glucose oxidase method, Analox GM9 Analyzer, Analox Instruments Ltd. London, U.K) were assessed.

In Study IV, fasting serum samples drawn in the morning were collected at baseline and after the 16-week intervention. The third sample was collected at follow-up visit. Serum samples were stored as aliquots at  $-80^{\circ}\text{C}$ . All samples were measured as duplicates and simultaneously at the end of the study. Serum sclerostin was measured with Sclerostin ELISA from Biomedica (Vienna, Austria) per manufacturer's instructions.

#### **4.7 Statistical methods**

Statistical analyses were conducted with SPSS 17.00, 21.00 and 22.00 for Windows or MacOS (studies I-IV). A Shaphiro-Wilk test was performed to test data normality (Studies I-IV). If the data was not normally distributed, then logarithmic, square root or inverse transformations with or without reflection were performed (Studies I-II). Differences among categorical data were tested by using a chi-square test (Studies II-IV). Results are denoted as mean  $\pm$  SD unless otherwise denoted (Studies I-IV). A p-value less than 0.05 was considered significant (Studies I-IV).

In Study I, differences between the healthy and diabetic pigs were tested with an independent samples t-test or a Mann–Whitney U-test. Bivariate correlations were calculated using the Pearson correlation coefficient.

In Study II, between-group differences were tested with independent samples t-test and ANCOVA when adjusting for possible confounders. Data were analyzed first in the overweight and normal-weight groups, as determined by the subjects' current BMI. Since some subjects with a history of early onset obesity had later achieved a normal weight, we subsequently analyzed the data also by determining the obese and control groups based on their weight status at the age of 7 years. Association of the bone marrow UI, a main outcome variable with other variables, was tested using a Pearson correlation.

In Study III, differences with groups at baseline were tested by using a parametric and non-parametric ANOVA. Differences between categorical data were tested by using a chi-square test. ANCOVA was used to adjust for the possible effect of handgrip strength at baseline. The effects of exercise between and within the groups were assessed with repeated measures ANOVA as a linear mixed model with unstructured covariance structure. Bonferroni-adjusted p-values were used in pairwise comparisons between the time points. Associations of bone marrow insulin GU, the main outcome variable with other variables were tested with Spearman or Pearson correlation analysis.

In Study IV, differences between the groups were tested with independent samples t-test or Mann-Whitney U-test if data was not normally distributed. Differences between pre-intervention and post-intervention parameters were assessed with repeated measures ANOVA with unstructured covariance structure. Bonferroni adjusted p-values were used in pairwise comparisons between the time points. Associations of BMD, the main outcome variable with other variables, were tested using Spearman's correlation.

## 5 RESULTS

Summary about the effects of factors of interest on main outcome variables in Studies I-IV are depicted in Table 2.

Table 2 Summary about the effects of obesity/maternal obesity and exercise intervention/recent physical activity on primary outcome variables. NA: not assessed.  $\leftrightarrow$ : no change.  $\uparrow$ : increases. VBM: vertebral bone marrow. FBM: femoral bone marrow. vBMF: vertebral bone marrow fat. tBMF: tibial bone marrow fat.

Study	Obesity (I, II)/Maternal obesity (III)	Exercise (III, IV)/Physical activity (II)
I	VBM GU $\leftrightarrow$ , vBMF $\leftrightarrow$	NA
II	tBMF UI $\leftrightarrow$	tBMF UI $\leftrightarrow$
III	VBM GU $\leftrightarrow$ , FBM GU $\leftrightarrow$ , vBMF $\leftrightarrow$	VBM GU $\leftrightarrow$ , FBM GU $\uparrow$ , vBMF $\leftrightarrow$
IV	NA	Total hip BMD $\uparrow$

### 5.1 Association between VBM GU and VBM fat content (Study I)

We found an inverse correlation between VBM GU and VBM fat content measured with  $^1\text{H}$  MR spectroscopy ( $r=-0.800$ ,  $p < 0.01$ ) as well as between VBM GU and VBM TAG assay ( $r=-0.846$ ,  $p < 0.05$ ) (Figure 12). A non-significant, but suggestive positive association in VBM fat content measured with  $^1\text{H}$  MR spectroscopy and VBM TAG assay was found ( $r=0.661$ ,  $p=0.07$ ). However, no association in VBM fat content measured with in-phase and out-of-phase MRI and VBM TAG assay was found ( $r=0.394$ ,  $p=0.33$ ). No association between VBM GU and VBM fat content measured with in-phase and out-of-phase MRI was found ( $r=-0.823$ ,  $p=0.11$ ). Differences in weight ( $p=0.008$ ) and serum fasting glucose ( $p=0.002$ ) were found between diabetic and healthy pigs. No differences between the groups were observed in tissue-specific GU (VBM, skeletal muscle, SAT) or VBM fat content measured with  $^1\text{H}$  MR spectroscopy, in-phase and out-of-phase MRI or VBM TAG assay (Table 3).

Table 3 Characteristics of obese diabetic and healthy pigs

	Diabetic (n=5)	Healthy (n=5)	p
VBM GU ( $\mu\text{mol/L}\cdot\text{min}$ )	$19.3 \pm 9.3$	$28.0 \pm 17.0$	0.22
VBM GCR ( $\text{mL/mL}\cdot\text{min}$ )	$1.4 \pm 0.7$	$6.4 \pm 5.1$	0.09
Skeletal muscle GU ( $\mu\text{mol/L}\cdot\text{min}$ )	$9.5 \pm 3.2$	$12.4 \pm 4.3$	0.26
SAT GU ( $\mu\text{mol/L}\cdot\text{min}$ )	$5.2 \pm 2.2$	$6.0 \pm 5.2$	0.75
VBM fat content (%)	$25.7 \pm 3.9^*$	$17.2 \pm 7.4$	0.12
Signal intensity index	$0.8 \pm 0.1^*$	$0.7 \pm 0.2$	0.45
VBM TAG concentration (mg/g)	$145.8 \pm 37.9^*$	$110.6 \pm 46.2$	0.29
Weight (kg)	$123.2 \pm 9.4$	$78.8 \pm 7.9$	0.008
Serum fasting glucose (mmol/L)	$15.4 \pm 4.1$	$5.8 \pm 2.4$	0.002

\* n=3 in diabetic group. Signal intensity index assessed with in-phase and out-of-phase MRI. VBM: vertebral bone marrow. GU: glucose uptake. GCR: glucose clearance rate. SAT: subcutaneous adipose tissue. TAG: triacylglycerol. Modified and reprinted with permission from Study I.

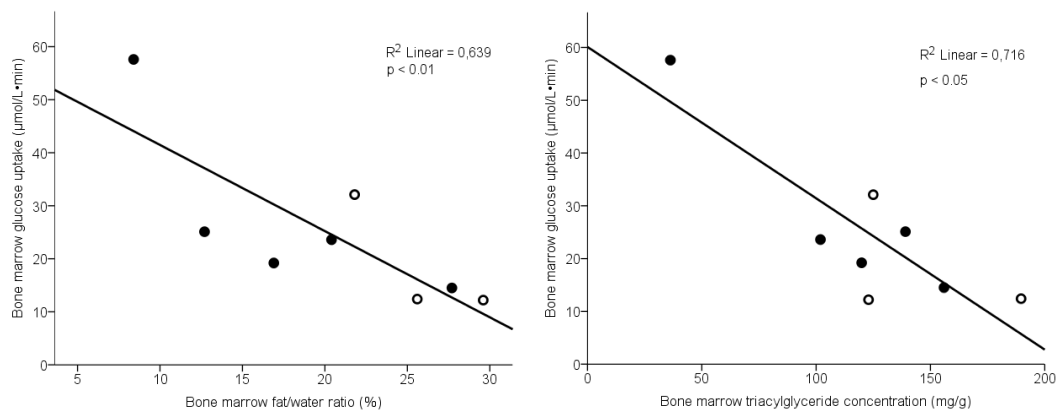


Figure 12 Correlation analyses of VBM GU, VBM fat content and VBM TAG concentrations. A negative correlation between VBM GU and VBM fat content measured with  $^1\text{H}$  MR spectroscopy (Left). A negative correlation between VBM GU and VBM TAG concentration in pigs (Right). Healthy pigs are represented by black dots (n = 5) and obese diabetic pigs are represented by white dots (n = 3). VBM: vertebral bone marrow. GU: glucose uptake. TAG: triacylglycerol. Reprinted with permission from study I.

## 5.2 Effect of obesity BMF UI (Study II)

BMI, total body fat, waist-to-hip -ratio, tissue fat, insulin and HOMA2-index were higher in overweight vs normal-weight group and subjects with early-onset obesity vs control group (Table 4). No differences were found in exercise habits (number of steps per days, distance travelled in km/days, energy expenditure in kcal/days, physical activi-

ty min/days) between the groups. A significant correlation between BMF UI and age was found in the whole cohort ( $r=0.408$ ,  $p=0.015$ ) (Figure 13). No confounding factors were found between BMF UI and age. Gender was not a confounder as the main outcome and confounders (UI, age, glucose, insulin, HOMA and PA) did not differ between males and females. We found no difference in BMF UI between overweight and normal-weight subjects. Furthermore, no difference was observed in BMF UI after dividing the subjects into obese and normal-weight control groups based on their weight status at the age of 7 years (Table 5).

Table 4 Baseline characteristics of the Study II subjects

	Overweight (n=17)	Normal-weight (n=18)	p	Subjects with early-onset obesity (n=13)	Controls (n=22)	p
Age (years)	20.3 ± 2.8	20.6 ± 2.9	0.79	19.7 ± 2.7	20.9 ± 2.9	0.22
Males (%)	53.0	11.0	0.01	53.8	18.2	0.045
BMI (kg/m <sup>2</sup> )	34.9 ± 8.7	21.1 ± 2.4	<0.001	36.8 ± 9.1	22.5 ± 3.7	<0.001
Waist-to-hip - ratio	0.9 ± 0.1	0.7 ± 0.1	<0.001	0.9 ± 0.1	0.7 ± 0.1	<0.001
Total body fat (kg)	41.8 ± 19.9	16.2 ± 5.2	<0.001	47.4 ± 19.2	17.6 ± 6.4	<0.001
Tissue fat (%)	40.6 ± 11.0	28.8 ± 6.8	0.005	43.5 ± 9.4	29.2 ± 7.5	<0.001
Fasting glucose (mmol/L)	5.3 ± 0.4	5.0 ± 0.4	0.08	5.2 ± 0.4	5.1 ± 0.4	0.74
HbA1c (mmol/L)	32.2 ± 3.5	32.9 ± 2.1	0.45	32.5 ± 3.8	32.6 ± 2.2	0.91
Insulin (mU/L)	14.6 ± 13.3	5.7 ± 3.1	0.04	17.9 ± 13.9	5.6 ± 3.0	<0.001
HOMA2-index	1.86 ± 1.63	0.76 ± 0.42	0.04	2.27 ± 1.69	0.74 ± 0.40	<0.001

Reprinted with permission from study II.

Table 5 BMF UI of the Study II subjects

	Overweight (n=17)	Normal-weight (n=18)	p	Subjects with early-onset obesity (n=13)	Controls (n=22)	p
UI (%)	9.4 ± 1.3	9.8 ± 1.5	0.43	9.6 ± 1.6	9.5 ± 1.3	0.85
UI (%) (corrected for age, physical activity and gender)	9.3 ± 0.4	9.5 ± 0.4	0.70	9.7 ± 0.4	9.3 ± 0.3	0.44
UI (%) (corrected for glucose, physical activity and gender)	9.4 ± 0.4	9.4 ± 0.4	0.97	9.6 ± 0.4	9.3 ± 0.3	0.68

Results are denoted as parameter estimates ± standard error of mean. BMF: bone marrow fat. UI: unsaturation index. Reprinted with permission from study II.

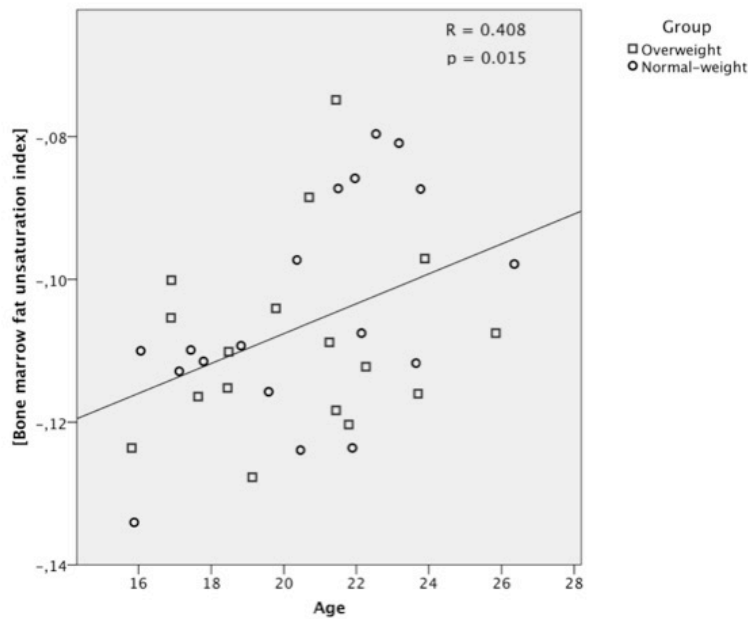


Figure 13 Correlation between tibial BMF UI and age in the pooled data of 35 Study II subjects. Inverse transformation with reflection was assessed for UI to obtain normal distribution. BMF: bone marrow fat. UI: unsaturation index. Reprinted with permission from study II.

### 5.3 Effects of obesity and exercise on bone marrow insulin-stimulated GU (Study III)

There were no differences in age, BMI, body fat %, systolic and diastolic blood pressure, waist-hip ratio, plasma fasting glucose, serum fasting insulin, VBM fat content, whole body GU (M-value) or prevalence of T2D between control vs frail, control vs OLM, control vs OOM and OLM vs OOM (Table 6). No differences were found in tissue-specific GU between OLM and OOM. After adjusting for muscle strength, no differences in VBM GU, FBM GU, SAT GU or psoas GU between control vs frail, control vs OLM, control vs OOM or OLM vs OOM (Figure 14) were observed. VBM GU was approximately 100 % higher compared to FBM GU. FBM, but not VBM GU, correlated with whole-body GU in frails and controls combined ( $r=0.487$ ,  $p=0.001$ ). VBM GU associated inversely to VBM fat content in frails and controls combined ( $r=-0.411$ ,  $p=0.03$ ).

No significant changes in anthropometric or biochemical characteristics were observed between or within the groups after resistance training intervention (Table 7). VBM fat

content remained unchanged. Resistance training increased FBM GU by 47 % ( $p=0.006$ ) in OOM. Similarly, psoas GU ( $p=0.039$ ) increased, while VBM and SAT GU remained unchanged after the intervention. In OLM, there were no significant changes in tissue-specific GU. Differences in exercise effects were found in FBM GU ( $p=0.022$ ) and SAT GU ( $p=0.021$ ) between OLM and OOM. VBM GU remained unchanged in both OOM and OLM (Figure 15). In OOM, the change in FBM GU correlated with change in whole body GU ( $r=0.601$ ,  $p=0.039$ ) but not with change in anthropometric characteristics or glycemic state indicators. In OLM, the change in FBM GU correlated with change in whole body GU ( $r=0.717$ ,  $p=0.001$ ). There was no correlation between change in VBM GU and change in whole body GU in OOM or OLM.

Table 6 Anthropometric and biochemical characteristics of the Study III subjects at the baseline

	Control (n=9)	Frail (n=37)	OLM (n=20)	OOM (n=17)
Age (years)	71.4 ± 3.1	71.9 ± 3.1	72.3 ± 2.6	71.5 ± 3.7
BMI (kg/m <sup>2</sup> )	27.8 ± 4.2	27.2 ± 4.7	26.6 ± 4.8	27.9 ± 4.6
Body fat %	40.1 ± 4.9	39.5 ± 5.9	38.6 ± 6.6	40.5 ± 4.9
Systolic BP (mmHg)	156 ± 13	162 ± 16	161 ± 12	163 ± 19
Diastolic BP (mmHg)	87 ± 11	90 ± 10	88 ± 10	93 ± 9
Waist/hip ratio	0.90 ± 0.03	0.91 ± 0.05	0.91 ± 0.05	0.90 ± 0.04
fP-glucose (mmol/L)	6.4 ± 0.4	6.0 ± 0.7	6.0 ± 0.7	5.9 ± 0.8
fS-insulin (mU/L)	8.8 ± 3.6	8.5 ± 4.3	9.6 ± 3.7	9.4 ± 4.9
Handgrip strength (kg) <sup>1</sup>	29.7 ± 2.6	17.7 ± 2.6*	17.2 ± 2.7*	18.2 ± 2.5*
Maternal BMI (kg/m <sup>2</sup> )	23.8 ± 2.0	26.0 ± 3.7	22.9 ± 1.4	29.7 ± 1.6*†
VBM fat content (%)	44.4 ± 6.6 <sup>a</sup>	43.8 ± 7.3 <sup>b</sup>	46.0 ± 7.0 <sup>c</sup>	42.2 ± 7.3 <sup>d</sup>
M-value (μmol/(kg·min))	22.3 ± 10.3	23.9 ± 10.6	26.5 ± 11.8	20.9 ± 8.3
T2DM (subjects/%)	2 (22.2%)	4 (10.8%)	3 (15.0%)	1 (5.9%)

Comparisons between control vs frail, control vs OLM, control vs OOM and OLM vs OOM are assessed. <sup>1</sup> Assessed in 2001-2004, \*  $p < 0.001$  vs control, †  $p < 0.001$  vs OLM, <sup>a</sup>  $n=7$ , <sup>b</sup>  $n=21$ , <sup>c</sup>  $n=9$ , <sup>d</sup>  $n=12$ . OLM: offspring of lean/normal-weight mothers. OOM: offspring of obese/overweight mothers. VBM: vertebral bone marrow. T2DM: type 2 diabetes mellitus. Reprinted with permission from study III.



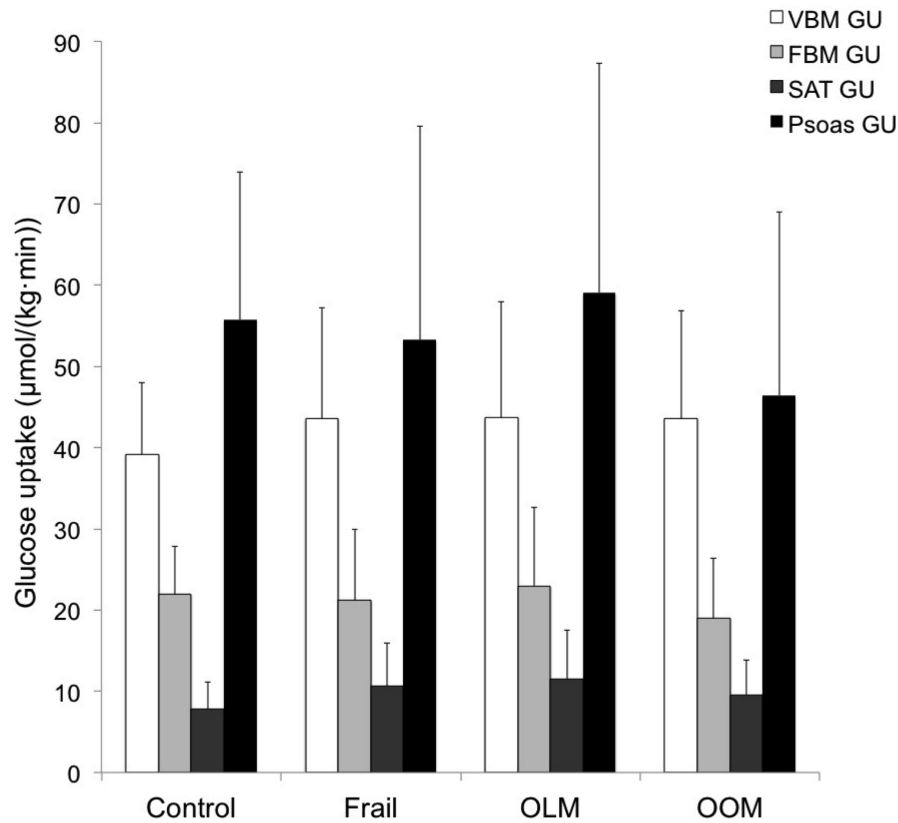


Figure 14 Tissue-specific GU of control, frail (OLM + OOM), OLM and OOM at baseline. There were no differences among the groups. OLM: offspring of lean/normal-weight mothers. OOM: offspring of obese/overweight mothers. Reprinted with permission from study III.

Table 7 Baseline and postintervention characteristics of OLM and OOM

	OLM			OOM		
	Baseline (n=20)	Exercise (n=19)	p	Baseline (n=17)	Exercise (n=16)	p
BMI (kg/m <sup>2</sup> )	26.6 ± 4.8	27.1 ± 4.7	0.55	27.9 ± 4.6	27.6 ± 4.8	0.96
Body fat %	38.6 ± 6.6	38.8 ± 6.3	0.48	40.5 ± 4.9	39.8 ± 4.5	0.19
Systolic BP (mmHg)	161 ± 12	154 ± 15	0.07	163 ± 19	158 ± 16	0.28
Diastolic BP (mmHg)	88 ± 10	84 ± 11	0.14	93 ± 9	89 ± 9	0.21
Waist/hip ratio	0.91 ± 0.05	0.89 ± 0.05	0.10	0.90 ± 0.04	0.88 ± 0.06	0.27
fP-glucose (mmol/L)	6.0 ± 0.7	6.1 ± 0.7	0.44	5.9 ± 0.8	5.8 ± 0.6	0.66
fS-insulin (mU/L)	9.6 ± 3.7	9.5 ± 4.1	0.79	9.4 ± 4.9	9.7 ± 5.6	0.32
VBM fat content (%)	46.0 ± 7.0 <sup>a</sup>	44.4 ± 6.1 <sup>b</sup>	0.25	43.7 ± 7.2 <sup>c</sup>	43.0 ± 6.2 <sup>d</sup>	0.85

<sup>a</sup> n=9, <sup>b</sup> n=17, <sup>c</sup> n=12, <sup>d</sup> n=12. OLM: offspring of lean/normal-weight mothers. OOM: offspring of obese/overweight mothers. BP: blood pressure. VBM: vertebral bone marrow. Reprinted with permission from Study III.

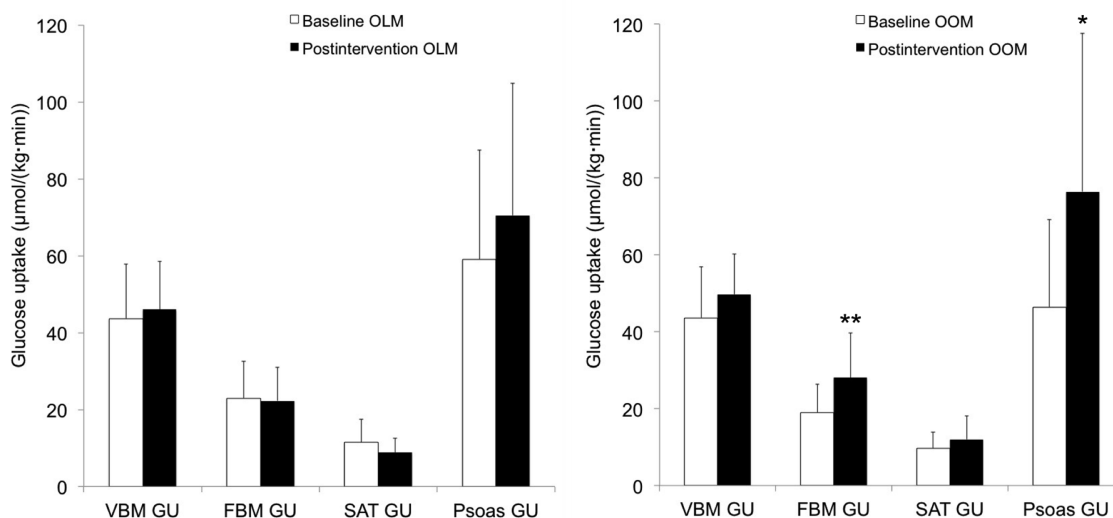


Figure 15 Tissue-specific GU at baseline and after the intervention in (left) OLM and (right) in OOM. There was no change in any tissue-specific GU after intervention in OLM. FBM GU ( $p=0.006^{**}$ ) and psoas muscle GU ( $p=0.039^{*}$ ) increased significantly after the intervention in OOM. GU: glucose uptake. OLM: offspring of lean/normal-weight mothers. OOM: offspring of obese/overweight mothers. FBM: femoral bone marrow. Reprinted with permission from Study III.

#### 5.4 Effects of exercise on BMD and serum sclerostin (Study IV)

Age, body mass index, waist to hip ratio, total body fat, supplemental vitamin D and calcium intake did not differ between the groups. 13.5 % of intervention subjects and 27.3 % of control subjects had calcium or vitamin D supplements ( $p=NS$ ). No differences were observed in the prevalence of an earlier diagnosis of osteoporosis or in the amount of subjects using current HRT. Total hip, femoral neck, trochanteric or intertrochanteric BMD did not differ between the groups. Quadriceps muscle mass was lower in the intervention group compared to controls ( $p=0.016$ ). No differences in adductor longus, adductor magnus or hamstring muscle masses were found. Serum sclerostin was higher in the controls ( $p=0.037$ ) (Table 8).

Total hip BMD increased by 6 % ( $p=0.005$ ) after resistance training (Figure 16). This was mainly induced by an increase in intertrochanteric area BMD (+10.7 %,  $p=0.001$ ). Trochanteric and femoral neck BMD remained unchanged ( $p=NS$ ). Serum sclerostin ( $p<0.001$ ) increased (Table 9). One year after the end of the resistance training interven-

tion, total hip BMD increased by 8.6 % ( $p < 0.001$ ) and serum sclerostin ( $p = 0.045$ ) decreased compared to post-intervention values. In controls, total hip BMD and serum sclerostin remained unchanged compared to pre-intervention values.

Mean quadriceps muscle mass was increased after resistance training by 9.2 % ( $p = 0.001$ ) and adductor magnus muscle mass was increased by 4.4 % ( $p = 0.012$ ), as previously reported by Bucci et al. (Bucci et al. 2015). Increases in hamstring or adductor longus muscle masses were not observed. Muscle strength measured by mean RM8 increased by 96 % during the seated row, 60 % during the leg press, 51 % during abdominal crunches, 118 % during the chest press, 70 % during seated leg curls, 43 % during hip abduction and 69 % during back extensions after the resistance training intervention ( $p < 0.001$  for all). No correlations were observed between the change in measured muscle group strength and BMD. BMI, total body fat percentage and waist-to-hip ratio remained unchanged.

An exercise diary of the leisure-time physical activity was kept by study subjects during the intervention and follow-up periods. Accordingly, the frequency of leisure-time physical activity per week was  $5.3 \pm 2.9$  during the intervention and  $5.2 \pm 2.4$  during the follow-up ( $p = 0.50$ ). The amount of leisure-time physical activity was  $55.6 \pm 32.1$  minutes per session during the intervention and  $60.9 \pm 32.2$  minutes per session during the follow-up ( $p = 0.19$ ).

Table 8 Baseline characteristics of the Study IV subjects.

	Control (n=11)	Intervention (n= 37)	p
Age (years)	71.8 ± 2.9	71.9 ± 3.1	0.79
Handgrip strength (kg) <sup>1</sup>	29.6 ± 2.5	17.7 ± 2.6	<0.001*
Body mass index (kg/m <sup>2</sup> )	26.8 ± 4.4	27.2 ± 4.7	0.82
Waist to hip ratio	0.89 ± 0.04	0.91 ± 0.05	0.44
Total body fat (%)	38.8 ± 5.3	39.5 ± 5.9	0.73
Earlier diagnosed osteoporosis (%)	9.1	13.5	0.70
Current HRT (%)	9.1	8.1	0.92
Total hip BMD (g/cm <sup>2</sup> )	0.740 ± 0.118	0.690 ± 0.115	0.26
Femoral neck BMD (g/cm <sup>2</sup> )	0.724 ± 0.130	0.724 ± 0.174	0.87
Trochanteric BMD (g/cm <sup>2</sup> )	0.657 ± 0.106	0.591 ± 0.111	0.09
Intertrochanteric BMD (g/cm <sup>2</sup> )	0.890 ± 0.193	0.801 ± 0.173	0.15
Quadriceps m. mass (g)	157.8 ± 22.0	140.5 ± 19.5	0.016*
Adductor magnus m. mass (g)	100.0 ± 17.1	92.9 ± 16.2	0.22
Hamstring m. mass (g)	52.4 ± 11.9	49.2 ± 11.2	0.42
Adductor longus m. mass (g)	26.1 ± 6.4	25.2 ± 7.4	0.70
Serum sclerostin (pmol/l)	74.9 ± 19.6	60.8 ± 17.9	0.037*

<sup>1</sup> Assessed in 2001-2004. Modified and reprinted with permission from Study IV.

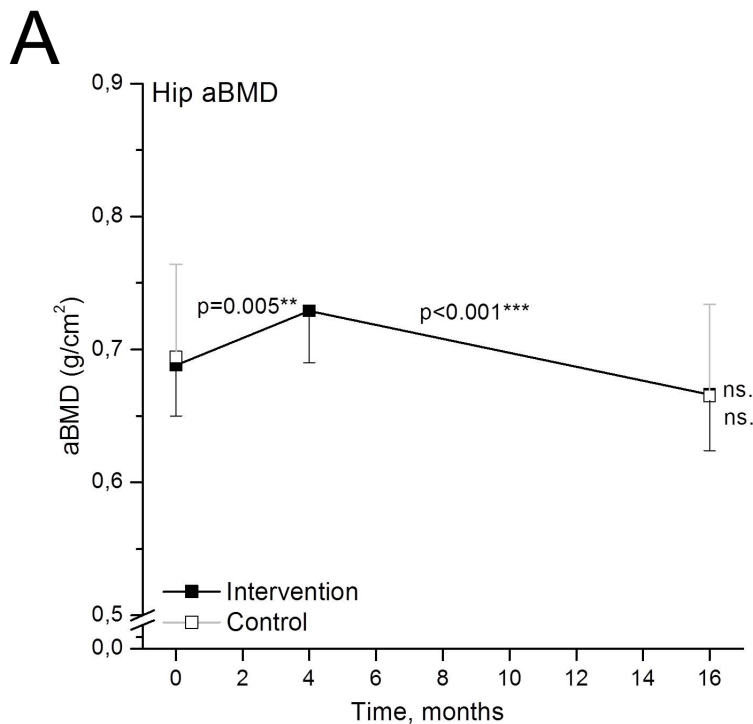


Figure 16 Changes in total hip BMD during the study. Total hip BMD at baseline, after the 16-week resistance training and one year after the end of the resistance training. Results are shown as estimated means with 95 % confidence intervals. \*\*  $p < 0.01$  baseline vs postintervention, \*\*\*  $p < 0.001$  postintervention vs one-year follow-up. aBMD: areal bone mineral density. Reprinted with permission from Study IV.

Table 9 Serum sclerostin concentrations at baseline, post-intervention and follow-up visits

	Intervention			Controls		
	Baseline (n=37)	Post (n=34)	Follow-up (n=19)	Baseline (n=11)	Post	Follow-up (n=6)
Serum sclerostin (pmol/l)	60.9 [54.1;67.6]	84.3 [77.4;91.1]**	69.5 [60.4;78.7]*	65.6 [41.2;90.0]	-	70.6 [46.2;95.0]

Results are denoted as estimated means with 95 % confidence intervals. \*\*  $p < 0.001$  vs pre, \*  $p=0.045$  vs post. Modified and reprinted with permission from study IV.

## 6 DISCUSSION

The primary purpose of this thesis was to achieve a better understanding of the possible negative effects exerted by obesity on bone health and whether exercise leads to favourable outcomes regarding bone health. The age distribution of the study subjects, parameters reflecting the bone health, modality of the imaging methods and type of obesity addressed varied greatly. The major outcomes in a connected order were first that BMF content or VBM GU uptake did not seem to differ between diabetic and healthy control experimental animals, but BMF content inversely associated with VBM GU in pooled data. Second, BMF unsaturation is not affected by current or early-onset obesity but is increased with age. Third, bone marrow insulin-stimulated GU is not affected by prenatal maternal obesity status, and FBM and VBM glucose metabolism reacts differently to a four-month resistance training intervention in elderly women according to their maternal obesity status. Lastly, BMD is increased after a four-month resistance training intervention, but the achieved increase in BMD is not sustained one year after the end of the intervention.

### 6.1 BMF (Bone marrow fat)

VBM fat content was determined in Studies I and III. Tibial BMF composition was assessed in Study II. Various methods were used in different cohorts. In Study I, VBM fat was assessed with  $^1\text{H}$  MR spectroscopy in addition to in-phase and out-of-phase MRI, which was validated with a chemical TAG concentration assay of VBM blocks extracted from the cadavers. However, no correlation between VBM in-phase and out-of-phase imaging and VBM TAG assay was found suggesting an insensitivity of in-phase and out-of-phase MRI to assess VBM fat content especially in low sample size populations. Nonetheless, in-phase and out-of-phase MRI have been previously used successfully in human studies in order to determine, for example, VBM fat content (Ojanen et al. 2014) and liver adiposity (Borra et al. 2009). Due to our validation findings in Study I, only  $^1\text{H}$  MR spectroscopy was used in Study III to assess VBM fat content. In Study I, there was a variation in the proportional amounts of fat content between the diabetic and healthy group measured with multiple methods ( $^1\text{H}$  MR spectroscopy 67 %, TAG analysis 75 %, in-phase and out-of-phase 88 %). In an earlier study using human subjects, VBM lipid peaks at 0.9-1.6 ppm and 2.0 ppm and water peak near 4.6 ppm were found (Liney

et al. 2007), and this was also the case in Study I. The discrepant results obtained with  $^1\text{H}$  MR spectroscopy and TAG concentration assay may have been caused by a lipid peak near 2.0 ppm that was not included in the spectra analysis. Main lipid peaks between 0.9 and 1.6 ppm correspond to methylene protons from lipids and terminal methyl protons in glycerols. Peaks near 2.0 ppm are assigned methylene protons  $\alpha$  to the carboxyl in the glycerol chains (Jagannathan et al. 1998). Another possible error source may have been the fact that in the TAG assay, the whole vertebral bone block was crushed meaning that non-VBM triglycerides have also been included in the analysis leading to a higher fat amount found compared to the findings in the  $^1\text{H}$  MR spectroscopy results.

In Study II, we investigated whether current or early-onset obesity affects the tibial BMF composition. Study subjects were male and female adolescents with a known history of early-onset obesity in addition to recent records of their physical activity and biochemical characteristics of their glycemic state. It was concluded that despite the body adiposity, current or childhood high body mass index does not affect BMF UI. This is in accordance with a recent study by Bredella et al (Bredella et al. 2014). They showed that no difference in BMF UI exists among young anorexia nervosa patients with different BMI. However, it seems that BMF unsaturation increases with age. This finding relates most likely to normal maturation of bone marrow during young adulthood, while red hematopoietic marrow is replaced with fatty marrow when also BMF content and fat cell size increases (Moore, Dawson 1990). Thus, this finding was not interpreted as a sign of risk or pathologic condition. Moreover, Study II was the first to investigate the effect of physical activity on BMF UI. It was concluded that physical activity seems not to influence BMF composition, but within the Study II setting, the BMF amount was not determined. Nevertheless, previous studies investigating the effect of exercise on BMF amount has been conducted. Exercise decreases femoral BMF in young children (Casazza et al. 2012), tibial shaft BMF in young female athletes (Rantalainen et al. 2013) and femoral BMF in young female mice (Styner et al. 2014). Based on this, it seems that exercise reduces site-specific BMF amount at least in young subjects. However, in Study III, a decrease in VBM fat content was not observed after a four-month resistance training intervention in elderly females. This suggests that BMF reacts differently to exercise at different ages and probably in a site-specific manner.

VBM fat contents were around 20 % and 45 % in Studies I and III measured with  $^1\text{H}$  MR spectroscopy, respectively. This demonstrates great variability in proportionate of fat and hematopoietic marrow depending on the age and gender of the subject (Kugel et al. 2001) and possibly depending on subject species. In Study III, there was no difference in VBM fat content between the study groups at baseline indicating that maternal obesity is not related to VBM fat content. In both Studies I and III, PRESS sequences were used to assess VBM fat content, but studies using STEAM to measure T2 fat component have also been conducted with quite similar results (LeBlanc et al. 1999). With different TE or TR, corrections for relaxation times, which were conducted in both Studies I and III, are necessary because due to shorter T2 of water than fat, increased T2 may lead to an increased fat signal (Kugel et al. 2001). In Study II, a novel long TE method was used to measure BMF UI, which is not vulnerable to disturbances caused by water resonance peak (Lundbom et al. 2011, Troitskaia, Fallone & Yahya 2013). None of the acquired spectra in Study II had observable water resonance present indicating that our results were not influenced by bone marrow water content. Previous  $^1\text{H}$  MR spectroscopy studies investigating VBM fat content have used short TE methods (Yeung et al. 2005, Patsch et al. 2013, Baum et al. 2012), which may have led to biased estimation of olefinic resonance while an intense water resonance is present.

## 6.2 Bone marrow GU (Glucose uptake)

Bone marrow GU was investigated in different settings of Studies I and II. Study I was a pilot study with a low sample size of experimental animals. It was conducted to define the role that VBM glucose metabolism plays in diabetes, which is a worldwide health problem (Shi, Hu 2014). In addition, because osteoporosis is prevalent in diabetes (Tuominen et al. 1999) and has been termed as “obesity of bone” (Rosen, Bouxsein 2006), whether VBM glucose metabolism and VBM fat content are connected was determined. It was concluded that VBM fat and VBM GU are inversely associated. This is in accordance with Study III’s results in which an inverse association was found between VBM fat content and VBM GU in elderly female subjects. One explanation to this finding may be that excess fat in the bone marrow niche inhibits bone marrow glucose metabolism. Bone marrow is the only place in the human body where the actual bone cells and fat are adjacently located (Fazeli et al. 2013). A second possible explanation could be that excess BMF replaces hematological cells resulting in blunted GU,



because it has been found that human adipose tissue depots tend to have low GU (Ng et al. 2012). Study I was conducted under a fasting state without insulin-stimulated conditions, and thus diabetic pigs tended to have quite high serum fasting glucose values compared to controls. To exclude the effect of hyperglycemia on GU, the VBM glucose clearance rates (GCR) were defined. However, a similar inverse correlation was found between VBM fat content and VBM GCR excluding hyperglycemia as a potential confounding factor.

Differences in VBM GU between obese diabetic and healthy pigs were not found in Study I. This led us to compare differences of site-specific GU (psoas muscle and SAT) between the groups to achieve a semi-quantitative measure for VBM GU. No differences were observed as found in an earlier study of obese and non-obese subjects (Virtanen et al. 2002). Possible explanations on not finding any differences may include low statistical power or conducting the study under a fasting state without insulin-stimulated conditions. Nonetheless, in Study I, VBM possessed highest GU in diabetic and control group compared to other sites showing that VBM is a metabolically active organ.

In Study I, VBM GU was approximately 2-times higher than skeletal muscle GU studied in pigs without an insulin-stimulated condition. In Study III, VBM GU was approximately 1.5-times higher than skeletal muscle studied in elderly female subjects during hyperinsulinemic euglycemic clamp. According to Iozzo et al., site-specific GU values tend to be approximately 3-fold higher during hyperinsulinemia than in the fasting state (Iozzo et al. 2006). Post-hoc comparison of VBM GU results between Studies I and III revealed that insulin-stimulated GU values tend to be approximately 2-times higher compared to non-insulin-stimulated condition. Moreover, psoas muscle GU values tend to be 6-times higher under insulin-stimulated compared to non-insulin stimulated conditions. However, in Study I, pigs were under anesthesia during the imaging which may partly, in addition to differences in study subjects, explain the differences in observed magnitudes of skeletal muscle GU between Studies I and III.

In Study III, it was found that FBM but not VBM insulin-stimulated GU increases after four-month resistance training intervention only in OOM. Studies investigating long-term effects of exercise on bone insulin sensitivity have not earlier been conducted. However, the effect of acute exercise has been found to increase femoral bone insulin

sensitivity in addition to femoral bone blood flow in young healthy male subjects (Heinonen et al. 2014, Heinonen et al. 2013). In this study, the ROI included the bone cortex in addition to the bone marrow cavity that differed from ROI placement in Study III in which the ROI was drawn to cover only the bone marrow cavity excluding the cortex. In addition, the study was not conducted under insulin-stimulated conditions as in Study III, and the subjects were young males aged  $24 \pm 2.6$  years meaning that FBM fat content probably differed between subjects in Study III and the study by Heinonen et al. (Heinonen et al. 2013). Different GU values resulted because it has been established that red bone marrow conversion to yellow bone marrow peaks at the age of 24 years (Moore, Dawson 1990). In Study III, the FBM blood flow was not assessed meaning that conclusions about the effect of long-term exercise on bone marrow blood flow cannot be drawn.

Considering the results of Study III, the most interesting question is why FBM insulin-stimulated GU increased only in OOM but not in OLM. It may be that FBM in OOM contains more insulin-resistant fat than in OLM. Femoral BMF was not measured in Study III, and to our knowledge no studies investigating the effect of maternal obesity on femoral BMF have been conducted. Another explanation could be that mechanistic role for maternal obesity-induced offspring insulin resistance could be developmentally programmed physical inactivity or altered adipocyte metabolism leading to a different behaviour of FBM GU between OLM and OOM (Samuelsson et al. 2008). Interestingly, it was also found that FBM insulin-stimulated GU very closely follows whole-body GU. If insulin resistance has developed, it may likely be alleviated with exercise in a relatively short time. The results in Study III highlight a novel role that FBM plays as a metabolically active fat depot. However, it remains unclear whether FBM GU would have increased after exercise regime in OOM and OLM combined.

Results of Study III are in accordance with the results by Bucci et al. who found that with the same cohort, whole-body GU and skeletal muscle GU increase after a four-month resistance training intervention (Bucci et al. 2016). Similar findings have been observed in obese sedentary young males in whom femoral skeletal muscle GU increased approximately 30 % after 11 weeks of resistance training (Reichkender et al. 2013). In Study III, the increase of psoas muscle in OLM was approximately 20 % and in OOM approximately 50 %. The differences in the skeletal muscle GU increases may

possibly be linked with the fact that intramyocellular lipid content of the tibialis anterior muscle decreased in OOM approximately 25 %, while in OLM, the intramyocellular lipid content remained unchanged (Bucci et al. 2016). This may reflect the possibility that a decrease of insulin-resistant fat in skeletal muscle leads to a mutual increase in skeletal muscle insulin sensitivity. This was not the case considering VBM GU suggesting that the mechanism behind the insulin-stimulated GU improvement is different between VBM and FBM or skeletal muscle. All in all, the results of Studies I and III suggest that glucose metabolism of VBM and FBM are regulated differently. FBM seems to be insulin sensitive, while VBM appears to be insulin resistant. According to the results, VBM GU was 1.5–2 times higher than FBM GU, which could be at least partly explained by the relatively high proportion of metabolically very active hematopoietic red marrow in VBM.

### **6.3 BMD (Bone mineral density)**

The effect of four-month resistance training on total hip BMD was studied with CTXA of QCT in Study IV. In addition, to study the long-term effect of resistance training on bone health, BMD was measured one year after the end of the intervention. Serum sclerostin concentration was assessed in parallel with BMD measurements. It was found that total hip BMD increased by 6 % after resistance training with a concomitant increase in serum sclerostin concentration. One year after the end of the intervention, BMD and serum sclerostin decreased back to baseline levels.

The increase in total hip BMD is in line with an earlier study in which BMD increased 3 % after 16-week resistance training in young male and female subjects (Lang et al. 2014). It may be that the BMD changes are a result of increased muscle strength through a spatially heterogenous response of bone to resistance training targeted to different muscle groups, such as hip abduction stimulating gluteus muscles inserting in the greater trochanter (Marques, Mota & Carvalho 2012). The increase in hip BMD was mainly located in the intertrochanteric area, which is the origin site of vastus muscles of quadriceps femoris. It was found in a study by Bucci et al. that the mass of this muscle group increased after exercise (Bucci et al. 2015). Ma et al. (Ma et al. 2014) studied the muscle-bone unit in subjects with varying BMD and found that in the subjects with osteopenia or osteoporosis, relatively larger muscle masses act on the weakened bones

independent of age, which, in other words, means that as BMD decreases abnormally, more bone than muscle is lost. On the other hand, a correlation between BMD and muscle strength increase was not observed in Study IV. This may indicate that increased muscle mass resulted in increased mechanical strain on bone that stimulates site-specific osteogenesis through osteoblast and osteocyte activation. Osteocytes are the mechanosensors in bone tissue (Clarke 2008) that coordinate the osteogenic response to mechanical loading at least in part through the expression of sclerostin (Tu et al. 2012).

In addition to an increase in BMD, serum sclerostin paradoxically increased after a resistance training regime, while a decrease was expected. Sclerostin is an osteocyte-secreted soluble antagonist of the Wnt/ $\beta$ -catenin signaling pathway, which regulates osteoblast differentiation and activity and is a negative regulator of bone mass (Clarke, Drake 2013). A correlation between BMD and serum sclerostin was expected as in earlier studies (Garnero et al. 2013, Modder et al. 2011, He et al. 2014). The strength of the associations found in earlier studies have been moderate with much larger sample sizes compared to Study IV in which the association was not found. It may be that a larger sample size is needed to find the correlation between BMD and serum sclerostin levels. Circulating sclerostin levels correlate closely with bone marrow sclerostin levels (Clarke, Drake 2013). However, it is not yet elucidated how well the changes in circulating sclerostin reflect the changes in bone microenvironment. The sources of biological variability are still unclear, and circulating sclerostin levels do not always correlate with observed BMD (Clarke, Drake 2013). Results that are consistent with found simultaneous increases in BMD and serum sclerostin in Study IV have earlier been observed by Polyzos et al. (Polyzos et al. 2012). They found that 6-month anti-osteoporotic treatment increased serum sclerostin levels in postmenopausal women, while a decrease was expected. Increased serum sclerostin levels found in Study IV may reflect the activation of sclerostin-synthesizing osteocytes (Clarke, Drake 2013) that may be caused by resistance training-induced mechanostimulation or bone microdamage (Luo et al. 2014). Thus, it is possible that exercise-induced effects on serum sclerostin levels are age- and sex-dependent and independent of BMD.

Study IV was first to assess BMD at one year after the end of the exercise regime. Total hip BMD decreased approximately back to baseline levels. This finding highlights the importance of continuous supervised resistance exercise in BMD maintenance. Engelke

et al. found in their study design that hip BMD decreased significantly by 1 % at a one-year timepoint in a control group without the history of previous exercise interventions (Engelke et al. 2006). In Study IV, the decrease in BMD was more rapid. The typical average BMD loss is 1.0-3.7 % per year in non-exercising postmenopausal women (Okano et al. 1998). Importantly, the expected decrease in BMD was not observed in non-exercising controls in Study IV, which may be a result of low statistical power within the control group.

In clinical practice, the gold standard for measuring BMD is DXA. The effect of resistance training on BMD is somewhat lower in earlier DXA studies (Bemben, Bemben 2011, Marques et al. 2011) compared to the effect achieved in Study IV. The magnitude in BMD changes among these studies may be explained by differences in the intensity of resistance training interventions or in demographic profiles of subjects as well as in methodology, i.e., QCT and DXA combined with interobserver and intraobserver precision errors. In Study IV, interobserver measurement error was not determined. Intraobserver error for CTXA of hip has been reported to be approximately 1.5 % (Li et al. 2006), which is slightly better compared to DXA. To achieve high precision with DXA, experienced and preferably the same radiographer performing the setting of the patient for the imaging is needed. DXA and CTXA results of the hip have a highly positive correlation (Cann 1988, Khoo et al. 2009). A one reason QCT was used in Study IV originates from the design of Study III, including whole body PET imaging, which was the main imaging modality in that particular study. PET sessions consisting of dynamic brain, heart, abdomen and thigh imaging lasted approximately 3-4 hours. QCT imaging was effortlessly assessed simultaneously and thus excluding logistical and schedule problems during the study sessions.

#### **6.4 Strengths and limitations**

The studies in this thesis consist of three modern imaging modalities and three novel study settings in three different and unique cohorts. Study I was first to investigate the interplay between VBM fat and VBM functional glucose metabolism. In addition, VBM TAG analysis was performed to validate VBM in-phase and out-of-phase MRI. This would have not been easily achieved in human studies. Study II was first to evaluate fatty acid composition of BMF in a cohort of young adult subjects including overweight

and severely obese individuals. Although the sample size was small, it was calculated that a 15 % difference in BMF UI could be detected between the obese and normal-weight subjects. Only a 4 % difference was found between these groups signifying that sample size was enough to conclude that no difference truly existed.

Study III was conducted under insulin-stimulated conditions to assess whole-body insulin sensitivity. This improved the validity and accuracy of the results. A strength of study III also was a unique HBCS II cohort that provided the possibility to study the effect of prenatal maternal obesity on glucose metabolism in the elderly offspring. Study IV was based on the same cohort than Study III without the conditions of maternal obesity. OOM and OLM were pooled together to form a group with decreased muscle strength to achieve a higher sample size. In addition, one may notice that the number of control subjects was higher than in Study III. This is explained by the fact that two control subjects in Study III were excluded because they were characterized as subjects with normal handgrip strength of OOM and not subjects with normal handgrip strength of OLM as the other controls. Thus, the number of controls in Study IV was 11 instead of nine as in Study III.

The strengths of Study IV were a well-characterized study population and the assessment of serum sclerostin simultaneously with high-quality CTXA hip BMD measurements. The resistance training intervention was efficient, as muscle strength and muscle masses increased. This reflects the compliance, adherence and motivation achieved by the study population. In addition, subjects kept exercise diaries during the intervention and the follow-up period. No differences were found in the frequency or amount of leisure-time physical activity between the intervention and follow-up period. This means that leisure-time physical activity did not probably influence the results. A major limitation of Study IV was a relatively small sample size. Also, controls were not re-examined after 16 weeks simultaneously with the intervention group, which may mean that a BMD gain of 6 % caused by technical issues cannot be completely ruled out. In addition, the follow-up consisted only of a subset of subjects, thus decreasing the statistical power. There was no possibility to analyse cortical and trabecular BMD simultaneously due to lack of advanced research tools. An additional limitation was lack of information about the age of menarche, years after menopause, parity and previous HRT treatment of the study subjects, possibly influencing the validity of the results.

The intention of Study I was to do a small pilot study to investigate the interplay between VBM fat and VBM glucose metabolism as well as to validate in-phase and out-of-phase MRI imaging of BMF. The original purpose of Study I was to investigate coronary artery disease in diabetic and obese models. Thus, the model was an obese diabetic model and not a true T2DM model because the insulin effect could have not been studied. In addition, only 8 samples were harvested, because Study I was conceived after the VBM samples were taken in conjunction to the study by Honka et al. (Honka et al. 2013). The low statistical power and the possible distortion of the interpretation of the results considering Study I was considered. However, the metabolically complicated condition in the diabetic group was observed including changes associated with diabetes. The groups were combined to conduct the correlation analysis but if diabetes interfered with the results, the correlation analysis would have been conducted separately. A limitation of Study II includes also a relatively low statistical power. In addition, male and female subjects were pooled. However, no differences were found between the characteristics of the male and female subjects justifying the pooling of these subjects. BMF UI was studied only at one time point. This prevented the investigation into possible changes in BMF UI in the longitudinal aspect of the study and studying the relation of BMF UI and BMI over time.

Weaknesses of Study III included the fact that the study subjects were termed as frail subjects, although they should have been termed as subjects with decreased handgrip strength or “semi-frail” subjects. The definition of frailty was based only on handgrip strength that is a valid marker to identify frail subjects (Syddall et al. 2003). Moreover, frailty is associated with insulin resistance (Abbatecola, Paolisso 2008), but differences in whole-body or any tissue-specific insulin sensitivity were not found at baseline. However, differences may possibly have been found if the sample size was larger. Nonetheless, sample size was thought satisfactory in study design including imaging techniques resulting in relatively high but acceptable radiation exposure to the study subjects. One might also doubt the maternal obesity aspect, because the follow-up time was approximately 70-80 years without precise and continuous information on lifestyle habits or medical records. However, the HBCS cohort is a one of a kind cohort and sufficiently wide amount of information is available. In addition, the absence of differences between OLM and OOM at baseline may be due to too small sample size or the fact that

the mothers were only moderately obese, which may originate from the lower prevalence of obesity during 1934 to 1944. During pregnancy, women gain weight very differently, which means that pre-delivery BMI may possibly be misleading as a health outcome predictor. However, the outcomes refer to prenatal maternal BMI, since pre-pregnancy BMI data is not available in the HBCS cohort. However, Eriksson et al. have found very substantial evidence in larger cohorts that prenatal maternal obesity truly exposes the offspring to cardiovascular disease and T2DM during the old age (Eriksson et al. 2014). One weakness in this study is that the control group was studied only at baseline, and hence it cannot be concluded how the resistance training intervention would have affected the tissue-specific and overall GU in controls. In addition, it must be pointed out that prenatal maternal BMI  $> 28.1 \text{ kg/m}^2$ , which was a definition for OOM subjects is only a cut-off value for highest quartile of the entire HBCS II population and not a value for actual clinical significance.

Study IV was the first of a kind to study the long-term effects of resistance training on BMD. One year after the end of the intervention, total hip BMD decreased back to baseline levels. Type II error of methodological causes, for example, intraobserver precision error cannot be completely ruled out because of the lack of the proper interventional control group. A small control group had a normal muscle strength, which may be a flaw in study design. However, the control group was only used to validate interventional group to possess decreased muscle strength, which phenotype appeared in decreased muscle mass and decreased handgrip strength. In conclusion, it is likely that the decrease in BMD was not caused by type II error over a one-year follow-up because a concomitant change was observed also in serum sclerostin reflecting the bone turnover.

## 6.5 Clinical implications and future directions

Diabetes is associated with increased risk for osteoporosis (Tuominen et al. 1999). In Study I, VBM GU was inversely associated with VBM fat. This result may give future insights into the pathogenesis, prevention and treatment of diabetes-induced osteoporosis. Pharmacological interventions promoting osteoblastogenesis in detriment of adipogenesis could be possible target for decreasing bone related co-morbidity of this chronic disease. However, further studies are required to define the causal mechanisms. In addition to diabetes, obesity may have undiscovered negative consequences on bone health.



---

Based on the results in Studies I and II, these do not seem to manifest as altered VBM GU or BMF in experimental animals or altered BMF composition in adolescents. It also seems that change in BMF UI during aging may be coupled with normal maturation of bone marrow and not to be risk or sign of disease condition.

Results of Study III showed that FBM is a metabolically active fat depot, and its glucose metabolism is regulated differently from VBM. This difference may reflect the distinct ability of red hematopoietic cells and yellow fatty marrow cells to consume glucose. In addition, resistance training increased FBM insulin-stimulated GU in OOM but not in OLM. This may reflect altered maternal obesity-induced bone marrow adipocyte metabolism. Implications of this finding are important, because they may offer new insights into more individualised and provide more accurately allocated lifestyle interventions in treating or preventing frailty of T2DM in subjects with known prenatal maternal obesity status. The findings of Study IV are valuable in providing new information regarding the production of sclerostin in response to exercise in older women. In addition, the findings in Study IV offer a new non-pharmacological aspect in treating decreased BMD in subjects with decreased muscle strength and probably thus having an implication in preventing osteoporotic fractures in correctly targeted patients.

For future directions, an interplay between BMF content and composition, bone marrow glucose metabolism and BMD would be of great interest to study because factors, for example, exercise and obesity, may be important in the determination of healthy bone aging.

## 7 CONCLUSIONS

The major conclusions of the work presented in this thesis may be summarized as follows

- 1) Vertebral bone marrow fat is inversely associated with vertebral bone marrow glucose uptake indicating that vertebral bone marrow glucose metabolism coupled with vertebral bone marrow fat content may impact diabetic-induced osteoporosis (I).
  
  - 2) Bone marrow fat unsaturation is not affected by current or early-onset obesity but increases with age reflecting the normal maturation of bone marrow and not a sign of risk or disease condition (II).
  
  - 3) Maternal obesity does not affect bone marrow insulin-stimulated glucose uptake in the elderly offspring. A reason not to find differences may be due to low sample size or the fact that subjects' mothers were only moderately obese (BMI 29.7 kg/m<sup>2</sup>), which may originate from the lower prevalence of obesity during 1934 to 1944 (III).
- Femoral bone marrow insulin-stimulated glucose uptake increases, but vertebral bone marrow insulin-stimulated glucose uptake remains unchanged after a four-month resistance training intervention in elderly women according to their maternal obesity status. This highlights the novel role of femoral bone marrow plays as a metabolically active fat depot (III).
- 4) Bone mineral density is increased with a simultaneous decrease in serum sclerostin after a four-month resistance training intervention in elderly female with decreased muscle strength. This highlights the importance of continuous resistance exercise in bone mineral density maintenance in addition to muscle strength maintenance (IV).

## **ACKNOWLEDGEMENTS**

The studies presented in this thesis were carried out during the years of 2012 to 2016 at Turku PET Centre, University of Turku and Department of Radiology, University of Turku and Turku University Hospital.

Professor Riitta Parkkola was the supervisor of my thesis. I wish to thank her for the opportunity to conduct this thesis under her supervision and for sharing her enormous experience in the field of MRI. Her calm, optimistic, cheerful and supportive features have helped me through the enormous amount of nerve-wrecking work required by this thesis.

Professor Pirjo Nuutila is the second supervisor of my thesis. She recruited me to the DORIAN project after I graduated in 2012 and helped me to start of my scientific career. I wish to thank her for the excellent guidance through this project and for sharing her enormous experience in the field of PET and metabolic studies. I consider myself privileged to have had a chance to work with her.

Robert M. Badeau is a colleague and a friend whom I met first time after starting the DORIAN project in 2012. He is one of the most positive people I know with unbelievable professional scientific writing, teaching and social skills. The articles would not have been published without his help. I owe my sincerest gratitude to Robert also for revising language of this thesis. In addition, the innumerable conversations of various topics with Robert and with my other colleagues and friends Miikka Honka and Marco Bucci during the working days cheered me up and kept me going and, most importantly, grew positive attitude toward my work.

Marco Bucci, Heta Lipponen, Juho Raiko, Riku Kiviranta, Kaisa Ivaska, Henri Honka, Virva Saunavaara, Samuel Sandboge, Johan Eriksson, Patricia Iozzo, Kalle Koskensalo, Suvi Koskinen, Miikka Tarkia, Christoffer Stark, Kaisa Linderborg, Pasi Tuomikoski, Julius Laine, Juhani Knuuti, Riitta Parkkola and Pirjo Nuutila have been the key players of the studies. I want sincerely to thank them to give me support, help, wisdom, knowledge and most importantly fruitful comments to my manuscripts. I want also thank all my friends and co-workers in Turku PET Centre and Department of Diagnos-

tic Radiology of Turku University Hospital, the study nurses Mia Koutu and Paula Nyholm, the personnel of the Turku PET Centre including the radiographers, the laboratory technicians, the IT-team, the physicians and secretary Mirja Jyrkinen for extremely helpful and friendly atmosphere. I also want to thank the official reviewers of this thesis, professor Seppo Koskinen and professor Ritva Vanninen, for their important and constructive comments. In addition, I want to thank the director of Medical Imaging Centre of Southwest Finland, adjunct professor Roberto Blanco Sequeiros and professor Hannu Aronen for positive attitude toward my work.

Professor Outi Mäkitie was the leading person in Study II. I want to thank her giving me an opportunity to widen my knowledge in the field of  $^1\text{H}$  MR spectroscopy imaging and eventually write an article of the unique material gathered in Helsinki in collaboration with Heli Viljakainen, Antti Hakkarainen, Tero Saukkonen, Sanna Toiviainen-Salo, Nina Lundbom and Jesper Lundbom.

I want to thank my parents, Pentti and Saara, my little sister Elisa and her fiancé Mindaugas, my elder sister Heidi-Maria and her husband Hannu as well as my grandmother Eira, for support and interest towards my studies. In addition, I want to thank Marit and Kalevi, parents of my wife Minna, for their friendly and warm attitude towards me.

My deepest thanks are to my wife Minna and my daughters Milla and Ellen. My family has been the voice-of-reason for this project. Minna has supported me, most importantly during challenging times, from the very beginning of my thesis. Her love and positive attitude are essential to me.

The written work of this thesis was financially supported by Per Oscar Klingendahl's Fund, Juho Vainio's Foundation, Department of Diagnostic Radiology of Turku University and Turku University Hospital, the Hospital District of Southwest Finland and Radiological Society of Finland.

Turku, March 2017



## REFERENCES

- Abbatecola, A.M. & Paolisso, G. 2008, "Is there a relationship between insulin resistance and frailty syndrome?", *Current pharmaceutical design*, vol. 14, no. 4, pp. 405-410.
- Adams, H.J., Kwee, T.C., de Keizer, B., Fijnheer, R., de Klerk, J.M., Littooi, A.S. & Nievelstein, R.A. 2014, "Systematic review and meta-analysis on the diagnostic performance of FDG-PET/CT in detecting bone marrow involvement in newly diagnosed Hodgkin lymphoma: is bone marrow biopsy still necessary?", *Annals of Oncology*, vol. 25, no. 5, pp. 921-927.
- Adams, J.E. 2009, "Quantitative computed tomography", *European Journal of Radiology*, vol. 71, no. 3, pp. 415-424.
- Adler, B.J., Kaushansky, K. & Rubin, C.T. 2014, "Obesity-driven disruption of haematopoiesis and the bone marrow niche", *Nature reviews. Endocrinology*, vol. 10, no. 12, pp. 737-748.
- Agren, J.J., Julkunen, A. & Penttila, I. 1992, "Rapid separation of serum lipids for fatty acid analysis by a single aminopropyl column", *Journal of lipid research*, vol. 33, no. 12, pp. 1871-1876.
- American College of Radiology 2008, , *Practice parameter for the performance of quantitative computer tomography (QCT) bone densitometry*. Available: <http://www.acr.org/guidelines>.
- Aras, M., Dede, F., Ones, T., Inanir, S., Erdil, T.Y. & Turoglu, H.T. 2014, "Evaluation of physiological FDG uptake in the skeleton in adults: is it uniformly distributed?", *Revista espanola de medicina nuclear e imagen molecular*, vol. 33, no. 5, pp. 286-289.
- Arimoto, M.K., Nakamoto, Y., Nakatani, K., Ishimori, T., Yamashita, K., Takaori-Kondo, A. & Togashi, K. 2015, "Increased bone marrow uptake of 18F-FDG in leukemia patients: preliminary findings", *SpringerPlus*, vol. 4, pp. 521-015-1339-2. eCollection 2015.
- Armamento-Villareal, R., Aguirre, L., Napoli, N., Shah, K., Hilton, T., Sinacore, D.R., Qualls, C. & Villareal, D.T. 2014, "Changes in thigh muscle volume predict bone mineral density response to lifestyle therapy in frail, obese older adults", *Osteoporosis international*, vol. 25, no. 2, pp. 551-558.
- Ballon, D., Jakubowski, A., Gabrilove, J., Graham, M.C., Zakowski, M., Sheridan, C. & Koutcher, J.A. 1991, "In vivo measurements of bone marrow cellularity using volume-localized proton NMR spectroscopy", *Magnetic Resonance in Medicine*, vol. 19, no. 1, pp. 85-95.
- Basu, S., Houseni, M., Bural, G., Chamroonrat, W., Udupa, J., Mishra, S. & Alavi, A. 2007, "Magnetic resonance imaging based bone marrow segmentation for quantitative calculation of pure red marrow metabolism using 2-deoxy-2-[F-18]fluoro-D-glucose-positron emission tomography: a novel application with significant implications for combined structure-function approach", *Molecular imaging and biology*, vol. 9, no. 6, pp. 361-365.

- Baum, T., Yap, S.P., Karampinos, D.C., Nardo, L., Kuo, D., Burghardt, A.J., Masharani, U.B., Schwartz, A.V., Li, X. & Link, T.M. 2012, "Does vertebral bone marrow fat content correlate with abdominal adipose tissue, lumbar spine bone mineral density, and blood biomarkers in women with type 2 diabetes mellitus?", *Journal of magnetic resonance imaging : JMRI*, vol. 35, no. 1, pp. 117-124.
- Bemben, D.A. & Bemben, M.G. 2011, "Dose-response effect of 40 weeks of resistance training on bone mineral density in older adults", *Osteoporosis international*, vol. 22, no. 1, pp. 179-186.
- Blake, G.M., McKeeney, D.B., Chhaya, S.C., Ryan, P.J. & Fogelman, I. 1992, "Dual energy x-ray absorptiometry: the effects of beam hardening on bone density measurements", *Medical physics*, vol. 19, no. 2, pp. 459-465.
- Borra, R.J., Salo, S., Dean, K., Lautamaki, R., Nuutila, P., Komu, M. & Parkkola, R. 2009, "Nonalcoholic fatty liver disease: rapid evaluation of liver fat content with in-phase and out-of-phase MR imaging", *Radiology*, vol. 250, no. 1, pp. 130-136.
- Botolin, S., Faugere, M.C., Malluche, H., Orth, M., Meyer, R. & McCabe, L.R. 2005, "Increased bone adiposity and peroxisomal proliferator-activated receptor-gamma2 expression in type I diabetic mice", *Endocrinology*, vol. 146, no. 8, pp. 3622-3631.
- Bredella, M.A., Fazeli, P.K., Daley, S.M., Miller, K.K., Rosen, C.J., Klibanski, A. & Torriani, M. 2014, "Marrow fat composition in anorexia nervosa", *Bone*, vol. 66, pp. 199-204.
- Bucci, M., Huovinen, V., Guzzardi, M.A., Koskinen, S., Raiko, J.R., Lipponen, H., Ahsan, S., Badeau, R.M., Honka, M.J., Koffert, J., Savisto, N., Salonen, M.K., Andersson, J., Kullberg, J., Sandboge, S., Iozzo, P., Eriksson, J.G. & Nuutila, P. 2016, "Resistance training improves skeletal muscle insulin sensitivity in elderly offspring of overweight and obese mothers", *Diabetologia*, vol. 59, no. 1, pp. 77-86.
- Burger, E.H., Klein-Nulend, J. & Smit, T.H. 2003, "Strain-derived canalicular fluid flow regulates osteoclast activity in a remodelling osteon--a proposal", *Journal of Biomechanics*, vol. 36, no. 10, pp. 1453-1459.
- Calvi, L.M. & Link, D.C. 2014, "Cellular complexity of the bone marrow hematopoietic stem cell niche", *Calcified tissue international*, vol. 94, no. 1, pp. 112-124.
- Cann, C.E. 1988, "Quantitative CT for determination of bone mineral density: a review", *Radiology*, vol. 166, no. 2, pp. 509-522.
- Cann, C.E., Adams, J.E., Brown, J.K. & Brett, A.D. 2014, "CTXA hip--an extension of classical DXA measurements using quantitative CT", *PloS one*, vol. 9, no. 3, pp. e91904.
- Casazza, K., Hanks, L.J., Hidalgo, B., Hu, H.H. & Affuso, O. 2012, "Short-term physical activity intervention decreases femoral bone marrow adipose tissue in young children: a pilot study", *Bone*, vol. 50, no. 1, pp. 23-27.
- Casciaro, S., Conversano, F., Pisani, P. & Muratore, M. 2015, "New per-

- spectives in echographic diagnosis of osteoporosis on hip and spine", *Clinical cases in mineral and bone metabolism*, vol. 12, no. 2, pp. 142-150.
- Catalano, P.M., Presley, L., Minium, J. & Hauguel-de Mouzon, S. 2009, "Fetuses of obese mothers develop insulin resistance in utero", *Diabetes care*, vol. 32, no. 6, pp. 1076-1080.
- Challen, G.A., Boles, N., Lin, K.K. & Goodell, M.A. 2009, "Mouse hematopoietic stem cell identification and analysis", *Cytometry.Part A : the journal of the International Society for Analytical Cytology*, vol. 75, no. 1, pp. 14-24.
- Chen, Q., Shou, P., Zheng, C., Jiang, M., Cao, G., Yang, Q., Cao, J., Xie, N., Velletri, T., Zhang, X., Xu, C., Zhang, L., Yang, H., Hou, J., Wang, Y. & Shi, Y. 2016, "Fate decision of mesenchymal stem cells: adipocytes or osteoblasts?", *Cell death and differentiation*, vol. 23, no. 7, pp. 1128-1139.
- Clarke, B. 2008, "Normal bone anatomy and physiology", *Clinical journal of the American Society of Nephrology : CJASN*, vol. 3 Suppl 3, pp. S131-9.
- Clarke, B.L. & Drake, M.T. 2013, "Clinical utility of serum sclerostin measurements", *BoneKEy reports*, vol. 2, pp. 361.
- Coe, L.M., Lippner, D., Perez, G.I. & McCabe, L.R. 2011, "Caspase-2 deficiency protects mice from diabetes-induced marrow adiposity", *Journal of cellular biochemistry*, vol. 112, no. 9, pp. 2403-2411.
- Cullum, I.D., Ell, P.J. & Ryder, J.P. 1989, "X-ray dual-photon absorptiometry: a new method for the measurement of bone density", *The British journal of radiology*, vol. 62, no. 739, pp. 587-592.
- Damilakis, J., Adams, J.E., Guglielmi, G. & Link, T.M. 2010, "Radiation exposure in X-ray-based imaging techniques used in osteoporosis", *European radiology*, vol. 20, no. 11, pp. 2707-2714.
- DeFronzo, R.A., Tobin, J.D. & Andres, R. 1979, "Glucose clamp technique: a method for quantifying insulin secretion and resistance", *The American Journal of Physiology*, vol. 237, no. 3, pp. E214-23.
- Delaisse, J.M. 2014, "The reversal phase of the bone-remodeling cycle: cellular prerequisites for coupling resorption and formation", *BoneKEy reports*, vol. 3, pp. 561.
- Devlin, M.J., Cloutier, A.M., Thomas, N.A., Panus, D.A., Lotinun, S., Pinz, I., Baron, R., Rosen, C.J. & Bouxsein, M.L. 2010, "Caloric restriction leads to high marrow adiposity and low bone mass in growing mice", *Journal of bone and mineral research*, vol. 25, no. 9, pp. 2078-2088.
- Devlin, M.J. & Rosen, C.J. 2015, "The bone-fat interface: basic and clinical implications of marrow adiposity", *The lancet.Diabetes & endocrinology*, vol. 3, no. 2, pp. 141-147.
- Dhawan, V., Moeller, J.R., Strother, S.C., Evans, A.C. & Rottenberg, D.A. 1989, "Effect of selecting a fixed dephosphorylation rate on the estimation of rate constants and rCMRGlucose from dynamic [18F] fluorodeoxyglucose/PET data", *Journal of nuclear medicine*, vol. 30, no. 9, pp. 1483-1488.

- Disler, D.G., McCauley, T.R., Ratner, L.M., Kesack, C.D. & Cooper, J.A. 1997, "In-phase and out-of-phase MR imaging of bone marrow: prediction of neoplasia based on the detection of coexistent fat and water", *AJR.American journal of roentgenology*, vol. 169, no. 5, pp. 1439-1447.
- Dobnig, H. & Turner, R.T. 1995, "Evidence that intermittent treatment with parathyroid hormone increases bone formation in adult rats by activation of bone lining cells", *Endocrinology*, vol. 136, no. 8, pp. 3632-3638.
- Donahue, H.J., McLeod, K.J., Rubin, C.T., Andersen, J., Grine, E.A., Hertzberg, E.L. & Brink, P.R. 1995, "Cell-to-cell communication in osteoblastic networks: cell line-dependent hormonal regulation of gap junction function", *Journal of bone and mineral research*, vol. 10, no. 6, pp. 881-889.
- Engelke, K., Adams, J.E., Armbrecht, G., Augat, P., Bogado, C.E., Bouxsein, M.L., Felsenberg, D., Ito, M., Prevrhal, S., Hans, D.B. & Lewiecki, E.M. 2008, "Clinical use of quantitative computed tomography and peripheral quantitative computed tomography in the management of osteoporosis in adults: the 2007 ISCD Official Positions", *Journal of clinical densitometry*, vol. 11, no. 1, pp. 123-162.
- Engelke, K., Kemmler, W., Lauber, D., Beeskow, C., Pintag, R. & Kalender, W.A. 2006, "Exercise maintains bone density at spine and hip EFOPS: a 3-year longitudinal study in early postmenopausal women", *Osteoporosis international*, vol. 17, no. 1, pp. 133-142.
- Eriksen, E.F. 1986, "Normal and pathological remodeling of human trabecular bone: three dimensional reconstruction of the remodeling sequence in normals and in metabolic bone disease", *Endocrine reviews*, vol. 7, no. 4, pp. 379-408.
- Eriksen, E.F., Diez-Perez, A. & Boonen, S. 2014, "Update on long-term treatment with bisphosphonates for postmenopausal osteoporosis: a systematic review", *Bone*, vol. 58, pp. 126-135.
- Eriksson, J.G., Sandboge, S., Salonen, M.K., Kajantie, E. & Osmond, C. 2014, "Long-term consequences of maternal overweight in pregnancy on offspring later health: findings from the Helsinki Birth Cohort Study", *Annals of Medicine*, vol. 46, no. 6, pp. 434-438.
- Fan, C., Hernandez-Pampaloni, M., Houseni, M., Chamroonrat, W., Basu, S., Kumar, R., Dadparvar, S., Torigian, D.A. & Alavi, A. 2007, "Age-related changes in the metabolic activity and distribution of the red marrow as demonstrated by 2-deoxy-2-[F-18]fluoro-D-glucose-positron emission tomography", *Molecular imaging and biology*, vol. 9, no. 5, pp. 300-307.
- Fazeli, P.K., Bredella, M.A., Freedman, L., Thomas, B.J., Breggia, A., Meenaghan, E., Rosen, C.J. & Klibanski, A. 2012, "Marrow fat and preadipocyte factor-1 levels decrease with recovery in women with anorexia nervosa", *Journal of bone and mineral research*, vol. 27, no. 9, pp. 1864-1871.
- Fazeli, P.K., Horowitz, M.C., MacDougald, O.A., Scheller, E.L., Rodeheffer, M.S., Rosen, C.J. & Klibanski, A. 2013, "Marrow fat and bone--new perspectives", *The*



- Journal of clinical endocrinology and metabolism*, vol. 98, no. 3, pp. 935-945.
- Fazzalari, N.L. 2011, "Bone fracture and bone fracture repair", *Osteoporosis international*, vol. 22, no. 6, pp. 2003-2006.
- Felsenberg, D. & Gowin, W. 1999, "Bone densitometry by dual energy methods", *Der Radiologe*, vol. 39, no. 3, pp. 186-193.
- Folch, J., Lees, M. & Sloane Stanley, G.H. 1957, "A simple method for the isolation and purification of total lipides from animal tissues", *The Journal of biological chemistry*, vol. 226, no. 1, pp. 497-509.
- Frost, H.M. & Schonau, E. 2000, "The "muscle-bone unit" in children and adolescents: a 2000 overview", *Journal of pediatric endocrinology & metabolism : JPEM*, vol. 13, no. 6, pp. 571-590.
- Gallagher, J.C. 2001, "Role of estrogens in the management of postmenopausal bone loss", *Rheumatic diseases clinics of North America*, vol. 27, no. 1, pp. 143-162.
- Garnero, P., Sornay-Rendu, E., Munoz, F., Borel, O. & Chapurlat, R.D. 2013, "Association of serum sclerostin with bone mineral density, bone turnover, steroid and parathyroid hormones, and fracture risk in postmenopausal women: the OFELY study", *Osteoporosis international*, vol. 24, no. 2, pp. 489-494.
- Georgiou, K.R., Hui, S.K. & Xian, C.J. 2012, "Regulatory pathways associated with bone loss and bone marrow adiposity caused by aging, chemotherapy, glucocorticoid therapy and radiotherapy", *American journal of stem cells*, vol. 1, no. 3, pp. 205-224.
- Gimble, J.M. & Nuttall, M.E. 2004, "Bone and fat: old questions, new insights", *Endocrine*, vol. 23, no. 2-3, pp. 183-188.
- Gimble, J.M., Robinson, C.E., Wu, X. & Kelly, K.A. 1996, "The function of adipocytes in the bone marrow stroma: an update", *Bone*, vol. 19, no. 5, pp. 421-428.
- Greco, E.A., Lenzi, A. & Migliaccio, S. 2015, "The obesity of bone", *Therapeutic advances in endocrinology and metabolism*, vol. 6, no. 6, pp. 273-286.
- Griffith, J.F., Yeung, D.K., Ahuja, A.T., Choy, C.W., Mei, W.Y., Lam, S.S., Lam, T.P., Chen, Z.Y. & Leung, P.C. 2009, "A study of bone marrow and subcutaneous fatty acid composition in subjects of varying bone mineral density", *Bone*, vol. 44, no. 6, pp. 1092-1096.
- Griffith, J.F., Yeung, D.K., Ma, H.T., Leung, J.C., Kwok, T.C. & Leung, P.C. 2012, "Bone marrow fat content in the elderly: a reversal of sex difference seen in younger subjects", *Journal of magnetic resonance imaging : JMRI*, vol. 36, no. 1, pp. 225-230.
- Hajek, M. & Dezortova, M. 2008, "Introduction to clinical in vivo MR spectroscopy", *European Journal of Radiology*, vol. 67, no. 2, pp. 185-193.
- Hallsten, K., Yki-Jarvinen, H., Peltoniemi, P., Oikonen, V., Takala, T., Kemppainen, J., Laine, H., Bergman, J., Bolli, G.B., Knuuti, J. & Nuutila, P. 2003, "Insulin- and exercise-stimulated skeletal muscle blood flow and glucose uptake in

- obese men", *Obesity research*, vol. 11, no. 2, pp. 257-265.
- Hamacher, K., Coenen, H.H. & Stocklin, G. 1986, "Efficient stereospecific synthesis of no-carrier-added 2-[18F]-fluoro-2-deoxy-D-glucose using aminopolyether supported nucleophilic substitution", *Journal of nuclear medicine*, vol. 27, no. 2, pp. 235-238.
- Hamilton, C.J., Swan, V.J. & Jamal, S.A. 2010, "The effects of exercise and physical activity participation on bone mass and geometry in postmenopausal women: a systematic review of pQCT studies", *Osteoporosis international*, vol. 21, no. 1, pp. 11-23.
- Hamilton, J.G. & Comai, K. 1988, "Rapid separation of neutral lipids, free fatty acids and polar lipids using prepacked silica Sep-Pak columns", *Lipids*, vol. 23, no. 12, pp. 1146-1149.
- Hamrick, M.W., McGee-Lawrence, M.E. & Frechette, D.M. 2016, "Fatty Infiltration of Skeletal Muscle: Mechanisms and Comparisons with Bone Marrow Adiposity", *Frontiers in endocrinology*, vol. 7, pp. 69.
- Hardouin, P., Pansini, V. & Cortet, B. 2014, "Bone marrow fat", *Joint, bone, spine : revue du rhumatisme*, vol. 81, no. 4, pp. 313-319.
- He, J., Zhang, H., Wang, C., Zhang, Z., Yue, H., Hu, W., Gu, J., Fu, W., Hu, Y., Li, M., Liu, Y., Zheng, H. & Zhang, Z. 2014, "Associations of serum sclerostin and polymorphisms in the SOST gene with bone mineral density and markers of bone metabolism in postmenopausal Chinese women", *The Journal of clinical endocrinology and metabolism*, vol. 99, no. 4, pp. E665-73.
- Heinonen, A., Sievanen, H., Kannus, P., Oja, P. & Vuori, I. 2002, "Site-specific skeletal response to long-term weight training seems to be attributable to principal loading modality: a pQCT study of female weightlifters", *Calcified tissue international*, vol. 70, no. 6, pp. 469-474.
- Heinonen, I., Kalliokoski, K.K., Hannukainen, J.C., Duncker, D.J., Nuutila, P. & Knuuti, J. 2014, "Organ-specific physiological responses to acute physical exercise and long-term training in humans", *Physiology (Bethesda, Md.)*, vol. 29, no. 6, pp. 421-436.
- Heinonen, I., Kemppainen, J., Kaskinoro, K., Langberg, H., Knuuti, J., Boushel, R., Kjaer, M. & Kalliokoski, K.K. 2013, "Bone blood flow and metabolism in humans: effect of muscular exercise and other physiological perturbations", *Journal of bone and mineral research*, vol. 28, no. 5, pp. 1068-1074.
- Heinonen, I., Nesterov, S.V., Kemppainen, J., Fujimoto, T., Knuuti, J. & Kalliokoski, K.K. 2012, "Increasing exercise intensity reduces heterogeneity of glucose uptake in human skeletal muscles", *PloS one*, vol. 7, no. 12, pp. e52191.
- Hesselink, J. 2005, , *Fundamentals of MR spectroscopy*. Available: <http://spinwarp.ucsd.edu/NeuroWeb/Text/mrs-TXT.htm>. 2016.
- Honka, H., Makinen, J., Hannukainen, J.C., Tarkia, M., Oikonen, V., Teras, M., Fagerholm, V., Ishizu, T., Saraste, A., Stark, C., Vahasilta, T., Salminen, P., Kirjavainen, A., Soinio, M., Gastaldelli, A., Knuuti,

- J., Iozzo, P. & Nuutila, P. 2013, "Validation of [18F]fluorodeoxyglucose and positron emission tomography (PET) for the measurement of intestinal metabolism in pigs, and evidence of intestinal insulin resistance in patients with morbid obesity", *Diabetologia*, vol. 56, no. 4, pp. 893-900.
- Howe, T.E., Shea, B., Dawson, L.J., Downie, F., Murray, A., Ross, C., Harbour, R.T., Caldwell, L.M. & Creed, G. 2011, "Exercise for preventing and treating osteoporosis in postmenopausal women", *The Cochrane database of systematic reviews*, vol. (7):CD000333. doi, no. 7, pp. CD000333.
- Hu, H.H. & Kan, H.E. 2013, "Quantitative proton MR techniques for measuring fat", *NMR in biomedicine*, vol. 26, no. 12, pp. 1609-1629.
- Hudec, S.M. & Camacho, P.M. 2013, "Secondary causes of osteoporosis", *Endocrine practice*, vol. 19, no. 1, pp. 120-128.
- Huh, J.H., Song, M.K., Park, K.H., Kim, K.J., Kim, J.E., Rhee, Y.M. & Lim, S.K. 2014, "Gender-specific pleiotropic bone-muscle relationship in the elderly from a nationwide survey (KNHANES IV)", *Osteoporosis international*, vol. 25, no. 3, pp. 1053-1061.
- Iozzo, P., Gastaldelli, A., Jarvisalo, M.J., Kiss, J., Borra, R., Buzzigoli, E., Viljanen, A., Naum, G., Viljanen, T., Oikonen, V., Knuuti, J., Savunen, T., Salvadori, P.A., Ferrannini, E. & Nuutila, P. 2006, "18F-FDG assessment of glucose disposal and production rates during fasting and insulin stimulation: a validation study", *Journal of nuclear medicine*, vol. 47, no. 6, pp. 1016-1022.
- Iozzo, P., Holmes, M., Schmidt, M.V., Cirulli, F., Guzzardi, M.A., Berry, A., Balsevich, G., Andreassi, M.G., Wesselink, J.J., Liistro, T., Gomez-Puertas, P., Eriksson, J.G. & Seckl, J. 2014, "Developmental ORIGins of Healthy and Unhealthy AgeiNg: the role of maternal obesity--introduction to DORIAN", *Obesity facts*, vol. 7, no. 2, pp. 130-151.
- Jagannathan, N.R., Singh, M., Govindaraju, V., Raghunathan, P., Coshic, O., Julka, P.K. & Rath, G.K. 1998, "Volume localized in vivo proton MR spectroscopy of breast carcinoma: variation of water-fat ratio in patients receiving chemotherapy", *NMR in biomedicine*, vol. 11, no. 8, pp. 414-422.
- Japur, C.C., Penaforte, F.R., Chiarello, P.G., Monteiro, J.P., Vieira, M.N. & Basile-Filho, A. 2009, "Harris-Benedict equation for critically ill patients: are there differences with indirect calorimetry?", *Journal of critical care*, vol. 24, no. 4, pp. 628.e1-628.e5.
- Kanis, J.A. 1994, "Assessment of fracture risk and its application to screening for postmenopausal osteoporosis: synopsis of a WHO report. WHO Study Group", *Osteoporosis international*, vol. 4, no. 6, pp. 368-381.
- Kanis, J.A., Johnell, O., Oden, A., Johansson, H. & McCloskey, E. 2008a, "FRAX and the assessment of fracture probability in men and women from the UK", *Osteoporosis international*, vol. 19, no. 4, pp. 385-397.
- Kanis, J.A., Johnell, O., Oden, A., Jansson, B., De Laet, C. & Dawson, A.

- 2000, "Risk of hip fracture according to the World Health Organization criteria for osteopenia and osteoporosis", *Bone*, vol. 27, no. 5, pp. 585-590.
- Kanis, J.A., McCloskey, E.V., Johansson, H., Cooper, C., Rizzoli, R., Reginster, J.Y. & Scientific Advisory Board of the European Society for Clinical and Economic Aspects of Osteoporosis and Osteoarthritis (ESCEO) and the Committee of Scientific Advisors of the International Osteoporosis Foundation (IOF) 2013, "European guidance for the diagnosis and management of osteoporosis in postmenopausal women", *Osteoporosis international*, vol. 24, no. 1, pp. 23-57.
- Kanis, J.A., McCloskey, E.V., Johansson, H., Strom, O., Borgstrom, F., Oden, A. & National Osteoporosis Guideline Group 2008b, "Case finding for the management of osteoporosis with FRAX--assessment and intervention thresholds for the UK", *Osteoporosis international*, vol. 19, no. 10, pp. 1395-1408.
- Kanis, J.A., Oden, A., Johansson, H., Borgstrom, F., Strom, O. & McCloskey, E. 2009, "FRAX and its applications to clinical practice", *Bone*, vol. 44, no. 5, pp. 734-743.
- Karlsson, M.K. & Rosengren, B.E. 2012, "Training and bone - from health to injury", *Scandinavian Journal of Medicine & Science in Sports*, vol. 22, no. 4, pp. e15-23.
- Kawai, M., de Paula, F.J. & Rosen, C.J. 2012, "New insights into osteoporosis: the bone-fat connection", *Journal of internal medicine*, vol. 272, no. 4, pp. 317-329.
- Khoo, B.C., Brown, K., Cann, C., Zhu, K., Henzell, S., Low, V., Gustafsson, S., Price, R.I. & Prince, R.L. 2009, "Comparison of QCT-derived and DXA-derived areal bone mineral density and T scores", *Osteoporosis international*, vol. 20, no. 9, pp. 1539-1545.
- Kreel, L. 1976, "The EMI whole body scanner in the demonstration of lymph node enlargement", *Clinical radiology*, vol. 27, no. 4, pp. 421-429.
- Krings, A., Rahman, S., Huang, S., Lu, Y., Czernik, P.J. & Lecka-Czernik, B. 2012, "Bone marrow fat has brown adipose tissue characteristics, which are attenuated with aging and diabetes", *Bone*, vol. 50, no. 2, pp. 546-552.
- Kugel, H., Jung, C., Schulte, O. & Heindel, W. 2001, "Age- and sex-specific differences in the 1H-spectrum of vertebral bone marrow", *Journal of magnetic resonance imaging : JMRI*, vol. 13, no. 2, pp. 263-268.
- Kylmaja, E., Nakamura, M. & Tuukkanen, J. 2015, "Osteoclasts and Remodeling Based Bone Formation", *Current stem cell research & therapy*, .
- Lang, T.F., Li, J., Harris, S.T. & Genant, H.K. 1999, "Assessment of vertebral bone mineral density using volumetric quantitative CT", *Journal of computer assisted tomography*, vol. 23, no. 1, pp. 130-137.
- Lang, T.F., Saeed, I.H., Streeper, T., Carballido-Gamio, J., Harnish, R.J., Frassetto, L.A., Lee, S.M., Sibonga, J.D., Keyak, J.H., Spiering, B.A., Grodzinsky, C.M., Bloomberg, J.J. & Cavanagh, P.R. 2014, "Spatial heterogeneity in the response of the proximal femur to

- two lower-body resistance exercise regimens", *Journal of bone and mineral research*, vol. 29, no. 6, pp. 1337-1345.
- Laval-Jeantet, A.M., Roger, B., Bouysee, S., Bergot, C. & Mazess, R.B. 1986, "Influence of vertebral fat content on quantitative CT density", *Radiology*, vol. 159, no. 2, pp. 463-466.
- LeBlanc, A., Lin, C., Evans, H., Shackelford, L., Martin, C. & Hedrick, T. 1999, "T2 vertebral bone marrow changes after space flight", *Magnetic resonance in medicine*, vol. 41, no. 3, pp. 495-498.
- Lecka-Czernik, B. 2012, "Marrow fat metabolism is linked to the systemic energy metabolism", *Bone*, vol. 50, no. 2, pp. 534-539.
- Lecka-Czernik, B., Stechschulte, L.A., Czernik, P.J. & Dowling, A.R. 2015, "High bone mass in adult mice with diet-induced obesity results from a combination of initial increase in bone mass followed by attenuation in bone formation; implications for high bone mass and decreased bone quality in obesity", *Molecular and cellular endocrinology*, vol. 410, pp. 35-41.
- Lehtonen-Veromaa, M., Mottonen, T., Svedstrom, E., Hakola, P., Heinenon, O.J. & Viikari, J. 2000, "Physical activity and bone mineral acquisition in peripubertal girls", *Scandinavian Journal of Medicine & Science in Sports*, vol. 10, no. 4, pp. 236-243.
- Lewiecki, E.M., Gordon, C.M., Baim, S., Leonard, M.B., Bishop, N.J., Bianchi, M.L., Kalkwarf, H.J., Langman, C.B., Plotkin, H., Rauch, F., Zemel, B.S., Binkley, N., Bilezikian, J.P., Kendler, D.L., Hans, D.B. & Silverman, S. 2008, "International Society for Clinical Densitometry 2007 Adult and Pediatric Official Positions", *Bone*, vol. 43, no. 6, pp. 1115-1121.
- Li, B., Jiang, Y., Sun, J., Liang, J. & Jin, Y. 2016, "MR spectroscopy for assessing the effects of oxytocin on marrow adipogenesis induced by glucocorticoid in rabbits", *Acta Radiologica (Stockholm, Sweden : 1987)*, vol. 57, no. 6, pp. 701-707.
- Li, W., Sode, M., Saeed, I. & Lang, T. 2006, "Automated registration of hip and spine for longitudinal QCT studies: integration with 3D densitometric and structural analysis", *Bone*, vol. 38, no. 2, pp. 273-279.
- Li, X., Kuo, D., Schafer, A.L., Porzig, A., Link, T.M., Black, D. & Schwartz, A.V. 2011, "Quantification of vertebral bone marrow fat content using 3 Tesla MR spectroscopy: reproducibility, vertebral variation, and applications in osteoporosis", *Journal of magnetic resonance imaging : JMRI*, vol. 33, no. 4, pp. 974-979.
- Lin, J.T. & Lane, J.M. 2008, "Non-pharmacologic management of osteoporosis to minimize fracture risk", *Nature clinical practice.Rheumatology*, vol. 4, no. 1, pp. 20-25.
- Liney, G.P., Bernard, C.P., Manton, D.J., Turnbull, L.W. & Langton, C.M. 2007, "Age, gender, and skeletal variation in bone marrow composition: a preliminary study at 3.0 Tesla", *Journal of magnetic resonance imaging : JMRI*, vol. 26, no. 3, pp. 787-793.
- Lundbom, J., Hakkarainen, A., Fielding, B., Soderlund, S., Westerbacka, J.,

- Taskinen, M.R. & Lundbom, N. 2010, "Characterizing human adipose tissue lipids by long echo time 1H-MRS in vivo at 1.5 Tesla: validation by gas chromatography", *NMR in biomedicine*, vol. 23, no. 5, pp. 466-472.
- Lundbom, J., Hakkarainen, A., Soderlund, S., Westerbacka, J., Lundbom, N. & Taskinen, M.R. 2011, "Long-TE 1H MRS suggests that liver fat is more saturated than subcutaneous and visceral fat", *NMR in biomedicine*, vol. 24, no. 3, pp. 238-245.
- Luo, Q., Leng, H., Wang, X., Zhou, Y. & Rong, Q. 2014, "The role of water and mineral-collagen interfacial bonding on microdamage progression in bone", *Journal of orthopaedic research*, vol. 32, no. 2, pp. 217-223.
- Ma, H.T., Griffith, J.F., Xu, L. & Leung, P.C. 2014, "The functional muscle-bone unit in subjects of varying BMD", *Osteoporosis international*, vol. 25, no. 3, pp. 999-1004.
- Ma, J. 2008, "Dixon techniques for water and fat imaging", *Journal of magnetic resonance imaging : JMRI*, vol. 28, no. 3, pp. 543-558.
- Machann, J., Stefan, N. & Schick, F. 2008, "(1)H MR spectroscopy of skeletal muscle, liver and bone marrow", *European Journal of Radiology*, vol. 67, no. 2, pp. 275-284.
- Maddalozzo, G.F. & Snow, C.M. 2000, "High intensity resistance training: effects on bone in older men and women", *Calcified tissue international*, vol. 66, no. 6, pp. 399-404.
- Marques, E.A., Mota, J. & Carvalho, J. 2012, "Exercise effects on bone mineral density in older adults: a meta-analysis of randomized controlled trials", *Age (Dordrecht, Netherlands)*, vol. 34, no. 6, pp. 1493-1515.
- Marques, E.A., Wanderley, F., Machado, L., Sousa, F., Viana, J.L., Moreira-Goncalves, D., Moreira, P., Mota, J. & Carvalho, J. 2011, "Effects of resistance and aerobic exercise on physical function, bone mineral density, OPG and RANKL in older women", *Experimental gerontology*, vol. 46, no. 7, pp. 524-532.
- Martyn-St James, M. & Carroll, S. 2006, "High-intensity resistance training and postmenopausal bone loss: a meta-analysis", *Osteoporosis international*, vol. 17, no. 8, pp. 1225-1240.
- Mastmeyer, A., Engelke, K., Fuchs, C. & Kalender, W.A. 2006, "A hierarchical 3D segmentation method and the definition of vertebral body coordinate systems for QCT of the lumbar spine", *Medical image analysis*, vol. 10, no. 4, pp. 560-577.
- Matsushita, M., Yoneshiro, T., Aita, S., Kameya, T., Sugie, H. & Saito, M. 2014, "Impact of brown adipose tissue on body fatness and glucose metabolism in healthy humans", *International journal of obesity (2005)*, vol. 38, no. 6, pp. 812-817.
- McClung, M.R., Geusens, P., Miller, P.D., Zippel, H., Bensen, W.G., Roux, C., Adami, S., Fogelman, I., Diamond, T., Eastell, R., Meunier, P.J., Reginster, J.Y. & Hip Intervention Program Study Group 2001, "Effect of risedronate on the risk of hip fracture in elderly women. Hip Intervention Program Study Group", *The New England journal*

- of medicine*, vol. 344, no. 5, pp. 333-340.
- Mingrone, G., Manco, M., Mora, M.E., Guidone, C., Iaconelli, A., Gniuli, D., Leccesi, L., Chiellini, C. & Ghirlanda, G. 2008, "Influence of maternal obesity on insulin sensitivity and secretion in offspring", *Diabetes care*, vol. 31, no. 9, pp. 1872-1876.
- Misra, M. & Klibanski, A. 2013, "Anorexia nervosa, obesity and bone metabolism", *Pediatric endocrinology reviews : PER*, vol. 11, no. 1, pp. 21-33.
- Modder, U.I., Hoey, K.A., Amin, S., McCready, L.K., Achenbach, S.J., Riggs, B.L., Melton, L.J., 3rd & Khosla, S. 2011, "Relation of age, gender, and bone mass to circulating sclerostin levels in women and men", *Journal of bone and mineral research*, vol. 26, no. 2, pp. 373-379.
- Moore KL, D.A. 2006, *Clinically Oriented Anatomy*, 5th edition edn, Lippincott Williams & Wilkins.
- Moore, S.G. & Dawson, K.L. 1990, "Red and yellow marrow in the femur: age-related changes in appearance at MR imaging", *Radiology*, vol. 175, no. 1, pp. 219-223.
- Nelson, M.E., Fiatarone, M.A., Morganti, C.M., Trice, I., Greenberg, R.A. & Evans, W.J. 1994, "Effects of high-intensity strength training on multiple risk factors for osteoporotic fractures. A randomized controlled trial", *Jama*, vol. 272, no. 24, pp. 1909-1914.
- Ng, J.M., Azuma, K., Kelley, C., Pencek, R., Radikova, Z., Laymon, C., Price, J., Goodpaster, B.H. & Kelley, D.E. 2012, "PET imaging reveals distinctive roles for different regional adipose tissue depots in systemic glucose metabolism in nonobese humans", *American journal of physiology. Endocrinology and metabolism*, vol. 303, no. 9, pp. E1134-41.
- NIH Consensus Development Panel on Osteoporosis Prevention, Diagnosis, and Therapy 2001, "Osteoporosis prevention, diagnosis, and therapy", *Jama*, vol. 285, no. 6, pp. 785-795.
- Nouh, M.R. & Eid, A.F. 2015, "Magnetic resonance imaging of the spinal marrow: Basic understanding of the normal marrow pattern and its variant", *World journal of radiology*, vol. 7, no. 12, pp. 448-458.
- Nuutila, P., Koivisto, V.A., Knuuti, J., Ruotsalainen, U., Teras, M., Haaparanta, M., Bergman, J., Solin, O., Voipio-Pulkki, L.M. & Wegelius, U. 1992, "Glucose-free fatty acid cycle operates in human heart and skeletal muscle in vivo", *The Journal of Clinical Investigation*, vol. 89, no. 6, pp. 1767-1774.
- Office of the Surgeon General (US) 2004, *Bone Health and Osteoporosis: A Report of the Surgeon General*. Office of the Surgeon General (US), Rockville (MD).
- Ojanen, X., Borra, R.J., Havu, M., Cheng, S.M., Parkkola, R., Nuutila, P., Alen, M. & Cheng, S. 2014, "Comparison of vertebral bone marrow fat assessed by (1)H MRS and inphase and out-of-phase MRI among family members", *Osteoporosis international*, vol. 25, no. 2, pp. 653-662.
- Okano, H., Mizunuma, H., Soda, M., Kagami, I., Miyamoto, S., Ohsawa, M., Ibuki, Y., Shiraki, M., Suzuki,

- T. & Shibata, H. 1998, "The long-term effect of menopause on postmenopausal bone loss in Japanese women: results from a prospective study", *Journal of bone and mineral research*, vol. 13, no. 2, pp. 303-309.
- Orava, J., Nuutila, P., Noponen, T., Parkkola, R., Viljanen, T., Enerback, S., Rissanen, A., Pietilainen, K.H. & Virtanen, K.A. 2013, "Blunted metabolic responses to cold and insulin stimulation in brown adipose tissue of obese humans", *Obesity (Silver Spring, Md.)*, vol. 21, no. 11, pp. 2279-2287.
- Pagnotti, G.M. & Styner, M. 2016, "Exercise Regulation of Marrow Adipose Tissue", *Frontiers in endocrinology*, vol. 7, pp. 94.
- Parfitt, A.M. 2002, "Targeted and non-targeted bone remodeling: relationship to basic multicellular unit origination and progression", *Bone*, vol. 30, no. 1, pp. 5-7.
- Patlak, C.S. & Blasberg, R.G. 1985, "Graphical evaluation of blood-to-brain transfer constants from multiple-time uptake data. Generalizations", *Journal of cerebral blood flow and metabolism*, vol. 5, no. 4, pp. 584-590.
- Patsch, J.M., Li, X., Baum, T., Yap, S.P., Karampinos, D.C., Schwartz, A.V. & Link, T.M. 2013, "Bone marrow fat composition as a novel imaging biomarker in postmenopausal women with prevalent fragility fractures", *Journal of bone and mineral research*, vol. 28, no. 8, pp. 1721-1728.
- Peltoniemi, P., Lonroth, P., Laine, H., Oikonen, V., Tolvanen, T., Gronroos, T., Strindberg, L., Knuuti, J. & Nuutila, P. 2000, "Lumped constant for [(18)F]fluorodeoxyglucose in skeletal muscles of obese and nonobese humans", *American journal of physiology. Endocrinology and metabolism*, vol. 279, no. 5, pp. E1122-30.
- Peltoniemi, P., Yki-Jarvinen, H., Oikonen, V., Oksanen, A., Takala, T.O., Ronnema, T., Erkinjuntti, M., Knuuti, M.J. & Nuutila, P. 2001, "Resistance to exercise-induced increase in glucose uptake during hyperinsulinemia in insulin-resistant skeletal muscle of patients with type 1 diabetes", *Diabetes*, vol. 50, no. 6, pp. 1371-1377.
- Phelps, M.E., Huang, S.C., Hoffman, E.J., Selin, C., Sokoloff, L. & Kuhl, D.E. 1979, "Tomographic measurement of local cerebral glucose metabolic rate in humans with (F-18)2-fluoro-2-deoxy-D-glucose: validation of method", *Annals of Neurology*, vol. 6, no. 5, pp. 371-388.
- Pittenger, M.F., Mackay, A.M., Beck, S.C., Jaiswal, R.K., Douglas, R., Mosca, J.D., Moorman, M.A., Simonetti, D.W., Craig, S. & Marshak, D.R. 1999, "Multilineage potential of adult human mesenchymal stem cells", *Science (New York, N.Y.)*, vol. 284, no. 5411, pp. 143-147.
- Polyzos, S.A., Anastasilakis, A.D., Bratengeier, C., Woloszczuk, W., Papatheodorou, A. & Terpos, E. 2012, "Serum sclerostin levels positively correlate with lumbar spinal bone mineral density in postmenopausal women--the six-month effect of risedronate and teriparatide", *Osteoporosis international*, vol. 23, no. 3, pp. 1171-1176.



- Pontikoglou, C., Deschaseaux, F., Sensebe, L. & Papadaki, H.A. 2011, "Bone marrow mesenchymal stem cells: biological properties and their role in hematopoiesis and hematopoietic stem cell transplantation", *Stem cell reviews*, vol. 7, no. 3, pp. 569-589.
- Provencher, S.W. 1993, "Estimation of metabolite concentrations from localized in vivo proton NMR spectra", *Magnetic resonance in medicine*, vol. 30, no. 6, pp. 672-679.
- Proytcheva, M. 2013, "Bone marrow evaluation for pediatric patients", *International journal of laboratory hematology*, vol. 35, no. 3, pp. 283-289.
- Ragab, Y., Emad, Y., Gheita, T., Mansour, M., Abou-Zeid, A., Ferrari, S. & Rasker, J.J. 2009, "Differentiation of osteoporotic and neoplastic vertebral fractures by chemical shift {in-phase and out-of phase} MR imaging", *European Journal of Radiology*, vol. 72, no. 1, pp. 125-133.
- Raggatt, L.J. & Partridge, N.C. 2010, "Cellular and molecular mechanisms of bone remodeling", *The Journal of biological chemistry*, vol. 285, no. 33, pp. 25103-25108.
- Rantalainen, T., Nikander, R., Heinenon, A., Cervinka, T., Sievanen, H. & Daly, R.M. 2013, "Differential effects of exercise on tibial shaft marrow density in young female athletes", *The Journal of clinical endocrinology and metabolism*, vol. 98, no. 5, pp. 2037-2044.
- Reeder, S.B., Hu, H.H. & Sirlin, C.B. 2012, "Proton density fat-fraction: a standardized MR-based biomarker of tissue fat concentration", *Journal of magnetic resonance imaging : JMRI*, vol. 36, no. 5, pp. 1011-1014.
- Reichkender, M.H., Auerbach, P., Rosenkilde, M., Christensen, A.N., Holm, S., Petersen, M.B., Lagerberg, A., Larsson, H.B., Rostrup, E., Mosbech, T.H., Sjodin, A., Kjaer, A., Ploug, T., Hoejgaard, L. & Stallknecht, B. 2013, "Exercise training favors increased insulin-stimulated glucose uptake in skeletal muscle in contrast to adipose tissue: a randomized study using FDG PET imaging", *American journal of physiology. Endocrinology and metabolism*, vol. 305, no. 4, pp. E496-506.
- Rosen, C.J., Ackert-Bicknell, C., Rodriguez, J.P. & Pino, A.M. 2009, "Marrow fat and the bone microenvironment: developmental, functional, and pathological implications", *Critical reviews in eukaryotic gene expression*, vol. 19, no. 2, pp. 109-124.
- Rosen, C.J. & Bouxsein, M.L. 2006, "Mechanisms of disease: is osteoporosis the obesity of bone?", *Nature clinical practice. Rheumatology*, vol. 2, no. 1, pp. 35-43.
- Rosen, E.D. & MacDougald, O.A. 2006, "Adipocyte differentiation from the inside out", *Nature reviews. Molecular cell biology*, vol. 7, no. 12, pp. 885-896.
- Rudroff, T., Kindred, J.H. & Kalliokoski, K.K. 2015, "[<sup>18</sup>F]-FDG positron emission tomography--an established clinical tool opening a new window into exercise physiology", *Journal of applied physiology (Bethesda, Md.: 1985)*, vol. 118, no. 10, pp. 1181-1190.

- Sachpekidis, C., Mai, E.K., Goldschmidt, H., Hillengass, J., Hose, D., Pan, L., Haberkorn, U. & Dimitrakopoulou-Strauss, A. 2015, "(18)F-FDG dynamic PET/CT in patients with multiple myeloma: patterns of tracer uptake and correlation with bone marrow plasma cell infiltration rate", *Clinical nuclear medicine*, vol. 40, no. 6, pp. e300-7.
- Sadie-Van Gijsen, H., Hough, F.S. & Ferris, W.F. 2013, "Determinants of bone marrow adiposity: the modulation of peroxisome proliferator-activated receptor-gamma2 activity as a central mechanism", *Bone*, vol. 56, no. 2, pp. 255-265.
- Sambrook, P. & Cooper, C. 2006, "Osteoporosis", *Lancet (London, England)*, vol. 367, no. 9527, pp. 2010-2018.
- Samuelsson, A.M., Matthews, P.A., Argenton, M., Christie, M.R., McConnell, J.M., Jansen, E.H., Piersma, A.H., Ozanne, S.E., Twinn, D.F., Remacle, C., Rowleson, A., Poston, L. & Taylor, P.D. 2008, "Diet-induced obesity in female mice leads to offspring hyperphagia, adiposity, hypertension, and insulin resistance: a novel murine model of developmental programming", *Hypertension*, vol. 51, no. 2, pp. 383-392.
- Schick, F., Einsele, H., Kost, R., Duda, S., Jung, W.I., Lutz, O. & Claussen, C.D. 1994, "Hematopoietic reconstitution after bone marrow transplantation: assessment with MR imaging and H-1 localized spectroscopy", *Journal of magnetic resonance imaging: JMRI*, vol. 4, no. 1, pp. 71-78.
- Schild, H. 2012, *MRI made easy*, Bayer Pharma Ag, Germany.
- Schwartz, A.V., Sigurdsson, S., Hue, T.F., Lang, T.F., Harris, T.B., Rosen, C.J., Vittinghoff, E., Siggeirsdottir, K., Sigurdsson, G., Oskarsdottir, D., Shet, K., Palermo, L., Gudnason, V. & Li, X. 2013, "Vertebral bone marrow fat associated with lower trabecular BMD and prevalent vertebral fracture in older adults", *The Journal of clinical endocrinology and metabolism*, vol. 98, no. 6, pp. 2294-2300.
- Seeman, E. 2013, "Age- and menopause-related bone loss compromise cortical and trabecular microstructure", *The journals of gerontology. Series A, Biological sciences and medical sciences*, vol. 68, no. 10, pp. 1218-1225.
- Shi, Y. & Hu, F.B. 2014, "The global implications of diabetes and cancer", *Lancet (London, England)*, vol. 383, no. 9933, pp. 1947-1948.
- Shreve, P.D., Anzai, Y. & Wahl, R.L. 1999, "Pitfalls in oncologic diagnosis with FDG PET imaging: physiologic and benign variants", *Radiographics*, vol. 19, no. 1, pp. 61-77; quiz 150-1.
- Singh, P., Yao, Y., Weliver, A., Broxmeyer, H.E., Hong, S.C. & Chang, C.H. 2008, "Vaccinia virus infection modulates the hematopoietic cell compartments in the bone marrow", *Stem cells (Dayton, Ohio)*, vol. 26, no. 4, pp. 1009-1016.
- Smit, T.H., Burger, E.H. & Huyghe, J.M. 2002, "A case for strain-induced fluid flow as a regulator of BMU-coupling and osteonal alignment", *Journal of bone and mineral research*, vol. 17, no. 11, pp. 2021-2029.
- Styner, M., Thompson, W.R., Galior, K., Uzer, G., Wu, X., Kadari, S.,

- Case, N., Xie, Z., Sen, B., Romaine, A., Pagnotti, G.M., Rubin, C.T., Styner, M.A., Horowitz, M.C. & Rubin, J. 2014, "Bone marrow fat accumulation accelerated by high fat diet is suppressed by exercise", *Bone*, vol. 64C, pp. 39-46.
- Syddall, H., Cooper, C., Martin, F., Briggs, R. & Aihie Sayer, A. 2003, "Is grip strength a useful single marker of frailty?", *Age and Ageing*, vol. 32, no. 6, pp. 650-656.
- Teitelbaum, S.L. 2000, "Bone resorption by osteoclasts", *Science (New York, N.Y.)*, vol. 289, no. 5484, pp. 1504-1508.
- Troitskaia, A., Fallone, B.G. & Yahya, A. 2013, "Long echo time proton magnetic resonance spectroscopy for estimating relative measures of lipid unsaturation at 3 T", *Journal of magnetic resonance imaging : JMRI*, vol. 37, no. 4, pp. 944-949.
- Trudel, G., Payne, M., Madler, B., Ramachandran, N., Lecompte, M., Wade, C., Biolo, G., Blanc, S., Hughson, R., Bear, L. & Uhthoff, H.K. 2009, "Bone marrow fat accumulation after 60 days of bed rest persisted 1 year after activities were resumed along with hemopoietic stimulation: the Women International Space Simulation for Exploration study", *Journal of applied physiology (Bethesda, Md.: 1985)*, vol. 107, no. 2, pp. 540-548.
- Tu, X., Rhee, Y., Condon, K.W., Bivi, N., Allen, M.R., Dwyer, D., Stolina, M., Turner, C.H., Robling, A.G., Plotkin, L.I. & Bellido, T. 2012, "Sost downregulation and local Wnt signaling are required for the osteogenic response to mechanical loading", *Bone*, vol. 50, no. 1, pp. 209-217.
- Tuominen, J.T., Impivaara, O., Puukka, P. & Ronnema, T. 1999, "Bone mineral density in patients with type 1 and type 2 diabetes", *Diabetes care*, vol. 22, no. 7, pp. 1196-1200.
- Vaag, A., Brons, C., Gillberg, L., Hansen, N.S., Hjort, L., Arora, G.P., Thomas, N., Broholm, C., Ribel-Madsen, R. & Grunnet, L.G. 2014, "Genetic, nongenetic and epigenetic risk determinants in developmental programming of type 2 diabetes", *Acta Obstetrica et Gynecologica Scandinavica*, vol. 93, no. 11, pp. 1099-1108.
- Van Damme, A., Vanden Driessche, T., Collen, D. & Chuah, M.K. 2002, "Bone marrow stromal cells as targets for gene therapy", *Current gene therapy*, vol. 2, no. 2, pp. 195-209.
- van den Berg, S.M., Seijkens, T.T., Kusters, P.J., Beckers, L., den Toom, M., Smeets, E., Levels, J., de Winther, M.P. & Lutgens, E. 2016, "Diet-induced obesity in mice diminishes hematopoietic stem and progenitor cells in the bone marrow", *FASEB journal*, vol. 30, no. 5, pp. 1779-1788.
- Vanhamme, L., van den Boogaart, A. & Van Huffel, S. 1997, "Improved method for accurate and efficient quantification of MRS data with use of prior knowledge", *Journal of magnetic resonance (San Diego, Calif.: 1997)*, vol. 129, no. 1, pp. 35-43.
- Viljanen, A.P., Lautamaki, R., Jarvisalo, M., Parkkola, R., Huupponen, R., Lehtimaki, T., Ronnema, T., Raitakari, O.T., Iozzo, P. & Nuutila, P. 2009, "Effects of weight loss on visceral and abdominal subcutaneous adipose tissue blood-flow and

insulin-mediated glucose uptake in healthy obese subjects", *Annals of Medicine*, vol. 41, no. 2, pp. 152-160.

Virtanen, K.A., Lidell, M.E., Orava, J., Heglind, M., Westergren, R., Nieminen, T., Taittonen, M., Laine, J., Savisto, N.J., Enerback, S. & Nuutila, P. 2009, "Functional brown adipose tissue in healthy adults", *The New England journal of medicine*, vol. 360, no. 15, pp. 1518-1525.

Virtanen, K.A., Lonroth, P., Parkkola, R., Peltoniemi, P., Asola, M., Viljanen, T., Tolvanen, T., Knuuti, J., Ronnema, T., Huupponen, R. & Nuutila, P. 2002, "Glucose uptake and perfusion in subcutaneous and visceral adipose tissue during insulin stimulation in nonobese and obese humans", *The Journal of clinical endocrinology and metabolism*, vol. 87, no. 8, pp. 3902-3910.

Wilson, C.L. & Ness, K.K. 2013, "Bone mineral density deficits and fractures in survivors of childhood cancer", *Current osteoporosis reports*, vol. 11, no. 4, pp. 329-337.

Yeung, D.K., Griffith, J.F., Antonio, G.E., Lee, F.K., Woo, J. & Leung, P.C. 2005, "Osteoporosis is associated with increased marrow fat content and decreased marrow fat unsaturation: a proton MR spectroscopy study", *Journal of magnetic resonance imaging : JMRI*, vol. 22, no. 2, pp. 279-285.

Zhao, R., Zhao, M. & Xu, Z. 2015, "The effects of differing resistance training modes on the preservation of bone mineral density in postmenopausal women: a meta-analysis", *Osteoporosis international*, vol. 26, no. 5, pp. 1605-1618.

# **ORIGINAL PUBLICATIONS**